

FINAL REPORT

Integrated Stable Isotope – Reactive Transport Model Approach
for Assessment of Chlorinated Solvent Degradation

ESTCP Project ER-201029

JUNE 2016

Tomasz Kuder and Paul Philp
University of Oklahoma

Boris van Breukelen
Delft University of Technology

Héloïse Thouement
VU University of Amsterdam

Mindy Vanderford
HydroGeoLogic Inc.

Distribution Statement A

This document has been cleared for public release



Page Intentionally Left Blank

This report was prepared under contract to the Department of Defense Environmental Security Technology Certification Program (ESTCP). The publication of this report does not indicate endorsement by the Department of Defense, nor should the contents be construed as reflecting the official policy or position of the Department of Defense. Reference herein to any specific commercial product, process, or service by trade name, trademark, manufacturer, or otherwise, does not necessarily constitute or imply its endorsement, recommendation, or favoring by the Department of Defense.

Page Intentionally Left Blank

REPORT DOCUMENTATION PAGE				Form Approved OMB No. 0704-0188	
Public reporting burden for this collection of information is estimated to average 1 hour per response, including the time for reviewing instructions, searching existing data sources, gathering and maintaining the data needed, and completing and reviewing this collection of information. Send comments regarding this burden estimate or any other aspect of this collection of information, including suggestions for reducing this burden to Department of Defense, Washington Headquarters Services, Directorate for Information Operations and Reports (0704-0188), 1215 Jefferson Davis Highway, Suite 1204, Arlington, VA 22202-4302. Respondents should be aware that notwithstanding any other provision of law, no person shall be subject to any penalty for failing to comply with a collection of information if it does not display a currently valid OMB control number. PLEASE DO NOT RETURN YOUR FORM TO THE ABOVE ADDRESS.					
1. REPORT DATE (DD-MM-YYYY) 16-06-2016		2. REPORT TYPE Final Report		3. DATES COVERED (From - To) Jan. 2011 - Feb. 2016	
4. TITLE AND SUBTITLE Integrating Stable Isotope Analysis and Reactive Transport Modeling for Assessing Chlorinated Solvent Degradation Final Report				5a. CONTRACT NUMBER W912HQ-10-C-0060	
				5b. GRANT NUMBER ER-201029	
				5c. PROGRAM ELEMENT NUMBER	
6. AUTHOR(S) Kuder, Tomasz; Philp, Richard, P.; vanBreukelen, Thouement, Heloise; Vanderford, Mindy				5d. PROJECT NUMBER ER-201029	
				5e. TASK NUMBER	
				5f. WORK UNIT NUMBER	
7. PERFORMING ORGANIZATION NAME(S) AND ADDRESS(ES) University of Oklahoma, 100 E. Boyd St., SEC 810 Norman, OK 73019-2115 Delft University of Technology, Stevinweg 1, 2628 CN Delft, The Netherlands VU University Amsterdam, De Boelelaan 1085, 1081 HV Amsterdam, The Netherlands GSI Environmental, Inc., 2211 Norfolk, Suite 1000 Houston, TX 77098				8. PERFORMING ORGANIZATION REPORT NUMBER	
9. SPONSORING / MONITORING AGENCY NAME(S) AND ADDRESS(ES) Environmental Security Certification Program (ESTCP) 4800 Mark Center Drive, Suite				10. SPONSOR/MONITOR'S ACRONYM(S) ESTCP	
				11. SPONSOR/MONITOR'S REPORT NUMBER(S) ER-201029	
12. DISTRIBUTION / AVAILABILITY STATEMENT					
13. SUPPLEMENTARY NOTES					
14. ABSTRACT This document presents the results of ESTCP Project ER-201029 Integrated Stable Isotope - Reactive Transport Model Approach for Assessment of Chlorinated Solvent Degradation. The objective of this guidance is to help site managers apply a Reactive Transport Modeling (RTM) approach for improved Compound-Specific Isotope Analysis (CSIA) data interpretation and to use models to estimate more accurate attenuation processes for chlorinated solvents. The quantification of various destructive and transport processes and how they contribute to plume size and longevity may help extend Monitored Natural Attenuation (MNA) remedies to sites that have, heretofore, not been able to apply this important technology. In comparison with traditional data interpretation, the approach presented has several important benefits: (1) improvement of a conceptual site models by identification and quantification of prevalent attenuation pathways and identification of secondary inputs from DNAPL dissolution or non-degradative sinks such as sorption or volatilization, diffusion or dispersion. (2) a more accurate assessment of degradation of the parent contaminant; (3) quantitative assessment of the net degradation/accumulation of the dechlorination intermediates.					
15. SUBJECT TERMS Compound-specific isotope analysis, reactive transport modeling, groundwater, chlorinated solvents					
16. SECURITY CLASSIFICATION OF:			17. LIMITATION OF ABSTRACT UU	18. NUMBER OF PAGES 130	19a. NAME OF RESPONSIBLE PERSON
a. REPORT	b. ABSTRACT	c. THIS PAGE			19b. TELEPHONE NUMBER (include area code)

Page Intentionally Left Blank

TABLE OF CONTENTS

1.0	INTRODUCTION.....	1
1.1	BACKGROUND.....	1
1.2	OBJECTIVE OF THE DEMONSTRATION.....	2
1.3	REGULATORY DRIVERS.....	3
2.0	TECHNOLOGY.....	3
2.1	TECHNOLOGY DESCRIPTION.....	3
	2.1.1 Compound-Specific Isotope Analysis (CSIA).....	3
	2.1.2 Reactive Transport Modeling (RTM).....	6
2.2	TECHNOLOGY DEVELOPMENT.....	11
	2.2.1 CSIA methods.....	11
	2.2.2 RTM methods.....	12
2.3	ADVANTAGES AND LIMITATIONS OF THE TECHNOLOGY.....	13
3.0	PERFORMANCE OBJECTIVES.....	15
3.1	PERFORMANCE OBJECTIVE 1: OPTIMIZE CSIA METHOD FOR C, H, Cl.....	17
3.2	PERFORMANCE OBJECTIVE 2: ADAPT 0/1-D PHREEQC MODEL FOR H ISOTOPE ENRICHMENT.....	18
3.3	PERFORMANCE OBJECTIVE 3: CALIBRATE 0/1-D GEOCHEMICAL MODEL FOR C, Cl AND H ENRICHMENT.....	19
3.4	PERFORMANCE OBJECTIVE 4: ADAPT MODEL TO 2/3-D IN PHAST AND PHT3D.....	19
3.5	PERFORMANCE OBJECTIVE 5: CALIBRATE 2/3-D MODEL WITH SITE-SPECIFIC DATA (REVISED: CALIBRATE 0-D MODEL WITH SITE-SPECIFIC DATA).....	20
3.6	PERFORMANCE OBJECTIVE 6: USE CSIA/MODEL TECHNOLOGY TO DEMONSTRATE THE PRESENCE OF MULTIPLE DEGRADATION PATHWAYS.....	21
3.7	PERFORMANCE OBJECTIVE 7: ESTIMATE DEGRADATION CONSTANTS FOR CONTAMINANTS OF CONCERN AT DEMONSTRATION SITE.....	22
3.8	PERFORMANCE OBJECTIVE 8: DEVELOP A NEW FRAMEWORK FOR INTERPRETING CSIA DATA.....	22
3.9	PERFORMANCE OBJECTIVE 9: REFINE CSM FOR DEMONSTRATION SITE.....	22
4.0	SITE DESCRIPTION.....	23
4.1	SITE LOCATION AND HISTORY.....	23
4.2	SITE GEOLOGY/HYDROGEOLOGY.....	23
4.3	CONTAMINANT DISTRIBUTION.....	27
5.0	TEST DESIGN.....	28

5.1	CONCEPTUAL EXPERIMENTAL DESIGN	28
5.2	BASELINE CHARACTERIZATION	29
5.3	LABORATORY STUDY RESULTS	29
5.4	DESIGN AND LAYOUT OF TECHNOLOGY COMPONENTS	32
5.5	FIELD TESTING	32
5.6	SAMPLING and ANALYSIS METHODS	32
5.7	SAMPLING RESULTS	35
6.0	PERFORMANCE ASSESSMENT	40
6.1	PERFORMANCE OBJECTIVE 1: OPTIMIZE CSIA METHOD FOR C, H, CL ISOTOPE ENRICHMENT	40
6.2	PERFORMANCE OBJECTIVE 2: ADAPT 0/1-D PHREEQC MODEL FOR H ISOTOPE ENRICHMENT	40
6.3	PERFORMANCE OBJECTIVE 3: CALIBRATE 0/1-D GEOCHEMICAL MODEL FOR C, CL AND H ENRICHMENT	41
6.4	PERFORMANCE OBJECTIVE 4: ADAPT MODEL TO 2/3-D IN PHAST AND PHT3D	42
6.5	PERFORMANCE OBJECTIVE 5: CALIBRATE 2/3-D MODEL WITH SITE-SPECIFIC DATA (REVISED: CALIBRATE 0-D MODEL WITH SITE-SPECIFIC DATA)	45
6.5.1	The rationale for the revision of the spatial dimensionality of the model to 0-D	45
6.5.2	Model approach	46
6.5.3	Modeling results: Shallow Plume	49
6.5.4	Modeling results: Deep Plume	52
6.6	PERFORMANCE OBJECTIVE 6: USE CSIA/MODEL TECHNOLOGY TO DEMONSTRATE THE PRESENCE OF MULTIPLE DEGRADATION PATHWAYS	64
6.7	PERFORMANCE OBJECTIVE 7: ESTIMATE DEGRADATION CONSTANTS FOR CONTAMINANTS OF CONCERN AT DEMONSTRATION SITE	65
6.8	PERFORMANCE OBJECTIVE 8: DEVELOP A NEW FRAMEWORK FOR INTERPRETING CSIA DATA	68
6.9	PERFORMANCE OBJECTIVE 9: REFINE CSM FOR DEMONSTRATIONSITE	68
7.0	COST ASSESSMENT	70
7.1	COST MODEL	70
7.2	COST DRIVERS	72
7.3	COST ANALYSIS	73
8.0	IMPLEMENTATION ISSUES	77
9.0	REFERENCES	78

TABLES

Table 2.1	Information required to construct reactive transport models.....	9
Table 2.2	Input data for various model levels.....	10
Table 2.3	Calibration process for various models.....	11
Table 3.1	Performance objectives.....	16
Table 5.1	Bulk isotope effects for individual RD transformation steps.....	31
Table 5.2	Analytical methods for sample analysis.....	33
Table 5.3	Project sampling program, analytes and analyses.....	36
Table 6.1	Parameter values selected for Case 3.....	43
Table 6.2	Description simulation scenarios.....	47
Table 6.3	Relative first-order degradation rate constants.....	48
Table 6.4A	Carbon isotope fractionation factors used in the models.....	49
Table 6.4B	Bulk chlorine isotope fractionation factors used in the models.....	49
Table 7.1	Cost model for a CSIA/model application.....	72
Table 7.2	CSIA, cost per sample (based on current costs at the OU laboratory).....	73
Table 7.3	Cost analysis: Case 1.....	74
Table 7.4	Cost analysis: Case 2.....	75
Table 7.5	Cost analysis: Case 3.....	76

FIGURES

Figure 2.1	Isotope ratios for a CE subjected to dilution versus biodegradation processes.....	4
Figure 2.2	Spatial dimensions of RTM.....	7
Figure 4.1	Hill AFB OU10 site location.....	24
Figure 4.2	Cross-sections of the aquifer.....	25
Figure 4.3	Lithological profile of selected monitoring wells.....	26

ESTCP Final Report:

Integrated Stable Isotope –

Reactive Transport Model Approach

for Assessment of Chlorinated

Solvent Degradation

Figure 4.4	Map of the Operable Unit (OU) 10	27
Figure 5.1	Rayleigh-type and 2D-CSIA plots, Lab Study.....	31
Figure 5.2	Locations of wells sampled for CSIA	37
Figure 5.3	CEs concentration and C isotope ratios, cross-section view.....	38, 39
Figure 6.1	A conceptual model of H isotope fractionation in RD of TCE to ethene	40
Figure 6.2	Calibration results for the C, Cl and H isotope fractionation model.....	42
Figure 6.3	Case 3 (ESTCP ER-201029, User's Guide)	43
Figure 6.4	Results of 2-D PHAST simulation	44
Figure 6.5	Results of 2-D PHT3D simulation	44
Figure 6.6	Carbon isotope ratios for TCE, cDCE and tDCE, versus the groundwater age.....	45
Figure 6.7	Dual-element CSIA plots, TCE in the Shallow Plume.....	50
Figure 6.8	Dual-element CSIA plots, TCE in the Deep Plume.....	53
Figure 6.9	Scenario 1: Model for TCE RD only, cis-DCE stall.....	55, 56
Figure 6.10	Scenario 2: Model of TCE RD, with RD products degradation.....	57, 58
Figure 6.11	Scenario 3: Sequential RD/oxidation model.....	59, 60
Figure 6.12	Scenario 4: Simultaneous RD/TCE oxidation model.....	61, 62
Figure 6.13	Scenario 5: Model for TCE RD only, using $\epsilon = -10\text{‰}$	63
Figure 6.14	Estimation of cumulative CEs mineralization.....	66
Figure 6.15	First-order integral degradation rate constants of TCE and DCE.....	67

APPENDICES

Appendix A. Points of Contact.....	81
Appendix B. List of Software	82
Appendix C. Tabulated Sampling Results	83
Appendix D. Chains of Custody of the Field Samples	98

ACRONYMS

AFB	Air Force Base
BTEX	Benzene, Toluene, Ethylbenzene and Xylenes
C	Carbon
CE	Chlorinated Ethenes
C-IMB	Carbon Isotope Mass Balance
cis-DCE	cis 1,2-Dichloroethene
Cl	Chlorine
COCs	Contaminants of Concern
CSIA	Compound-Specific Isotope Analysis
CSM	Conceptual Site Model
cVOC	Chlorinated Volatile Organic Compound
DCE	Dichloroethene
DNAPL	Dense Non-aqueous Phase Liquid
DO	Dissolved Oxygen
EPA	U.S. Environmental Protection Agency
GC	Gas Chromatography
GC-IRMS	Gas Chromatography Isotope Ratio Mass Spectroscopy
GIS	Geographic Information System
GUI	Graphical User Interface
H	Hydrogen
HST3D	Model software. See Appendix B
IMB	Isotope Mass Balance
IRMS	Isotope Ratio Mass Spectrometry
KIE	Kinetic Isotope Effect
MCL	Maximum Contaminant Level
MNA	Monitored Natural Attenuation
MT3DMS	Model software. See Appendix B
MtBE	tert-Methyl Butyl Ether
OU	Operable Unit
OX	Aerobic Oxidation
P&T	Purge and Trap
PAH	Polyaromatic Hydrocarbon
PCE	Tetrachloroethene (Perchloroethene)
PHAST	Model software. See Appendix B
PHREEQC	Model software. See Appendix B
PHT3D	Model software. See Appendix B
QAQC	Quality Assurance Quality Control
RD	Reductive Dechlorination
RTM	Reactive Transport Modeling
SMOC	Standard Mean Ocean Chloride (Cl isotope ratio standard)
TCE	Trichloroethene
trans-DCE	trans 1,2-Dichloroethene
USEPA	U.S. Environmental Protection Agency

ESTCP Final Report:

Integrated Stable Isotope –

Reactive Transport Model Approach

for Assessment of Chlorinated

Solvent Degradation

USGS	U.S. Geological Survey
VC	Vinyl Chloride
VPDB	Vienna Pee Dee Belemnite (C isotope ratio standard)
VSMOW	Vienna Standard Mean Ocean Water (H isotope ratio standard)
δ	Delta. See Eq. 1 for “delta” notation of isotope ratios

ACKNOWLEDGEMENTS

This report presents the results and conclusions from a collaborative project between researchers at University of Oklahoma (OU), VU University Amsterdam (Vrije Universiteit Amsterdam in Dutch) and Delft University of Technology, the Netherlands, and GSI Environmental, Inc. (GSI). This demonstration project was funded by the Environmental Security Technology Certification Program (ESTCP), with the main goal of demonstrating the utility of combining Compound-Specific Isotope Analysis (CSIA) and Reactive Transport Modeling (RTM) to quantify and strengthen support for Monitored Natural Attenuation (MNA) remedies for groundwater contaminated with chlorinated ethene constituents (CEs).

Investigators for this project included Dr. Paul Philp (Principal Investigator, OU), Dr. Tomasz Kuder (Co-Principal Investigator, OU), Dr. Boris van Breukelen (VU), and Dr. Mindy Vanderford and Dr. Charles Newell (GSI). The modeling tool that was generated as part of this project was developed by Boris van Breukelen, Philip Stack and Héloïse Thouement. The microcosm experiment was modeled as part of a research project of Philip Stack. The Hill AFB OU10 site case study was evaluated as part of the dissertation of Héloïse Thouement.

We gratefully acknowledge Kyle Gorder (US Air Force) for his help in identifying potential demonstration sites and coordinating the field work at Hill Air Force Base (AFB), Operable Unit (OU) 10. We also acknowledge the support of AEEC in conducting the field sampling at Hill OU10.

Finally, the project team wishes to thank Dr. Andrea Leeson, Dr. Jeff Marqusee, and the support staff from the ESTCP program office for their help and guidance throughout the demonstration.

EXECUTIVE SUMMARY

OBJECTIVES OF DEMONSTRATION

Monitored Natural Attenuation (MNA) is an important groundwater remediation technology based on a carefully controlled and monitored demonstration of contaminant attenuation. However, demonstrating *contaminant mass destruction* can be challenging. Compound-specific isotope analysis (CSIA) is a specialized laboratory method that can provide a direct signal of biological or abiotic degradation and support assessment of the strength of physical attenuation processes. The popularity of CSIA has risen rapidly among project managers as a line of evidence supporting MNA remedies. While CSIA results help to refine conceptual site models, CSIA data can be difficult to interpret, especially at sites with complex hydrogeology or with competing degradation pathways. The overall goal of the project is to present methods for quantitative assessment of natural attenuation processes, including mass destruction, for chlorinated solvents, using a combination of CSIA with modeling-assisted data interpretation.

TECHNOLOGY DESCRIPTION

Many elements, such as carbon, hydrogen and chlorine, occur as different isotope species, differing in their atomic mass. CSIA permits the determination of the isotopic makeup of the contaminants present in environmental samples and the information obtained can be used as a line of evidence in contaminant studies. The majority of CSIA applications concerns the assessment of VOC contaminant degradation in groundwater. The principle of the approach is that isotope ratios of a contaminant, for example $^{13}\text{C}/^{12}\text{C}$, remain constant as the groundwater is diluted, while the fraction of the heavy isotope, ^{13}C , typically increases with degradation. The difference between ^{12}C and ^{13}C behavior originates from energetically favored reactions for the molecules containing the lower atomic mass isotope (e.g., ^{12}C). The benefit of the CSIA approach for contaminant studies lies in its ability to distinguish mass destruction (by biodegradation and/or abiotic degradation) from other types of mass attenuation. However, interpretation of field CSIA data can be difficult due to competing degradation pathways and/or complex transport conditions in the aquifer. The value added to contaminated site assessment by the use of CSIA ultimately depends on the specificity of the interpretation. This study centers on demonstration of numerical modeling to improve the capabilities for attenuation pathway identification and quantitative assessment of CSIA data.

Reactive transport modeling (RTM) simulates transport and contaminant degradation, using a simplified representation of the features of the modeled site. RTM enables one to simulate complex reaction networks (e.g., sequential reductive dechlorination along with oxidative transformation) together with isotope fractionation (C, H, Cl), while accounting for physical processes that may influence isotope ratios, such as hydrodynamic dispersion. However, as discussed below, RTMs also enable sound data interpretation through simulating fewer dimensions like 2-D cross-sections, 1-D flow paths or even 0-D batch degradation.

DEMONSTRATION RESULTS

The demonstration followed two main tracks, a development and initial calibration of the modeling software and a demonstration of the combined CSIA/RTM approach through an assessment of a contaminated site (Hill AFB, Operable Unit 10, consisting of the Shallow TCE & PCE Plume and the Deep TCE Plume). The success of the technology demonstration was defined in terms of producing results that are useful for development/improvement of the Conceptual Site Model and are superior to those obtained by the “classic” CSIA alone.

The performance objectives for the software development & validation were met successfully: (i) 0/1-D PHREEQC model templates for simulation of isotope fractionation in reductive dechlorination, for carbon, chlorine and hydrogen were developed and calibrated using a data set from a microcosm experiment (dechlorination of trichloroethylene by a *Dehalococcoides* culture); and (ii) two different 2/3-D model platforms, PHAST and PHT3D were adopted to simulate the same set of reactions as PHREEQC.

The performance objectives for evaluation of the Demonstration Site had to be revised, after initial evaluation of the data collected at the site. Observed trends of isotope enrichments did not correlate to the distance from the plume source, the distance across the plume fringe or to the groundwater age. Instead, degradation in the Shallow Plume was localized in disconnected zones of the plume. Degradation in the Deep Plume was occurring primarily in an irregular area in the proximity to the plume source zone. Since no meaningful trends of isotope fractionation could be identified along 1-D flow lines, the exercise of 1/2/3-D modeling would be meaningless. Instead, the modeling was conducted using the batch (0-D) mode of the 0/1-D PHREEQC software. Spatial and temporal dimensions were thus not explicitly simulated. Even so, in comparison with the “classical” CSIA evidence, the combined CSIA/modeling approach (using the model to test alternative attenuation scenarios; the scenarios were defined using the “classical” CSIA evidence) permitted: (i) a reduction of uncertainties in identification of specific degradation pathways; and (ii) more accurate identification of the range of isotope enrichment factors, leading to more accurate quantitation of contaminant mass destruction.

IMPLEMENTATION ISSUES

The benefits of the proposed methodology are that: (i) the cost added by basic 0-D modeling of CSIA data is relatively low in comparison to the complete cost of sample collection and CSIA analytical work; and (ii) the only requirement for implementation of CSIA/modeling is a reasonable completeness of the CSIA and contaminant concentration data. A decision to involve RTM-assisted data interpretation can be made after the “classical” CSIA data interpretation. RTM may potentially eliminate question remaining, by testing alternative attenuation scenarios.

As indicated above, site heterogeneity complicates implementation of the modeling in data interpretation. Even after the model dimensions were downgraded to 0-D, simulation of the degradation processes in the Deep Plume using the existing model template was difficult and less successful than in the case of the Shallow Plume. It is likely that the problems were caused by significant contribution of diffusion/back-diffusion to the distribution of contaminants in the aquifer, a process that was not included in the model template.

1.0 INTRODUCTION

Monitored Natural Attenuation (MNA) is an important groundwater remediation technology based on a carefully controlled and monitored demonstration of contaminant attenuation from natural subsurface processes (USEPA 1998).

MNA remedies have several advantages over active remedies in terms of cost, effort, carbon footprint, and energy savings. However, demonstrating the strength of attenuation processes, particularly *contaminant mass destruction* can be challenging. For this reason, recent research efforts have focused on improving methods for demonstrating contaminant mass destruction processes in the subsurface.

Conventional MNA analyses rely on “*lines of evidence*” such as concentration vs. distance or concentration vs. time plots and other simple data visualization techniques to demonstrate contaminant destruction. Compound-specific isotope analysis (CSIA) is a specialized laboratory method that can provide a more direct signal of biological or abiotic degradation and support assessment of the strength of physical attenuation processes. The popularity of CSIA has risen rapidly among project managers as one line of evidence supporting MNA remedies.

While CSIA results help to document contaminant degradation and refine conceptual site models (CSM), CSIA data can be difficult to interpret, especially at sites with complex hydrogeology or release histories. This project’s focus is a combination of CSIA data and simple reactive transport models (RTMs), to strengthen interpretation of both CSIA and conventional analytical data. The overall goal of the project is to present methods for quantitative assessment of natural attenuation processes, including mass destruction, for chlorinated solvents, using a combined compound-specific isotope analysis (CSIA) and numerical reactive transport modeling (RTM) approach.

1.1 BACKGROUND

Management of sites impacted by chlorinated solvent contaminants presents an on-going challenge for the Department of Defense (SERDP-ESTCP 2006). Finding new ways to characterize and manage these sites is a priority. The microbial degradation of chlorinated solvents in aquifers has been demonstrated in both laboratory and in situ over the past 25 years. However, a number of aspects of the mechanisms and rates of in-situ degradation have yet to be determined. For example, while the potential for aerobic oxidation of chlorinated volatile organic compounds (cVOCs) in subsurface has been recently recognized, little empirical evidence is available to demonstrate this process in situ. Over the last decade, CSIA has been applied to environmental samples to demonstrate the occurrence of biological degradation and chemical transformation processes for a variety of contaminants, with most studies focusing on chlorinated ethene solvents such as PCE and TCE (USEPA, 2008). The principle of the application of this technology is that stable isotope ratios (e.g., $^{13}\text{C}/^{12}\text{C}$) of contaminant molecules change as degradation proceeds, providing direct evidence for contaminant degradation.

The application of the CSIA technology can potentially help to refine a number of aspects of CSMs, including the following:

- Identification of prevalent degradation pathways.
- Identification of non-destructive contaminant sinks such as sorption, dilution or volatilization.
- Delineation of the areas of strong degradation processes within the plume.
- Providing more accurate assessment of the rate and extent of degradation of the parent contaminant.
- Providing quantitative assessment of the net degradation/accumulation of the dechlorination intermediates.

On the most basic level, CSIA can simply provide qualitative evidence of contaminant mass destruction. More detailed results, including quantitative estimates of the contaminant mass degraded and identification of degradation pathways can be also obtained at certain sites, as demonstrated in the past. However, interpretation of field CSIA data can be difficult due to competing degradation pathways and/or complex transport conditions in the aquifer. The value added to contaminated site assessment by the use of CSIA ultimately depends on the specificity of the interpretation. This study centers on demonstration of numerical modeling to improve the capabilities for attenuation pathway identification and quantitative assessment of CSIA data.

1.2 OBJECTIVE OF THE DEMONSTRATION

The key objective of the project was to validate a combined CSIA and numerical RTM approach as an advanced assessment tool for attenuation of chlorinated solvents. The specific technical objectives of the validation are described in Section 3. The Demonstration Site was Operable Unit 10 (OU 10) at Hill AFB, Utah, a site where groundwater is impacted by plumes of chlorinated ethenes. The comprehensive data set collected at the demonstration site served as a model case study for the RTM-CSIA approach.

The project deliverables include freeware RTM templates (Appendix B) applicable to chlorinated ethenes degradation and the User's Guide document, describing the applications of classic CSIA and the CSIA/RTM for chlorinated solvents sites (ESTCP ER-201029, User's Guide). The User's Guide will help site managers and regulators to determine if CSIA and/or CSIA/RTM is appropriate for their site, and how the data can be used to support remedial decision making, including decisions on reducing monitoring effort, discontinuation of active remedies, and on facilitating property redevelopment. The freeware made available to consulting and academic communities should facilitate widespread availability of the technology for commercial applications at DoD sites and elsewhere.

1.3 REGULATORY DRIVERS

For the majority of DoD sites with chlorinated solvent contamination, the primary regulatory driver is attainment of relevant cleanup goals in the affected media. Until cleanup goals are met, site managers must establish and demonstrate conditions protective of potential receptors. For sites regulated under CERCLA (Superfund), demonstration of protective conditions must be made every five years. Part of the demonstration of protectiveness can include showing that plumes are well controlled and that remedial systems are making progress toward site cleanup goals. MNA remedies can be very cost effective, but require regulatory approval. Use of MNA as a treatment and/or control strategy requires evidence of intrinsic degradation. CSIA may supply the type of information to support regulatory approval of MNA.

2.0 TECHNOLOGY

The present project combines CSIA (chemical analysis technology) with RTM (data analysis technology).

2.1 TECHNOLOGY DESCRIPTION

2.1.1 Compound-Specific Isotope Analysis (CSIA)

In organic contaminant chemistry applications, the most significant stable isotope ratios are $^{13}\text{C}/^{12}\text{C}$, $^2\text{H}/^1\text{H}$, $^{37}\text{Cl}/^{35}\text{Cl}$, and $^{15}\text{N}/^{14}\text{N}$ ($^{15}\text{N}/^{14}\text{N}$ will not be discussed in this report). CSIA measures the ratios of stable isotopes of common elements for specific chemical compounds present in the analyzed samples. In recent years, CSIA became a widely accepted tool in the studies of groundwater contaminants (USEPA, 2008). A detailed discussion of CSIA theory and application is provided in the User's Guide, Section 3.0 prepared as a deliverable of this project (ESTCP ER-201029, User's Guide).

CSIA has been applied in groundwater contaminant studies since late 1990's, initially exclusively for analysis of carbon isotope ratios. CSIA has been used extensively in investigations of environmental releases to characterize the source and fate of several significant VOC-class contaminants. The majority of CSIA applications concerns the assessment of biodegradation (and, to lesser extent, chemical abiotic degradation) of VOCs in groundwater, including CEs, MtBE and BTEX (USEPA, 2008). Isotope signatures have been also used to identify sources of CEs (USEPA, 2008).

The benefit of CSIA applied to groundwater contamination lies in its ability to distinguish mass destruction (by biodegradation and/or abiotic degradation) from other types of mass attenuation. The principle of the approach is that stable isotope ratios of a contaminant, for example $^{13}\text{C}/^{12}\text{C}$, remain constant as the groundwater is diluted, while degradation often causes **isotope fractionation** between the reactant (degrading contaminant) and the degradation product. Typically, the fraction of the heavy isotope, ^{13}C , increases as degradation proceeds (Figure 2.1). The enrichment of ^{13}C in partially degraded contaminant residue is the result of lower activation energy in bond cleavage in the contaminant molecules with the lighter isotope, ^{12}C , at the reaction center. Consequently, the degradation products, e.g., TCE produced by reductive dechlorination of PCE, are depleted in ^{13}C related to the parent compounds (Figure 2.1). The

ESTCP Final Report:

Integrated Stable Isotope –

Reactive Transport Model Approach

for Assessment of Chlorinated

Solvent Degradation

same pattern of isotope fractionation, where the heavy isotope is enriched in degradation residue, usually applies to other elements, including H and Cl. However, the mechanisms of the isotope ratio changes for H and Cl have been studied less extensively and are not as well understood as those of C isotopes.

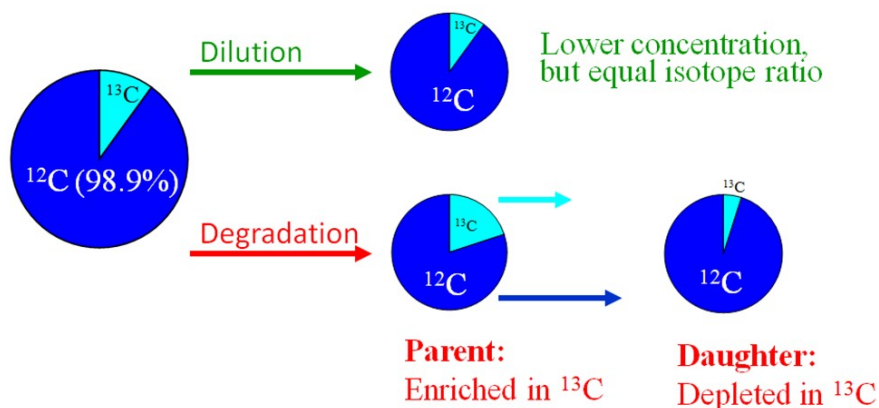


Figure 2.1. Isotope ratios for a CE subjected to dilution versus biodegradation processes. Dilution results in no change in isotope ratios. Degradation results in isotope fractionation: The proportion of the heavy isotope in the parent compound increases, while the daughter compound (product) is depleted in the heavy isotope.

In contaminant chemistry studies, isotope ratios are typically reported using the so-called delta delta (δ) notation (Equation 1). Note that a δ value does not show the absolute isotope abundance but rather a deviation from the international standard (USEPA, 2008). The δ values are typically written with a ‰ (per mill) symbol to reduce the number of decimals (e.g., $\delta^{13}\text{C} = 0.0013$ is written as $\delta^{13}\text{C} = 1.3$ ‰).

$$\delta^{13}\text{C} = (R_{\text{sample}}/R_{\text{standard}} - 1) \quad (\text{Eq. 1})$$

A change of isotope ratios of a contaminant undergoing degradation can, in most cases, be described by the Rayleigh model (Eq. 2 written for the example of C isotopes). The model predicts $\delta^{13}\text{C}_t$ (an isotope ratio of the degraded contaminant at time t) as a function of the fraction of the contaminant mass remaining (f). The enrichment factor (ϵ) is a reaction-specific magnitude of the isotope effect and $\delta^{13}\text{C}_0$ is the pre-degradation isotope ratio of the contaminant, $\delta^{13}\text{C}_t$ is the isotope ratio of the contaminant in a groundwater sample, measured by CSIA.

Eq. 2 can be rewritten to calculate the value of f , to assess the contaminant mass destruction (Equation 3). The estimates obtained by Eq. 3 are usually very conservative because the constants ϵ and δ_0 tend to display certain margins of uncertainty and the f determination must be based on conservative end-member values ϵ and δ_0 . Moreover, the Rayleigh model is directly applicable when degradation is the only sink for the reactant, i.e., in batch reactors or in homogenous steady-state contaminant plumes. As the Rayleigh model does not account for spatial heterogeneity of a contaminant plume (van Breukelen and Prommer 2008), the obtained

values of f are further masked by mixing of more or less degraded material within the hydraulic radius of a monitoring point. Finally, the Rayleigh model applies directly only to the parent contaminant (e.g., PCE present in a DNAPL spill) but Eq. 3 cannot be used to accurately calculate the extend of degradation of the daughter compounds (e.g., cDCE that eventually reduces to VC).

$$\ln [(\delta^{13}\text{C}_t + 1000) / (\delta^{13}\text{C}_0 + 1000)] = \varepsilon \times \ln f \quad (\text{Eq. 2})$$

$$f = \exp\{\ln [(\delta^{13}\text{C}_t + 1000) / (\delta^{13}\text{C}_0 + 1000)] / \varepsilon\} \quad (\text{Eq. 3})$$

Due to the setup of analytical technique, CSIA determines isotope fractionation at whole molecule level (“bulk” isotope data). In (bio)chemical reactions, isotope effects occur at the level of individual atoms within the molecules. “Bulk” isotope effects combine so-called kinetic isotope effects (KIEs) for all atoms of the element present in the reacting molecule (for example, in dechlorinating of TCE to cis-DCE, the bulk Cl isotope effect combines the contributions from the Cl atom undergoing dechlorination and the two atoms remaining in the cis-DCE product, respectively). While discussion of KIEs is beyond the scope of this report, noting the difference between the “**bulk**” effects and the **position-specific KIEs** will help to understand the principle of the isotope modeling, where position-specific inputs, in particular for Cl and H modeling, may be required (see User’s Guide, Section 3, ER-201029 and USEPA, 2008 for more information on KIEs).

Analytical techniques: CSIA involves extraction of the target compounds from environmental sample matrix, followed by separation of the compounds using gas chromatography (GC), and then followed by mass spectrometry to determine isotope ratios in individual compounds. Details of the analytical methods used in this study are given in Section 5.6.

- **Sample extraction** – in this project, VOCs were extracted from samples using the Purge and Trap method.
- **Chromatography** – for the majority of the samples, standard GC separation approach was used, similar to the approach for conventional VOCs analysis. For selected samples collected in 2014, where the presence of interfering non-target VOCs was observed previously, two-dimensional GC separation was used, similar to the method described in the technical report of ESTCP ER-201025 (ESTCP ER-201025, Technical Report).
- **C CSIA** – The effluent from the GC column is passed through an in-line oxidation reactor. C isotope ratios are determined after combustion of the target compounds to surrogate gas, CO₂. The surrogate gas is analyzed by isotope ratio mass spectrometry (IRMS) to determine the isotope ratio.
- **Cl CSIA** – Cl isotope ratios are determined by spectrometry of ionized molecules introduced into the spectrometer without thermal conversion. Cl CSIA methods utilize IRMS or standard quadrupole MS detectors. The latter option was used in the present project.
- **H CSIA** – The effluent from the GC column is passed through an in-line reduction reactor. H isotope ratios are determined after reduction of the target compounds to

surrogate gas, H₂. The surrogate gas is analyzed by isotope ratio mass spectrometry (IRMS) to determine the isotope ratio.

2.1.2 Reactive Transport Modeling (RTM)

A model is a simplified representation of the features of interest of a site. Models can be developed with varying levels of complexity to simulate a variety of conditions. Most groundwater models are developed around either physical processes (e.g. advection, dispersion, diffusion, and sorption, described above) or chemical reactions (e.g. spontaneous or enzymatically catalyzed Monod-type rate equations). **Reactive Transport Models (RTMs) constitute a set of interpretive tools to simulate complex interactions between linked chemical and physical processes across multiple space and time scales.** Linking CSIA results (isotope fractionation resulting from contaminant degradation) with contaminant transport requires integration of chemical reactions and physical processes and is, therefore, best approached through RTM.

RTMs, in principle, enable users to simulate complex reaction networks (sequential reductive dechlorination together with oxidative transformation) together with isotope fractionation (C, H, Cl), while accounting for physical processes that may influence isotope ratios such as hydrodynamic dispersion (Abe, 2006; van Breukelen and Prommer, 2008), diffusion as part of vertical transverse dispersion (Jin et al, 2014 ; van Breukelen and Rolle, 2012), and sorption (Eckert, 2013; van Breukelen and Prommer, 2008). RTMs allow 3-D simulation of concentration and CSIA patterns at contaminated sites. However, as discussed below, RTMs also enable sound data interpretation through simulating fewer dimensions like 2-D cross-sections, 1-D flow paths or even 0-D batch degradation.

RTM model and software platforms used as modeling tools for CSIA interpretation for this project include:

- **PHREEQC** – A zero/one dimensional (0/1-D) geochemical transport model developed by the US Geological Survey (USGS). 0-D PHREEQC represents batch degradation system, where transport phenomena are not simulated.
- **PHAST** – A two/three dimensional (2/3-D) groundwater flow and transport model capable of simulating the same set of reactions as PHREEQC. PHAST couples PHREEQC to the groundwater flow and solute transport model HST3D.
- **PHT3D** – A three dimensional (2/3-D) groundwater flow and transport model capable of simulating the same set of reactions as PHREEQC. PHT3D couples PHREEQC to the groundwater flow model MODFLOW and the solute transport model MT3DMS.

RTM Spatial Dimensions

Figure 2.2 illustrates the number of spatial dimensions that can be simulated using RTM techniques. Site data occur in 3-D space. However, this does not imply that RTMs in 3-D are

required to interpret concentrations and CSIA data. Many relevant site characterization questions can be answered by models created in 0, 1 or 2 dimensions.

Provided hydraulic head contours are more or less parallel (Figure 2.2A), observations can usually be projected to a 2-D cross-section of the pollution plume (Figure 2.2B), because a sampling network typically follows the groundwater flow direction. Monitoring of a 2-D cross-section is cost-effective and sound for many sites where environmental conditions are relatively homogeneous perpendicular to the groundwater flow direction at a certain depth level. Furthermore, 2-D model development is simpler and computationally less intensive. Still, a 2-D cross-sectional model is only required if degradation processes vary between the core and the fringe of the plume. Figure 2.2B shows the spreading of ethylbenzene and its degradation following anaerobic core and aerobic fringe degradation results in complex CSIA patterns and enrichment at the fringe (D'Affonseca, 2011). Clearly, for this case a 2-D model is required as well as multi-level sampling.

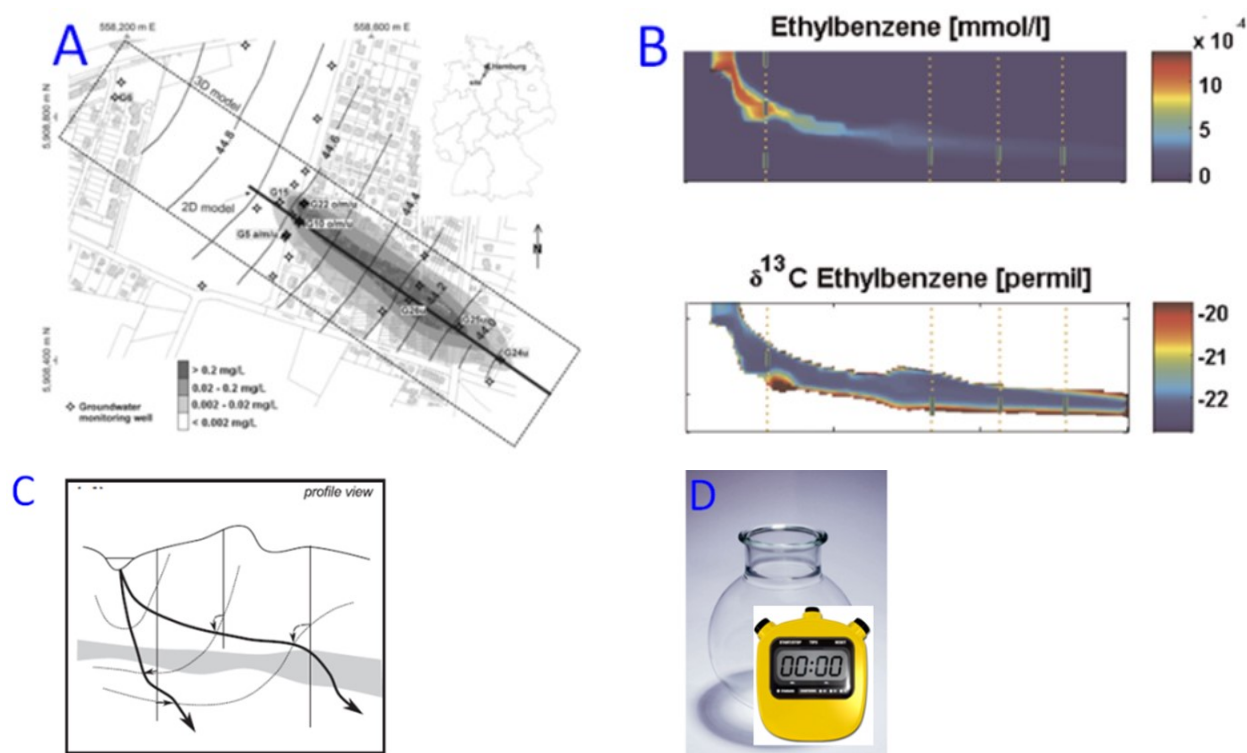


Figure 2.2. Spatial dimensions of RTM. A) 2-D plan view of 3-D pollution plume (D'Affonseca, 2011). The black line following the groundwater flow direction shows the position of a 2-D cross-section shown in B. B) 2-D cross-section of pollution plume depicted in A showing simulated ethylbenzene concentrations and carbon isotope ratios (D'Affonseca, 2011). C) 1-D flow paths simulating observations in 2-D space (Karlsen, 2012). D) A well-mixed closed 0-D batch system where the properties only change as function of time or reaction progress.

In a case where degradation processes are homogenous across the vertical dimension of the plume, a 1-D flow path model may suffice to simulate observations. In the User's Guide, Scenario Case 1 illustrates the 1-D approach (Sections 4.2 and Section 7). The example shows that a 1-D model is not able to accurately simulate concentration levels, as transverse dilution is not accounted for in a 1-D model. Model calibration to molar concentration ratios instead of absolute CE concentrations provides a solution. Optionally, several flow paths can be modeled to simulate observations in 2-D cross section (Figure 2.2C). Flow path models are easy to setup and are computationally fast.

A typical assumption in any 1-/2-/3-D model is that degradation rates are spatially constant. In fact this is a sound assumption to limit model complexity and to prevent non-uniqueness of the set of calibrated model parameters. However, it is questionable if rate constants are truly spatially homogeneous. In reality, the spatial heterogeneity of reaction rates should reflect heterogeneities in the distribution of hydrogeochemical properties. For cases of high spatial heterogeneity in geochemical environments, it will be hard for a 1-D model to accurately simulate observations as a function of travel distance. A potential approach is to consider the subsurface as a black box reaction vessel and to apply a 0-D batch RTM (actually a "reaction model", as transport does not occur). In such a setup (Figure 2.2D) the changes in molar concentration ratios and CSIA data are evaluated versus reaction progress as previously performed by van Breukelen et al. (2005). Such a model setup enables a fast evaluation of the appropriateness of the conceptual reaction network, the proportion of degradation rate constants, and isotope fractionation factors. However, an important drawback to this approach is the omission of hydrodynamic dispersion as an attenuation process. Calibrated fractionation factors will, consequently, deviate somewhat from actual values. This latter 0-D approach was applied to interpret the field site data from the Demonstration Site (Section 6.5).

Model Input Data

Several types of information are required to construct different types of RTMs (see Table 2.1 and above, Section ***RTM Spatial Dimensions***). Basic categories of data include hydrogeologic data such as groundwater flow direction, porosity, gradient and hydraulic conductivity. Data sources for hydrogeologic characteristics include site-specific groundwater elevations, results of pump tests and boring logs. These types of data are normally collected during the site investigation and are part of the CSM. Lithology datasets are sometimes maintained in a relational database, like the concentration data, but other parameters are normally found in site characterization reports and regulatory decision documents.

The second category of model information includes transport data such as effective porosity, bulk density of soil and fraction of organic matter as well as longitudinal and transverse dispersivity. Often data in the second category are estimated for specific lithology from literature sources, but data derived from actual site conditions can improve the quality of the model.

The third category of site data includes contaminant concentrations over both space and time. CSIA and other analytical data collected from the site would be included in this category. These data are normally found in a site relational database including details of the media sampled, analytical methods and the dates and locations of samples collected.

ESTCP Final Report:

Integrated Stable Isotope –

Reactive Transport Model Approach

for Assessment of Chlorinated

Solvent Degradation

For RTM models using CSIA results, a fourth category of data is required: reaction rates (k) and enrichment factors (ϵ) for reacting compounds. These input values can be taken from literature sources for the reactants and the geochemical conditions of the site. Values for ϵ for a number of elements and CEs have been collected from the literature and are shown in based on the recent compilation shown in Appendix B of the User's Guide (ESTCP ER-201029, User's Guide). Estimates of rate constants are likewise available in the literature (For example, see for first-order rate constant van Breukelen et al., 2005 cf. Table 1 and literature references herein).

Table 2.1. Information required to construct reactive transport models

Conceptual Info	<ul style="list-style-type: none"> • Site history • Key contaminants • Base map 	<ul style="list-style-type: none"> • A good conceptual site model • Source identity and history
Hydrogeologic Data	<ul style="list-style-type: none"> • Hydraulic conductivity at several locations • Effective porosity • Configuration of the transmissive zone (layers, location of any no-flow boundaries) • Confined vs. unconfined conditions 	<ul style="list-style-type: none"> • Any recharge/discharge zones • Recharge rates to transmissive zone • Hydraulic gradient information • Location, pumping rate of any major wells
Transport Data	<ul style="list-style-type: none"> • Bulk density of soil in aquifer matrix • Total porosity of soils in aquifer matrix • Fraction organic carbon in aquifer matrix • Partition coefficients 	<ul style="list-style-type: none"> • Estimates of longitudinal and transverse dispersivity • Diffusion coefficient estimates • Tortuosity or effective diffusion coefficients • General ranges of expected degradation coefficients
Reaction Data	<ul style="list-style-type: none"> • Reaction rates (k) for various CEs under different biogeochemical conditions 	<ul style="list-style-type: none"> • Isotope fractionation factors (ϵ)
Contaminant Data	<ul style="list-style-type: none"> • Decay chain for the contaminants of interest • Parent compound concentration at multiple locations and multiple times • Daughter compound concentration at multiple locations and multiple times 	<ul style="list-style-type: none"> • C isotope data at multiple locations (probably 10 or more) for at least one sampling event. • Cl isotope data at multiple locations (probably 10 or more) for at least one sampling event. • H isotope data (optional)

Different RTM software platforms have been developed for CSIA data interpretation, and require different types of input data. (Key model platforms are described in Section 5; detailed description of the model platforms is given in the User's Guide published previously). Table 2.2 indicates more specifically which general input data or information are needed for the various types of RTMs (0/1/2/3-D) relevant to CSIA interpretation. Specific attributes of the reaction network and type of kinetics are usually fine-tuned during model development. Once the reaction network is properly determined, the values of degradation rate constants and isotope fractionation factors can be fine-tuned within literature ranges in the process of model calibration. All models need prior information on the source composition. Detailed information on hydrogeological properties is needed to develop 2-D and 3-D models, whereas for 1-D models information on the average groundwater flow velocity and trajectory of the flow path are sufficient.

Table 2.2. Input data for various model levels

Input data/information	0-D Batch	1-D Flow path	2-D Cross-section	3-D Aquifer
Model platform	<i>PHREEQC</i>	<i>PHREEQC</i>	<i>PHAST, PHT3D</i>	<i>PHAST, PHT3D</i>
Reaction network	<i>Y (MD)</i>	<i>Y (MD)</i>	<i>Y (MD)</i>	<i>Y (MD)</i>
Reaction kinetics	<i>Y (MD)</i>	<i>Y (MD)</i>	<i>Y (MD)</i>	<i>Y (MD)</i>
Degradation rate constants	<i>Y (MC)</i>	<i>Y (MC)</i>	<i>Y (MC)</i>	<i>Y (MC)</i>
Isotope Fractionation factors	<i>Y (MC)</i>	<i>Y (MC)</i>	<i>Y (MC)</i>	<i>Y (MC)</i>
Source composition	<i>Y</i>	<i>Y</i>	<i>Y</i>	<i>Y</i>
Source concentrations	<i>Y</i>	<i>Y</i>	<i>Y</i>	<i>Y</i>
Source isotope ratios	<i>Y</i>	<i>Y</i>	<i>Y</i>	<i>Y</i>
Age of source	<i>na</i>	<i>Y</i>	<i>Y</i>	<i>Y</i>
Time	<i>Y</i>	<i>na</i>	<i>na</i>	<i>na</i>
Groundwater flow velocity	<i>na</i>	<i>Y</i>	<i>na</i>	<i>na</i>
Hydraulic heads	<i>na</i>	<i>na</i>	<i>Y</i>	<i>Y</i>
Hydraulic permeability	<i>na</i>	<i>na</i>	<i>Y</i>	<i>Y</i>
Porosity	<i>na</i>	<i>na</i>	<i>Y</i>	<i>Y</i>
Hydrogeological architecture	<i>na</i>	<i>y</i>	<i>Y</i>	<i>Y</i>
Solid-water partitioning coefficient	<i>Y</i>	<i>Y</i>	<i>Y</i>	<i>Y</i>
Longitudinal dispersion coefficient	<i>na</i>	<i>Y</i>	<i>Y</i>	<i>Y</i>
Transverse dispersion coefficients	<i>na</i>	<i>na</i>	<i>Y: αV</i>	<i>Y: αV & αH</i>
Concentration and CSIA data	<i>Y</i>	<i>Y</i>	<i>Y</i>	<i>Y</i>
Y = Yes na = not applicable (MD) = will also follow out of model development (MC) = could also be determined through model calibration				

Calibration

Model calibration is the systematic adjustment of model input parameters so that model outputs more accurately reflect field or “ground truth” conditions. Calibration involves the estimation of values of constants and parameters used in the model algorithms. This is normally accomplished by solving approximation equations for the desired constants and parameters using values of field observed variables. All models require some level of calibration to be useful for a specific site. Table 2.3 provides a brief summary of calibration processes for the RTMs used to interpret CSIA

Model Output

After the trial-and-error process of model calibration indicated in Table 2.3, the model results can be presented as illustrated in the four example case models described in Section 4.2 of the User’s Guide (ESTCP ER-201029, User’s Guide), and as illustrated for the field site interpretation in Section 6 of this report.

Table 2.3. Calibration process for various models

<i>Model Name</i>	<i>Model Type</i>	<i>Calibration Process</i>
PHREEQC	0-D	Adjusting degradation rate constants and isotope fractionation factors to fit isotope ratio versus molar concentration ratio plots
	1-D	Adjusting degradation rate constants, isotope fractionation factors, and the longitudinal dispersion coefficient to fit isotope ratio and molar concentration ratio versus travel distance plots
PHAST/ PHT3D	2-D	Assuming the flow field has been properly calibrated: Adjusting degradation rate constants, isotope fractionation factors, and the longitudinal and transverse vertical dispersion coefficients to fit CSIA and concentration data in the 2-D cross-section. Fitting should be regarded as approximately reproducing the observed concentration and CSIA patterns.
	3-D	The same as for 2-D. However, also the horizontal transverse dispersion coefficient should be fitted. The model-data comparison will be a considerably larger challenge than for a 2-D model. Fitting should be regarded as roughly reproducing the observed concentration and CSIA patterns.

2.2 TECHNOLOGY DEVELOPMENT

Technology development was conducted both in the area of analytical chemical methods and in the area of modeling software.

2.2.1 CSIA methods

At the outset of the project, the status of the analytical techniques for determining the C, Cl and H isotope ratios of chlorinated ethenes was as follows:

- C CSIA methods were well established at the OU laboratory and elsewhere, no additional development was necessary for routine application.
- Cl CSIA methods were established at the OU laboratory and elsewhere but were not optimized to the same extent as C CSIA, specifically, the detection limits of the method were ~ 5 ug/L vs ~ 1 ug/L of C CSIA.
- H CSIA methods for chlorinated compounds were in early stages of development and not available for routine applications.

The main item for CSIA technology development was the novel method permitting H CSIA of chlorinated compounds. The detailed description of the H CSIA method is given in a paper published in *Environmental Science and Technology* (Kuder and Philp, 2013). A description of the methods is included in Section 5.6.

Given relatively low concentrations of the contaminants in a number of monitoring wells at the Demonstration Site, further optimization of Cl CSIA was conducted prior to the 2014 sampling event. Currently, the Cl CSIA method permits determination of Cl isotope ratio in TCE at concentrations as low as ~0.5 µg/L. A description of the Cl CSIA method is included in Section 5.6.

2.2.2 RTM methods

Technology development was also required in the area of numerical modeling. At the outset of the project the status of isotope fractionation modeling was as follows:

- A 0/1-D PHREEQC model was available for simulating carbon isotope fractionation during sequential reductive dechlorination of chlorinated ethenes (van Breukelen et al., 2005).
- A 0/1-D PHREEQC model was available for simulating chlorine isotope fractionation during sequential reductive dechlorination of chlorinated ethenes (Hunkeler et al., 2009). The model did not account for optional secondary KIEs.
- 2/3-D PHT3D models (PHREEQC coupled to MODFLOW-MT3DMS) were developed for 2-D simulations of carbon isotope fractionation of aromatic hydrocarbons (Prommer, 2009; van Breukelen, 2008), but not for CEs.
- Except for the 0/1-D PHREEQC model simulating C isotope effect in reductive dechlorination, none of the above was validated using actual experimental data on CEs degradation, from field or laboratory experiments.

The technology development goal of this project was to continue this model development with the following aims:

- Development of a 0/1-D PHREEQC model simulating hydrogen isotope fractionation during sequential reductive dechlorination of chlorinated ethenes.
- Validation of the complete (C, Cl, H) PHREEQC model using experimental data obtained in a laboratory study (a microcosm developed with a culture conducting reductive dechlorination of TCE to ethene). The results from the laboratory study are described in Section 5.3.
- Development of 2/3-D PHT3D and 2/3-D PHAST reactive transport models to simulate carbon and chlorine isotope fractionation during both reductive dechlorination and oxidative transformation of DCE and VC.

The model employed for this study was developed as part of this project (van Breukelen et al., 2016, manuscript submitted). The model includes C, Cl, and H isotope fractionation, through both RD ($\text{PCE} \rightarrow \text{TCE} \rightarrow \text{cis-DCE/trans-DCE} \rightarrow \text{VC} \rightarrow \text{ETH}$) and oxidation ($\text{cis-DCE/trans-DCE} \rightarrow \text{CO}_2$, $\text{VC} \rightarrow \text{CO}_2$). Reaction kinetics are modeled as first-order and independent from the redox conditions. The model utilizes the PHREEQC platform developed by the USGS for simulating chemical reactions and transport processes in natural or contaminated water (USGS 2011). Previously, a model was developed on the PHREEQC platform to simulate C isotope fractionation during sequential reductive dechlorination (van Breukelen, 2005). As part of this project, the model was expanded to simulate multi-position Cl isotope fractionation and H isotope fractionation. The three-isotope model was validated using data from the anaerobic microcosm experiment for reductive dechlorination processes.

Due to the complexity of this aquifer system and the prevalence of localized contaminant degradation (discussed in more detail in Section 6.5), we followed a similar modeling approach

as van Breukelen et al. (2005). The aquifer was considered as a black-box and modeled with a batch model. Spatial and temporal dimensions were thus not explicitly simulated. By neglecting transport, the modeling still enabled: (i) reduction of uncertainties about the occurrence of specific degradation pathways; (ii) narrowing the range of field enrichment factors for C, Cl, and H; and (iii) obtaining a quantitative snapshot of degradation of the reductive degradation intermediates.

Two main models were developed for this project (Table 2.4). First, the “plume” model was developed to simulate C and Cl isotope fractionation during sequential reductive dechlorination of PCE to ethene and during oxidation of DCE and VC. The model was implemented in PHAST and partially in PHT3D as the number of solutes was limited in the applied PHT3D GUI PMWIN such that only TCE to ethene could be simulated for both C and Cl. Secondary KIEs in Cl isotope fractionation were not simulated as these were not known to be relevant at the time. C isotope fractionation was simulated with the isotopologue method to optionally account for potential isotope diffusion effects. Isotopologue-dependent diffusion can be simulated with PHT3D but not with PHAST. The model assumed first-order kinetics with respect to CE concentration and was extended with Monod terms to describe either oxygen inhibition of reductive dechlorination or oxygen dependent DCE and VC oxidation.

Second, the “microcosm” model was developed to simulate the microcosm experiment performed as part of this project. This model simulates TCE to ethene sequential reductive dechlorination and C/Cl/H isotope fractionation. The model is implemented in PHREEQC and application in 3-D PHAST is thus straightforward. The model simulated secondary Cl KIEs. The model was further extended with oxidative transformation of VC together with C and Cl isotope fractionation (see sample scenarios of degradation chains in section 6.5). The model simulates concentration-dependent Monod kinetics and optional lag phases for individual reactions, but does not accommodate oxygen dependent inhibition/promotion of reductive dechlorination/oxidation, respectively. However, oxidation of VC was added in Case 2 (see the User’s Guide) and degradation processes can be simulated for specific and fixed model domains. Note the models are not cast in stone and can be adjusted by an experienced user for specific needs and model parts can be exchanged. The results from 0-D modeling of the Demonstration Site data (Section 6) were obtained using the latter “microcosm” model.

2.3 ADVANTAGES AND LIMITATIONS OF THE TECHNOLOGY

Advantages of the technology. At many sites, CSIA data may be an important tool in attaining approval for monitored natural attenuation (MNA) remedies or as part of a demonstration of plume stability and control. The decision to implement an MNA remedy must be accompanied by quantitative support for mass removal and risk reduction, and achieving remediation goals within a reasonable time frame. CSIA is the only technology that is currently available that has the power to directly identify the effects of in-situ degradation on contaminant plumes through analysis of groundwater samples collected at standard monitoring points. CSIA provides a footprint of degradation (in the form of ^{13}C enrichment) which is specific of given contaminant of interest, unlike the traditional geochemical footprints utilized in MNA assessment.

Unlike CSIA, “traditional” technologies rely on indirect evidence, such as decreases in plume mass and the presence of degrading bacteria, or on limited direct evidence in the form of presence of recalcitrant daughter products. CSIA data are obtained by analysis of the isotope ratios in the contaminants of interest so that the evidence of degradation applies directly to the contaminant pool present at the study site. The primary advantages of CSIA for the assessment of chlorinated solvents sites can be itemized as follows:

- CSIA data are by definition “compound-specific”, directly applying to the analyzed contaminants of concern (COCs).
- CSIA evidence is independent from contaminant concentration data. CSIA evidence is not affected by contaminant dilution etc. so that the evidence of in-situ degradation is unequivocal.
- CSIA permits identification of degradation of a contaminant even in the absence of the specific degradation products.
- Isotope ratios of the cDCE and/or VC product can be used to determine if dechlorination stalls at those intermediates.
- Another advantage of CSIA is being able to distinguish different sources of parent material using isotopic signatures.

In comparison to “classic” interpretation of CSIA data, the combined use of CSIA-RTM approach has better potential to quantify the extent of contaminant mass attenuation and to resolve the contributions from different mechanisms of attenuation. In summary, CSIA and CSIA-RTM data can potentially expand MNA decision process. MNA remediation strategies often provide significant cost savings during long-term restoration of groundwater.

Limitations of the technology. Limitations can arise from physical parameters of the aquifer and from complications during chemical analysis. In MNA applications, the aim of CSIA is to detect the evidence of degradation. At certain sites, it is possible that certain sections of the plume were never impacted by degradation or the degradation occurred only in limited scale. Monitoring points intersecting heterogeneous aquifers can yield mixed samples dominated by groundwater parcels with undegraded contaminant. Some types of aquifer lithology are therefore inherently problematic for CSIA work, such as those with strong channelization of the flow (Lesser et al., 2008). CSIA of such samples would produce isotope ratio signatures dominated by the undegraded material. On one hand, increasing the effective sampling radius decreases the specificity of the CSIA data and spatially localized zones of degradation may be missed if the spatial resolution of sampling is not adequate. On the other hand, samples collected across a larger radius (e.g., a monitoring screened for a large depth interval) provide isotope signatures that are representative of average degradation applying to the remaining contaminant. Such data may be informative on the overall plume-wide mass attenuation (Mak et al., 2006). Consequently, the decision on whether or not to implement CSIA and the evidence likely to be obtained by CSIA should consider the site’s comprehensive hydrogeologic CSM. Complex hydrogeology can also be problematic for groundwater fate and transport modeling. Multiple source areas with original contaminants produced from multiple feed stocks may produce isotope signatures that are difficult to interpret. Sites where basic groundwater modeling is not productive may not benefit from reactive transport modeling using CSIA data.

The heterogeneity limitations were indeed encountered in this project. As discussed in detail in Section 6.5, the spatial patterns of isotope fractionation at the Demonstration Site suggested localized and irregular zones of reductive dechlorination, as opposed to 1st order kinetics that is conducive to reactive transport modeling.

Applicability of the proposed technology can be also limited by the difficulties in obtaining isotope data by CSIA. Two potential limitations are: 1) the analyte concentrations that are below current detection limits; and 2) interferences from excessive content of non-target VOCs present in the same samples. Routine CSIA methods permit analysis of C and Cl isotopes in the key CEs at concentrations as low as 1 µg/L (recent OU methodology), while H CSIA requires the TCE at concentration as low as 20 µg/L (recent OU methodology). In regards to handling non-target VOCs, one broad category of samples that may be difficult to handle are those with CEs commingled with fuel hydrocarbons (due to problems with GC resolution of the target CEs) or those where low µg/L concentrations of target CEs occur with high mg/L-level concentrations of other organics (such samples may require dilution prior to analysis, decreasing the effective detection limits).

Ongoing CSIA technology progress opens opportunities for analyzing samples formerly inaccessible to CSIA. One example is recent work on vapor intrusion CEs, where major improvement of GC resolution was obtained by the use of the so-called 2D-chromatography (ESTCP ER-201025, Technical Report). A potential user is advised to consult analytical service providers for up to date information on performance benchmarks of commercial CSIA services.

Finally, interpretation of field data can be hampered by the absence of published references, defining isotope effects to be expected for relevant degradation mechanisms. For example, as of today, no reference data exist to benchmark hydrogen isotope fractionation in CEs degradation. Therefore, the information potential of dual-element CSIA (C+H) remains unknown and unrealized in field studies.

3.0 PERFORMANCE OBJECTIVES

The overall objective of this project was to develop the CSIA+RTM approach to better interpret CSIA data collected at PCE and TCE plumes, to permit more specific and confident conclusions. The CSIA+RTM applications will ultimately assist in CSM development. The hypothesis of this technology demonstration is that the combined CSIA+RTM approach brings an added benefit relative to the traditional CSIA in contaminated site assessment, through identification of individual degradation mechanisms and permitting quantitative assessment of the progress of contaminant attenuation independently from the contaminant concentrations and the presence of diagnostic degradation products (the traditional non-CSIA approach) and independently from the constraints of the Rayleigh model of isotope fractionation (the classical approach in interpretation of field CSIA data). Quantitative and qualitative performance objectives are summarized in Table 3.1.

Table 3.1. Performance objectives

Performance Objective	Data Requirements	Success Criteria	Results
Quantitative Performance Objectives			
1. Optimize CSIA methods for C, H, Cl	Analyses for microcosm and field data	Isotope analysis results for concentrations of COCs above the MCLs	The performance objective was met. C, Cl and H CSIA methods were developed for this project
2. Adapt 1-D PHREEQC Model for H isotope enrichment	Microcosm data of sufficient quality and quantity	The model fits H CSIA observations and thereby gives information on isotope fractionation during the degradation steps and on the control of environmental conditions on the H CSIA values.	The performance objective was met. The model of H isotope fractionation was developed and calibrated to experimental data.
3. Calibrate 0/1-D geochemical model for C, Cl and H enrichment	Microcosm data of sufficient quality and quantity to calibrate model	1. C and Cl data confirm earlier model assumptions 2. H data sufficient to develop enrichment model (see above) 3. Model functions as a baseline geochemical model for anaerobic sequential decay	The performance objective was met. The model was accurate in simulation of the experimental data. The validated model serves as a baseline for applications in field data assessment.
4. Adapt model to 3-D in PHAST and PHT3D	1-D Model and microcosm data	Comparison of PHAST and PHT3D models give similar results as kind of benchmark validation; mass balances of all isotopes are met.	The performance objective was met. The model outputs of PHAST and PHT3D are almost identical in simulation of RD reductive dechlorination of TCE with oxidative degradation at the plume fringe.
5. Calibrate 2/3 D model with site – specific data	Data from field demonstration site	The model fits (concentration and CSIA data are close to the observation values) in most (75%) of the monitoring points.	The original performance objective was not met. The spatial complexity of the degradation zones at the site was too great to permit 2/3-D simulation. The redefined performance objective (validation of 0-D model) was met. The 0-D model provide informative evidence for understanding contaminant transformations.

6. Use CSIA/model technology to demonstrate the presence of multiple degradation pathways	Data from field demonstration site	As above; the model needs inclusion of multiple degradation pathways to explain field data.	The performance objective was met. Evidence of RD, oxidation and physical attenuation of CEs was identified.
7. Estimate degradation constants for COCs at demonstration site	CSIA/modeling results	Estimation of rate constants as result of model calibration. Comparison of model uncertainty with calibration using only concentration data vs. both concentration and CSIA data, to address the benefit of CSIA data.	The performance objective was met. The model permitted narrowing the uncertainty range of parameters used in rate determination, relative to the CSIA-only approach.
Qualitative Performance Objectives			
8. Develop a new framework for interpreting CSIA data	CSIA and modeling results	Develop a model that can be applied at different sites to <ul style="list-style-type: none"> visualize and interpret CSIA data, demonstrate the presence of degradation processes, predict future plume behavior and support remedial decision making. 	The performance objective was met. The framework for the use of the CSIA/model approach was presented in the User's Guide deliverable (ER-201029), published online in 2014.
9. Refine CSM for demonstration site	CSIA and modeling results	<ul style="list-style-type: none"> Comparison of CSIA-RTM modeling with alternative data processing options (CSIA-conventional Rayleigh model; RTM calibrated by concentrations only) Data sufficient to update CSM on the strength of attenuation mechanisms at various locations in the plume 	The performance objective was met. Adding the model-based interpretation of CSIA data helped to identify degradation pathways and advanced the accuracy of the biodegradation assessment.

3.1 PERFORMANCE OBJECTIVE 1: OPTIMIZE CSIA METHODS FOR C, H, Cl

As described in Section 5.1, the present technology demonstration required a field site data set, consisting of three element (C, Cl, H) isotope data of the parent CEs and the dechlorination products. At the outset of the project, existing in-house analytical methods at the University of Oklahoma were already available for analysis of C and Cl isotope ratios of CEs at low-ppb concentrations. No suitable method was available at OU or elsewhere, for analysis H isotope

ratios in chlorinated compounds at reasonable range of analyte concentrations. The focus of demonstration was the development of functional H CSIA methodology.

Data requirements

To provide a useful data set for the purpose of the contaminated site assessment, the isotope ratios obtained must be reliable. Method performance is determined by analysis of QAQC samples, as discussed in Section 5.6.

Success Criteria

There are two elements defining the success of the demonstration: 1) QAQC samples results conforming to established performance criteria in terms of the analytical error of the isotope ratios obtained; 2) detection limits of the methods (the minimum concentration of the target analyte sufficient to determine the isotope ratio) should permit analysis of the samples collected at the Demonstration Site.

Result

The performance objective was met. The data were obtained within stated QAQC goals (Section 6.1) The analytical method optimization status at the outset of the field sample analysis season (samples collected in 2011) was satisfactory, with effective detection limits for C and Cl CSIA at, or below, MCL of the contaminants of concern and the novel H CSIA permitting analysis of TCE and DCE at low tens of $\mu\text{g/L}$. Given relatively low concentrations of the contaminant in a number of monitoring wells at the Demonstration Site, further optimization was conducted prior to the 2014 sampling event, most significantly for Cl CSIA. Currently, Cl CSIA method permits determination of Cl isotope ratios in chlorinated ethenes at concentrations as low as $0.5 \mu\text{g/L}$.

3.2 PERFORMANCE OBJECTIVE 2: ADAPT 0/1-D PHREEQC MODEL FOR H ISOTOPE ENRICHMENT

At the outset of this project, no PHREEQC model was available to model of hydrogen isotope fractionation in RD. Moreover, existing results on hydrogen isotope fractionation in RD experiments were insufficient to propose mechanisms of hydrogen isotope fractionation in RD. Therefore, a controlled experiment (microcosm) was a prerequisite to the model development (the results from the microcosm study, including the proposed mechanism of H fractionation, have been described by Kuder et al., 2013). The present objective was the development of H isotope fractionation model, using the mechanistic insight from the RD experiment.

Data requirements

H isotope ratios were determined in the microcosm experiment, for TCE and the degradation products: cDCE, VC and ethene. The experimental data were used to propose a mechanism of H isotope fractionation to be then translated into the numerical model.

Success Criteria

The success of the present performance objective required microcosm data of sufficient quality (QAQC criteria identical as for Objective 3.1) and completeness to permit proposing a mechanistic scenario of hydrogen isotope fractionation in RD. The PHREEQC model should yield a good fit to the microcosm data.

ESTCP Final Report:

*Integrated Stable Isotope –
Reactive Transport Model Approach
for Assessment of Chlorinated
Solvent Degradation*

Result

The performance objective was met. The PHREEQC model of H isotope fractionation in reductive dechlorination was developed and tested by fitting to the experimental values of isotope ratios of TCE and reductive dechlorination products.

3.3 PERFORMANCE OBJECTIVE 3: CALIBRATE 0/1-D GEOCHEMICAL MODEL FOR C, CL AND H ENRICHMENT

After completing the H CSIA model development (Section 3.2), and extension of the Cl fractionation model to include secondary KIEs, a complete three-element isotope fractionation 0/1-D PHREEQC model was available. While examples of less comprehensive models (only C or Cl isotope fractionation) were described previously (Hunkeler et al., 2009), only the C isotope fractionation model was validated using experimental data. The focus of this objective is validation of the complete, three-element model.

Data requirements

C+Cl+H isotope data and concentrations of TCE and RD products from the microcosm experiment.

Success Criteria

The data quality criteria are identical as in Section 3.1. The PHREEQC model should yield a good fit to the microcosm data for the C, Cl, H isotope ratios and the concentrations of individual compounds. Good fit would confirm model assumptions.

Result

The performance objective was met. The PHREEQC model was accurate in simulation of the experimental data from the microcosm study. The validated 0/1-D model serves as a baseline for applications in field data assessment/modeling, for field sites where RD is part of the CSM.

3.4 PERFORMANCE OBJECTIVE 4: ADAPT MODEL TO 2/3-D IN PHAST AND PHT3D

The base model (PHREEQC) simulates transformations of reactants in 0/1-D and can only address longitudinal dispersion along the flow line. Therefore, attenuation of contaminant concentrations caused by transverse dispersion is not accounted for, except in the leading edge of the simulated plume. For more accurate representation of the overall concentration decreases, a 2/3-D transport model should be used. Two 2/3-D software platforms, PHAST and PHT3D were adopted to simulate the same set of reactions as PHREEQC.

Data requirements

The 2/3-D PHAST and PHT3D models that incorporate the developed PHREEQC model. The only difference with the PHREEQC model is that the 3-D models simulate 3-D groundwater flow and solute transport. The developed models were verified (benchmarked) through comparing the outputs from the two models. Benchmarking is a common approach to verify the validity of a complex reactive transport model (Steeff et al., 2015).

Success Criteria

ESTCP Final Report:

Integrated Stable Isotope –

Reactive Transport Model Approach

for Assessment of Chlorinated

Solvent Degradation

PHAST to PHT3D comparison (benchmarking) should yield identical results for the two models and the simulations should show closed mass balances for the C, Cl and H isotope ratios.

Result

The performance objective was met. Figures 6.4 and 6.5 illustrate that the model outputs of PHAST and PHT3D are almost identical in a scenario simulation of reductive dechlorination of TCE to ethene in the plume core with oxidative transformation of VC at the plume fringe. Small deviations in model outputs relate to the different numerical solution schemes for computing hydrodynamic dispersion.

3.5 PERFORMANCE OBJECTIVE 5: CALIBRATE 2/3-D MODEL WITH SITE-SPECIFIC DATA (REVISED: CALIBRATE 0-D MODEL WITH SITE-SPECIFIC DATA)

After software development and model validation using the microcosm experiment data (Sections 3.2 and 3.4), the model must be tested and validated using the field data collected from the Demonstration Site. In principle, a model including contaminant attenuation mechanisms included in the Demonstration Site's CSM should provide a reasonable fit of the simulated and field data (concentrations and the isotope ratios of the contaminants of concern).

The original proposal discussed using a 2/3-D model, i.e., validation of the 2/3-D PHAST and PHT3D software. That approach had to be revised after initial evaluation of the field CSIA data collected at the Demonstration Site, as described in detail in Section 6.5. In brief, mapping of the CSIA results suggested that the zones with isotope enrichments (indicating the location of degradation activity) were distributed irregularly over the two CEs plumes studied. Accordingly, the observed trends of isotope fractionation did not correlate to the distance from the plume source, the distance across the plume fringe or to the groundwater age. The observed data distribution was therefore inconsistent with the 1st order and the fringe degradation scenarios (cf. Figure 3-13 in the User's Guide; ESTCP ER-201029, User's Guide). Since no meaningful trends of isotope fractionation could be identified along 1-D flow lines, the exercise of 1/2/3-D modeling would be meaningless.

Instead, the modeling was conducted using the batch (0-D) mode of the 0/1-D PHREEQC software. Spatial and temporal dimensions were thus not explicitly simulated. Even so, the modeling still permitted: (i) a reduction of uncertainties in identification of specific degradation pathways; and (ii) more accurate identification of the range of enrichment factors for C, Cl, and H. The information obtained enabled a quantitative assessment of contaminant degradation using the classic Rayleigh model approach (see Section 6.7).

Data requirements

This performance objective required determination of the concentrations and the isotope ratios of the contaminants occurring at the Demonstration Site. The field data were initially processed following conventional CSIA evaluation protocols, to better understand the processes responsible for contaminant attenuation at the site and to revise the existing CSM, if necessary. The CSIA data were used to identify potential attenuation mechanisms active at the site and to better understand the spatial distribution of the degradation activity. The modeling was then performed for the attenuation scenarios consistent with the revised version of the CSM.

ESTCP Final Report:

Integrated Stable Isotope –

Reactive Transport Model Approach

for Assessment of Chlorinated

Solvent Degradation

Typically, alternative CSM scenarios must be tested to identify those most consistent with the field data.

Success Criteria

The success criterion for model validation is that the model exhibits a reasonable fit to the field data. In practice, determination of objective numerical criteria of what constitutes a reasonable fit is difficult. While reactive transport model output provides quantitative parameters (e.g., reaction rates, for 1,2,3-D models), the practice of reactive transport model validation (in peer reviewed literature and in environmental applications) tends to stress qualitative or semi-quantitative criteria, such as the ability to simulate average well heads and flow directions and historical trends in contaminant concentrations. For a 0-D model, direct comparison of contaminant concentrations and the reaction rates is not possible. Instead, the field-to-model comparison could be made using molar fractions of the individual contaminants, the isotope ratios and the dual-CSIA slopes. Finally, there is a qualitative element of the validation, in the sense of the model yielding information useful for site's CSM development. Such information may include a more robust evidence for degradation mechanisms (Section 3.6) or better constrained degradation rate constants (Section 3.7) in comparison with the conclusions from standard evaluation of CSIA data.

Result

The original performance objective was not met. The spatial complexity of the degradation zones at the site was too great to permit 2/3-D simulation, as indicated in the opening paragraphs of Section 3.5. The redefined performance objective (validation of 0-D model) was met. The 0-D model provided informative evidence for understanding contaminant transformations.

3.6 PERFORMANCE OBJECTIVE 6: USE CSIA/MODEL TECHNOLOGY TO DEMONSTRATE THE PRESENCE OF MULTIPLE DEGRADATION PATHWAYS

This performance objective is an element of the model validation, and it specifically addresses the CSIA/model utility in identification of the degradation mechanisms, or, in more general sense, attenuation occurring through degradative and non-degradative mechanisms. Identification of the degradation/attenuation mechanism is valuable in assessing the fate of the contaminants of concern and in the design and management of site remediation.

Data requirements

Data requirements are identical to those described in Section 3.5.

Success Criteria

The mechanism identification is achieved as follows:

- Dual-element CSIA trends in the field data sets are examined. The trends in field samples are compared to reference data on various attenuation mechanisms to identify similarities.
- Modeling is conducted for the degradation scenarios, for specific mechanisms or a combination of various mechanisms. A good fit of the model to field data confirms the scenario's assumptions.

Dual-element CSIA trends for the field samples should be consistent with those produced in known attenuation mechanisms, and the CSIA data alone should be sufficient to propose viable

ESTCP Final Report:

Integrated Stable Isotope –

Reactive Transport Model Approach

for Assessment of Chlorinated

Solvent Degradation

attenuation scenarios that can be further tested by modeling. Similarly to the success criteria in Section 3.5, the model should exhibit a reasonable fit to the field data. The comparison of the results for different scenarios tested should permit identification of the likely scenario(s) and elimination of unlikely scenarios.

Result

The performance objective was met. Both subunits of the Demonstration Site exhibited evidence of reductive dechlorination of PCE and TCE and of an additional process responsible for partial removal of the reductive dechlorination products (likely, aerobic biodegradation). Moreover, evidence of significant TCE mass attenuation by diffusion out of the mobile dissolved phase was observed.

3.7 PERFORMANCE OBJECTIVE 7: ESTIMATE DEGRADATION CONSTANTS FOR CONTAMINANTS OF CONCERN AT DEMONSTRATION SITE

This performance objective is an element of the model validation, and it specifically addresses the CSIA/model utility for constraining the rates of degradation. In 0-D modeling, the reaction rates are not obtained directly from the simulation (as the rate constants used in the model) but have to be determined indirectly using the estimates of the isotope fractionation factors obtained through the 0-D modeling and the available groundwater age (tritium-helium) data.

Data requirements

Data requirements are identical to those described in Section 3.5. In addition, an estimate of contamination age is necessary, either from site's historical data or by groundwater dating. Groundwater age (tritium-helium) data were collected previously by Hill AFB (CH2MHILL, 2011).

Success Criteria

The CSIA + model yield degradation rates with lower uncertainty margin than the CSIA alone.

Result

The performance objective was met. Model fitting permitted narrowing the uncertainty range of parameters used in rate determination, relative to the CSIA-only approach.

3.8 PERFORMANCE OBJECTIVE 8: DEVELOP A NEW FRAMEWORK FOR INTERPRETING CSIA DATA

The performance objective was met. The framework for the use of the CSIA/model approach was presented in the User's Guide deliverable (ER-201029), published online in 2014. The model templates (Cases 1-4, described in the User's Guide and available for download) can be tailored to the site specific conditions for future applications.

3.9 PERFORMANCE OBJECTIVE 9: REFINE CSM FOR DEMONSTRATION SITE

The objective of the CSIA/model implementation is ultimately to assist in the development or refinement of CSM for the Demonstration Site.

Data requirements

ESTCP Final Report:

*Integrated Stable Isotope –
Reactive Transport Model Approach
for Assessment of Chlorinated
Solvent Degradation*

Complete data and interpretation results from the CSIA/model implementation at the Demonstration Site

Success Criteria

Comparison of CSIA/model results with the alternative data processing options (CSIA-conventional Rayleigh model; RTM calibrated by concentrations only).

Result

The performance objective was met. Adding the model-based interpretation of CSIA data advanced the accuracy of the contaminant attenuation assessment.

4.0 SITE DESCRIPTION

4.1 SITE LOCATION AND HISTORY

The demonstration site is Hill Air Force Base Operable Unit 10 (OU10), located in northern Utah, approximately 25 miles north of Salt Lake City. Figure 4.1 illustrates the site location, the extent of groundwater contamination and the monitoring well locations. OU10 encompasses the Building 1200 Area along the western boundary of Hill AFB and extends off-base into the cities of Clearfield, Sunset, and Clinton. Aircraft/vehicle maintenance activities at Building 1200 Area began in approximately 1940 and continued through 1959, at which point the building complex was converted to administrative offices. Chlorinated solvents were released in 1940-1959.

The primary COCs at OU10 are TCE, cis-1,2-DCE and PCE. Two primary sources of contamination have been identified. PCE was probably spilled incidentally on a parking lot the parking lot west of Building 1274. The TCE plume originated from the continuous releases from an oil/water separator at the north end of Building 1244 (CH2MHILL, 2009).

An extensive groundwater monitoring well network which includes over 100 piezometers and monitoring wells form the basis of the data collection system and allow for the high-density sample collection that is required for an accurate application of CSIA technology (CH2MHILL, 2009). Hill AFB also utilizes Barcad® technology for many of the wells at OU10. Barcad wells permit obtaining multiple samples from discrete intervals within the same borehole. Site monitoring began in 1995 with semiannual sampling since 2002. Active remedies at the OU10 included soil excavation in the area of the oil/water separator, in 2003. In 2007, an Enhanced Reductive Dechlorination (ERD) treatment was tested in an area of high dissolved TCE (approximately 900 m to 1000 m away from the assumed source area).

4.2 SITE GEOLOGY/HYDROGEOLOGY

The subsurface lithology is characterized by detailed cross-sections and soil profiles (Figures 4.2 and 4.3; the lithology recorded for individual monitoring wells samples in this study is shown in Figure 4.3) (CH2MHILL, 2009). The subsurface consists of two saturated units (Unit A and Unit C) separated by an aquitard (Unit B). Below Unit C, a thick aquitard (Unit D) prevents further

ESTCP Final Report:

Integrated Stable Isotope –

Reactive Transport Model Approach

for Assessment of Chlorinated

Solvent Degradation

downwards migration of pollutants. Units A and C consist of sand (fine- to medium-grained) and silt, with moderate to high permeability. Groundwater velocities were determined previously, using slug or pump tests and groundwater dating (CH2MHILL, 2009). In Unit A, average groundwater flow velocity is about 0.15 m/d. The calculated retardation factors for PCE, TCE, c-DCE, and t-DCE, are relatively low (≤ 3.1 , 1.7, 1.6, and 2.0, respectively), due to the low organic carbon content (0.03 % in sand; 0.07 % in silty sand). In Unit C, the groundwater velocity decreases abruptly between the easternmost area (0.58 m/d), where the sand layers are thin and interbedded with clay layers, and the western area (0.18 m/d), where the sand packages are thicker. The organic carbon content of Unit C is higher (0.2 %), resulting with higher sorption and higher retardation factors (TCE migrates at half the rate of DCE).

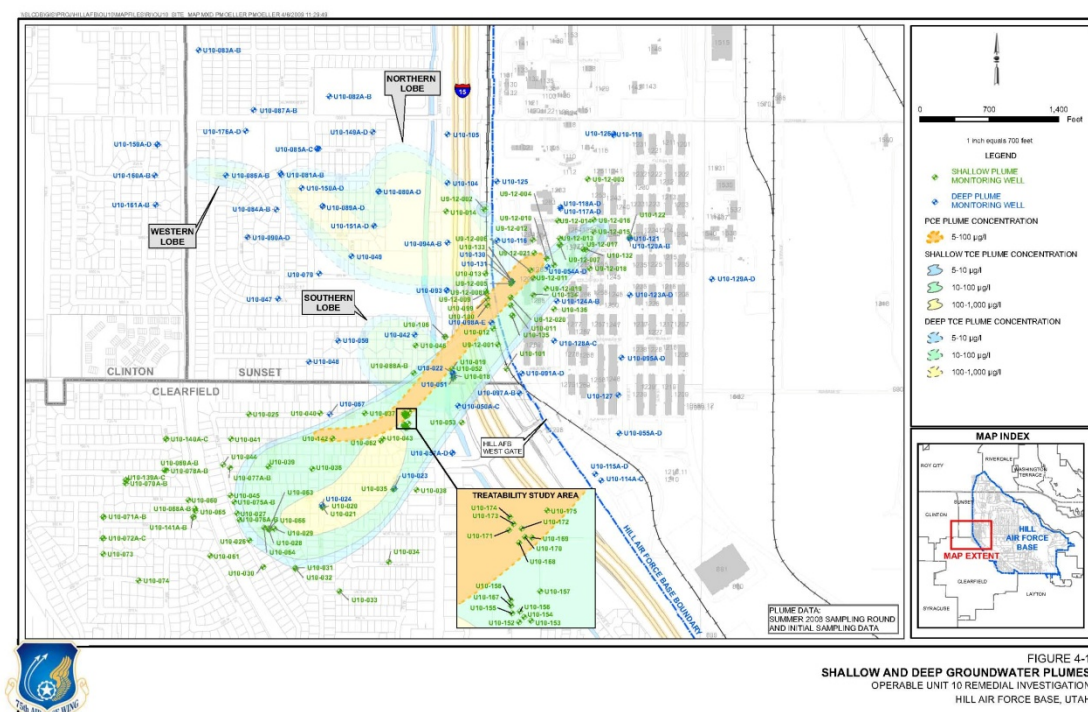


Figure 4.1. Hill AFB OU10 site location.

Redox Conditions and Microbiology. The site exhibits significant variability of redox conditions (CH2MHILL, 2009). Based on dissolved O_2 , nitrate and sulfate levels, Unit A was classified as overall oxic, while Units B and C were classified as mildly reducing. Detections of methane in some wells in Unit C indicated methanogenic conditions, while other wells in Unit C showed high nitrate. In Unit A, aerobic cometabolic CEs degraders were identified. Aerobic methanotrophs (potentially capable of CEs cometabolism) were also detected in the Lower Zone (CH2MHILL, 2009). In the Lower Zone, RD bacteria *Desulfuromonas* and *Dehalobacter* have been identified. On the other hand, DO and ORP levels in Units B and C were high, suggesting a potential for aerobic biodegradation, probably in the mobile porosity.

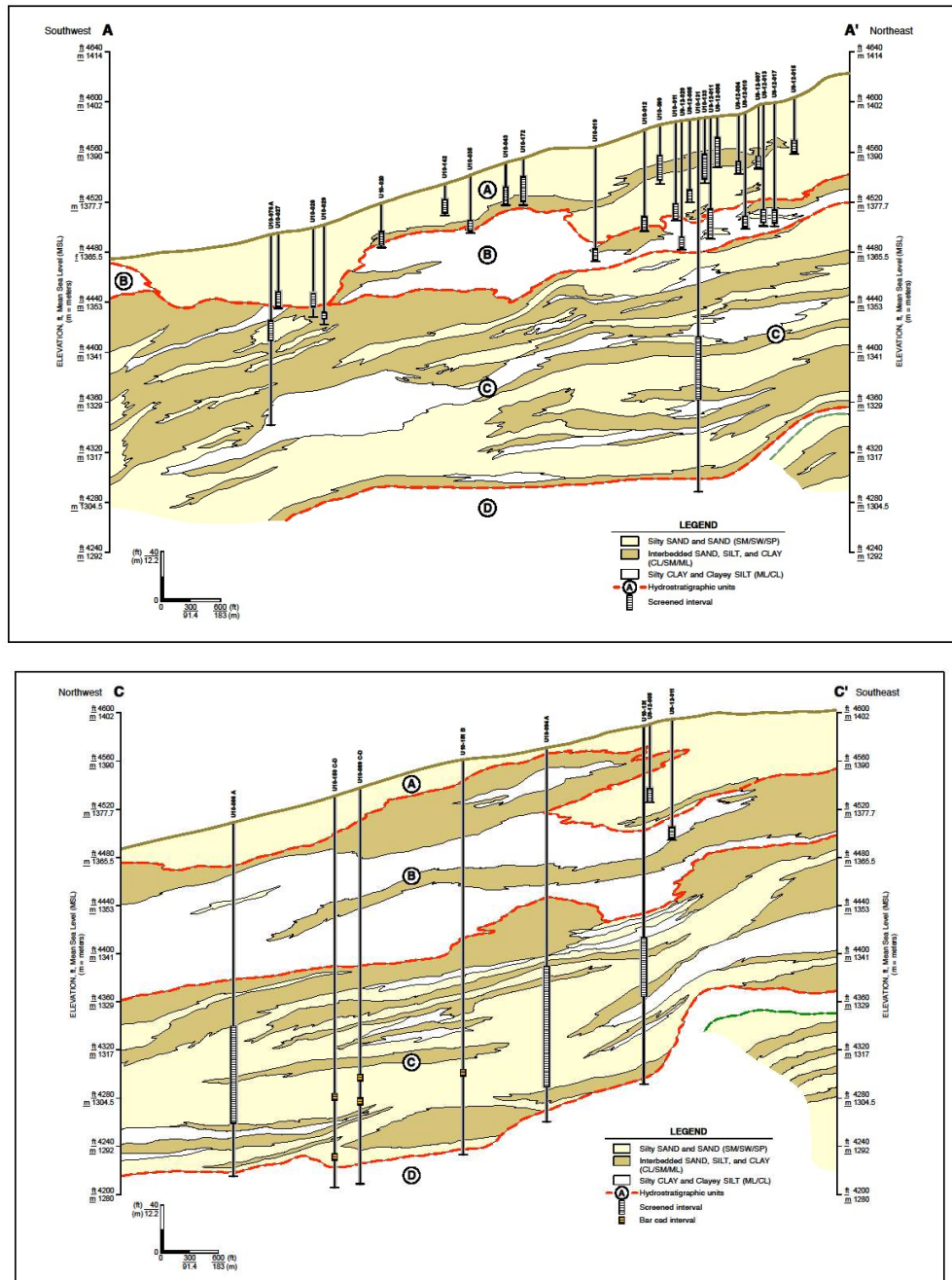


Figure 4.2. Cross-sections of the aquifer. NE-SW transect (top) and SE-NW transect (bottom) (CH2MHILL, 2009)

4.3 CONTAMINANT DISTRIBUTION

Two primary sources of contamination have been identified. TCE was spilled continuously over an extended period of time, from an oil/water separator (CH2MHILL, 2009). The resulting contaminant plume extends from the source area to the SW and off-base (Figure 4.1). PCE was probably spilled incidentally on the parking lot west of Building 1274, and the PCE occurrences are limited to the shallow Unit A.

In Unit A, the Shallow TCE Plume travels along the surface of the aquitard (Unit B). The plume is thin (6 - 12 m), 90-425 m wide, and has traveled approximately 1,500 m southwest from the source, across the Hill AFB boundary and underneath a residential area. PCE travels to the SW close to the groundwater surface and partially mixes with the Shallow TCE Plume.

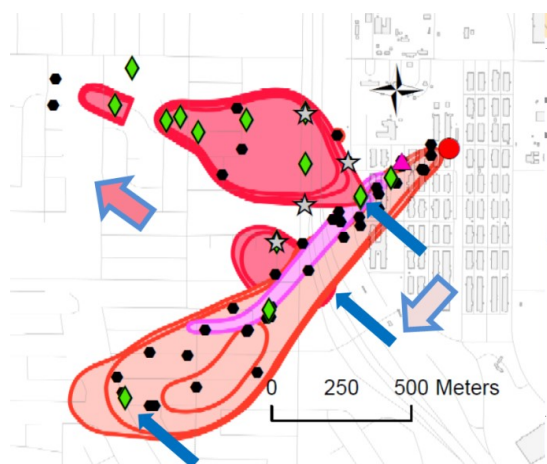


Figure 4.4. Map of the Operable Unit (OU) 10. Shown are the shallow PCE plume (purple), the Shallow TCE Plume beneath (pink), and the Deep TCE Plume (red). The groundwater flow directions are indicated by large arrows. The black dots represent the wells sampled for CSIA. The estimated spill locations are indicated by a purple triangle (PCE) and a red circle (TCE). The blue arrows indicate the leakage areas connecting the Shallow with the Deep Plume. The green diamonds indicate wells where either VC or ethene

The Unit B aquitard is entirely eroded in some areas and leakage from Unit A to Unit C leads to formation of the Deep TCE Plume in Unit C (Figure 4.4), moving to the northwest, between 53 m and 88 m BGS. Locally, TCE is also detected in wells screened within Unit B. The Deep TCE Plume includes Northern and Southern Lobes. The Northern Lobe is 425 m wide at its maximum, and 800 m long. The Southern Lobe is 245 m wide and 425 m long.

The original TCE source is likely exhausted, as DNAPL was not detected in the probable source area during site investigations, and since the present CE concentrations are low in the source zone. The highest TCE concentrations in the Shallow Plume are located 900-1300 m downgradient from the source zone, which also suggests that the source is depleted. Consequently, the water flowing into Unit C to form the upgradient part of the Deep Plume is

ESTCP Final Report:

Integrated Stable Isotope –

Reactive Transport Model Approach

for Assessment of Chlorinated

Solvent Degradation

less polluted today than in the past, as suggested by the decreasing concentrations in well U10-131, at the junction between the Shallow Plume and the northern lobe of the Deep Plume (CH2MHILL, 2009).

The observed RD products are mostly cis-DCE and, at lower concentrations, trans-DCE. DCE species are present locally in the Shallow Plume, mostly in wells screened in or near Unit B. DCE species are present in nearly all samples collected at the Deep Plume. Low concentrations of VC, ethene and ethane were observed historically and in the 2011 samples, in several wells screened in Units B and C (Figure 4.4).

5.0 TEST DESIGN

5.1 CONCEPTUAL EXPERIMENTAL DESIGN

The broad objective of this project was to develop groundwater modeling tools and approaches to better interpret CSIA data collected from PCE and TCE plumes, to assist site managers in the integration of CSIA evidence into remediation efforts. Accurate interpretation of CSIA data has the potential to quantify and predict mass destruction of contaminants by multiple mechanisms. Better estimates of mass attenuation mechanisms can be used to demonstrate progress toward remedial goals and predict the life-span of contaminant plumes.

The experimental design for this project consisted of three main components:

- 1) Initial development and calibration of the modeling software, including a calibration of the initial model (PHREEQC) with the CSIA data from a laboratory microcosm.
- 2) Application of the developed model for evaluation of chlorinated ethenes attenuation at the Demonstration Site.
- 3) An assessment of the added benefit of the CSIA/model approach in evaluation of chlorinated ethenes sites.

Software development and initial calibration

1. The PHREEQC model existing at the outset of the project was extended and calibrated for simulation of carbon, chlorine and hydrogen isotope fractionation in reductive chlorination of TCE. The calibration used an experimental data set (a microcosm study, described in Section 5.3).
2. The base model (0/1-D PHREEQC) was integrated into 2/3-D model software platforms, PHAST and PHT3D, which were adopted to simulate the same set of reactions as the PHREEQC.
3. After the software development and initial calibration with the laboratory study data, the next stage was an application using field data from the Demonstration Site.

Field-scale application of the model

1. Field Data Collection: Groundwater samples for CSIA were collected at high spatial density from the Demonstration Site. CSIA and concentration analysis of the samples provided the field data set for the validation of the model.
2. The main data set was obtained in the second half of 2011. Additional samples were collected and analyzed in 2014, to close gaps in the 2011 data.
3. The field data were evaluated (conventional, “classical” CSIA data evaluation) in combination with existing CSM of the Demonstration Site, to identify alternative attenuation scenarios to be tested by the model. For example, a scenario of cDCE stall can be compared to a scenario where cDCE degrades in aerobic cometabolism.
4. The modeling approach was revised. The originally planned 2/3-D modeling was impossible due to the spatial heterogeneity of degradation at the site. The modeling was conducted using 0-D dimensionality.
5. Scenarios identified in the preliminary data assessment were tested, using the 0-D modeling approach. The output of the model (fit of the model to the field data) served to validate or disqualify the proposed scenarios.

Assessment of the added benefit of the CSIA/model approach

1. The information from the “classic” CSIA and from the CSIA/model approach was used to advance the existing CSM.
2. The information from the CSIA/model approach was compared to the following: (i) contaminant concentration model (Buscheck-Alcantar model of the site, available from the Hill AFB; (ii) “classic” CSIA (no model-based scenario testing), utilizing the full data set at full spatial resolution; (iii) former “classic” CSIA utilizing a limited data set, included in the CSM report of the site (CH2MHILL, 2009).

5.2 BASELINE CHARACTERIZATION

Selection of the Demonstration Site was based on existing site characterization data (CH2MHILL, 2009). Since this project did not involve actual activities of contaminant remediation and comparison of before-after the treatment, baseline characterization *sensu stricto* was not required.

5.3 LABORATORY STUDY RESULTS

A laboratory study was conducted, to facilitate the development and calibration of the modeling software (see Sections 3.2 and 3.3). The complete results from the study have been published in the form of a peer-reviewed paper (Kuder, T.; van Breukelen, B. M.; Vanderford, M.; Philp, P., *3D-CSIA: Carbon, Chlorine, and Hydrogen Isotope Fractionation in Transformation of TCE to Ethene by a Dehalococcoides Culture. Environmental Science and Technology* 2013, 47, 9668–9677). In summary, the study was a microcosm experiment on dechlorination of TCE to ethene by Bio-Dechlor Inoculum (BDI) bacterial culture, a consortium of *Dehalococcoides* species

(Liang et al., 2007). The C isotope effects observed for the RD steps were consistent with data published in the past for *Dehalococcoides*. A somewhat unexpected result was the observation that daughter compounds (DCE and VC) were depleted in the heavy ^{37}Cl isotope. That depletion implied that isotope fractionation occurred not only at the C-Cl bond undergoing dechlorination, but also at the nominally inert Cl positions (so-called secondary KIEs). The implication of the latter was the need to modify the Cl fractionation model, to include isotope effect contributions from all Cl positions of the reacting molecules.

An assessment of H isotope effect was the first of its kind, due to recent availability of the H CSIA analytical technique. The observed isotope effect in TCE degradation was opposite to the typical enrichment of the heavy isotope. Instead, the H isotope ratios of TCE became depleted in ^2H over the progress of biodegradation. The H isotope ratios of the degradation products showed very significant preference for incorporation of the light ^1H isotope as discussed in the following paragraph. The published paper also attempted to advance the understanding of the mechanism of RD employed by *Dehalococcoides*. The latter issue is peripheral to this demonstration.

Mechanistic model of hydrogen isotope fractionation in RD

The results described in the following paragraph were used to develop the principles of the H isotope fractionation model (Section 3.2 and 6.2). The following is cited after Kuder et al. (2013). As determined in the laboratory study, reductive dechlorination of TCE by a *Dehalococcoides* culture led to RD products that were significantly depleted in ^2H relative to their CE precursors (Figure 6.2). The initial $\delta^2\text{H}$ of TCE was +530 ‰. The values of $\delta^2\text{H}$ in the progressively dechlorinated products decreased, to -270 ‰ for ethene. RD involves protonation of the precursor CE (Figure 6.1). The $\delta^2\text{H}$ of the newly added hydrogen atom ($\delta^2\text{H}_{\text{addition}}$) of the daughter CEs can be obtained by Equation 4, where n is the number of hydrogen atoms in a given daughter product. In the equation, the “bulk” $\delta^2\text{H}$ refers to average $\delta^2\text{H}$ of parent and daughter compounds, e.g., TCE and cDCE, respectively. Equation 4 assumes that the protonation conserves the isotope ratios of the hydrogen inherited from the parent CEs and that CEs do not undergo hydrogen isotope exchange while residing in the environment.

$$\delta^2\text{H}_{\text{addition}} = n \times \delta^2\text{H}_{\text{daughter-bulk}} - (n-1) \times \delta^2\text{H}_{\text{parent-bulk}} \quad (\text{Eq. 4})$$

The values of $\delta^2\text{H}_{\text{addition}}$ decreased from -150 ‰ (transformation of TCE to cDCE), to -650 ‰ (cDCE to VC) to -770 ‰ (VC to ethene) and were strongly depleted relative to the microcosm water ($\delta^2\text{H}$ of -42 ‰). *Dehalococcoides* species require molecular hydrogen as the immediate electron donor. In the microcosm, H_2 was produced by fermentation of lactate. It was previously reported that H_2 and water undergo fast isotope equilibration in the presence of active hydrogenases, resulting in a major depletion of the ^2H of the hydrogen pool. Therefore, it is proposed that $\delta^2\text{H}$ of the RD product is ultimately controlled by the $\delta^2\text{H}$ of the water medium, with superimposed depletion upon $\text{H}_2/\text{H}_2\text{O}$ equilibrium rather than being tied to the H isotope composition of the fermentation substrate (see Kuder et al., 2013 for more information).

Table 5.1. Bulk isotope effects for individual RD transformation steps*

RD step	ϵ (‰)	$\epsilon_{\text{Cl}}/\epsilon_{\text{C}}$
• TCE to cDCE	$\epsilon_{\text{C}} = -16.4 \pm 0.4$ $\epsilon_{\text{C}} = -15.3$ $\epsilon_{\text{Cl}} = -3.6 \pm 0.3$ $\epsilon_{\text{Cl-A,B}} = -3.3$ $\epsilon_{\text{H}} = +34 \pm 11$	0.21 ± 0.2
• cDCE to VC	$\epsilon_{\text{C}} = -26.8$ $ \epsilon_{\text{Cl}} < -3.2 $ $\epsilon_{\text{Cl,VC}} = -1.7$	< 0.12
• VC to ethene	$\epsilon_{\text{C}} = -26.7 \pm 1.9$ $\epsilon_{\text{C}} = -28.1$ $\epsilon_{\text{Cl}} = -2.7 \pm 0.4$	0.10 ± 0.1

* See Kuder et al. (2013) for detailed explanation of how these values were obtained. See Figure 5.1 for graphic presentation of the trends of isotope fractionation in the microcosm experiment.

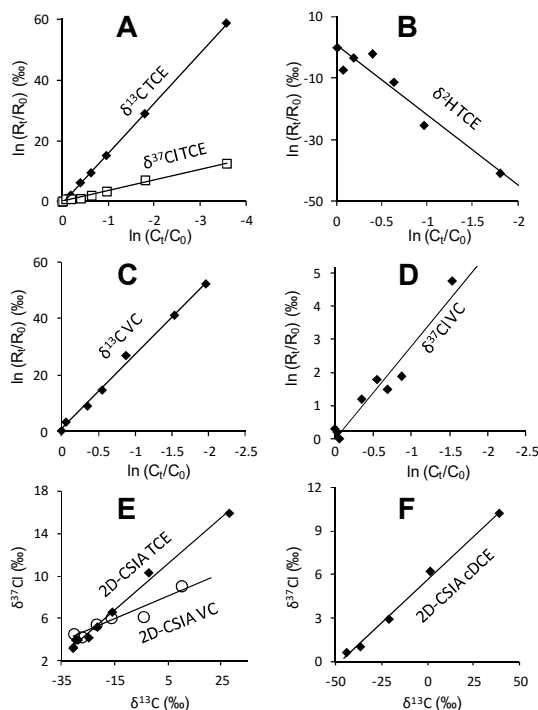


Figure 5.1 Rayleigh-type and 2D-CSIA plots for TCE, cDCE, and VC. After Kuder et al., 2013. Calibrated PHREEQC yielded best model-data fit for enrichment factors very similar to those obtained independently in using the Rayleigh approach and listed in Table 5.1.

5.4 DESIGN AND LAYOUT OF TECHNOLOGY COMPONENTS

The project does not require extensive new design components. Technical summary of the non-standard CSIA methods are summarized in Section 5.6. The technical details of setup and operation of the modeling software were described previously in the User's Guide (ESTCP ER-201029, User's Guide).

5.5 FIELD TESTING

The project did not involve field activities other than collection of groundwater samples for CSIA. The sampling techniques are identical to those applies in routine MNA application. Further sampling information is provided in Section 5.6.

5.6 SAMPLING and ANALYSIS METHODS

Groundwater sample collection

Groundwater sampling was conducted through a subcontract with the Hill AFB contractor, AEEC. Groundwater was collected from existing monitoring wells by a variety of methods, specific to the well type and construction. Sample volumes required for CSIA are higher than those collected in routine MNA work. For this project, approximately 500 mL of groundwater was collected from each location to allow enough material to potentially determine isotope ratios of C, Cl and H in several target compounds. Because of the variety of wells and sampling methods used on site (BarCad, low flow, permeable diffusion bags), and the spatial distribution of wells, it was determined that contracting with the base contractor was the most efficient sample collection strategy. AEEC's SAP and Health and Safety Plan for Hill AFB OU10 were followed for sample collection. A low-flow sampling method was used for most wells. For low-flow sampling, field instruments were used to continuously monitor physical parameters such as pH, dissolved oxygen and conductivity.

Wells with longer screens were sampled using passive diffusion bags (PDBs). Because of the higher sample volumes required for CSIA, 750 mL PDBs were used. PDBs were placed in the well at depths corresponding to the 2-3 ft interval with highest concentrations (see Tables D1 and D2 for the screen depths). PDBs were allowed to equilibrate with groundwater between 1 and 2 weeks prior to sample collection. PDBs were retrieved and poured into sample vials for shipment. Hill OU10 has several wells with BarCad sampling ports. These wells were sampled according to the AEEC site SAP. Variety in sampling methods is not anticipated to introduce artifacts into CSIA results.

Samples collected by AEEC on site were shipped under chain of custody to U of O (Appendix E). Each sample consisted of approximately twelve 40 mL VOA bottles with 0.2 mL of sulfuric acid (H_2SO_4 , pH < 2) as a preservative. Samples were maintained at 4°C in coolers prior to and during shipment. Concentrations of the CEs were analyzed within two weeks of shipment. One trip blank, for VOC analysis, was collected per sample cooler.

ESTCP Final Report:

Integrated Stable Isotope –

Reactive Transport Model Approach

for Assessment of Chlorinated

Solvent Degradation

QAQC samples: Field duplicates were collected at the rate of 1 duplicate per every 10 samples collected. Field duplicates were prepared and analyzed alongside the primary sample to determine the precision for the field sampling program (Appendix D).

Laboratory Analytical Methods

Table 5.2 summarizes the analytical methods used in this project.

VOC concentrations in groundwater were determined using a modified EPA Method 8260 at U of O, prior to CSIA analysis. In-house analysis, if possible, is the preferred option in CSIA work, because examination of full scan GCMS data helps to detect potential problems with GC resolution. On the other hand, chromatographic interferences from non-target compounds are not easily predicted if only a standard Method 8260 report is available.

Table 5.2. Analytical methods for sample analysis

Matrix	Analyte	Method	Container	Preservative	Holding Time
Groundwater	Chlorinated ethenes	8260 ¹	VOA	H ₂ SO ₄ , 4°C	2 weeks
	C Isotope ratios	C CSIA ²	VOA	H ₂ SO ₄ , 4°C	n/a ³
	Cl Isotope ratios	Cl CSIA ²	VOA	H ₂ SO ₄ , 4°C	n/a ³
	H Isotope ratios	Cl CSIA ²	VOA	H ₂ SO ₄ , 4°C	n/a ³
Microcosm water	Chlorinated ethenes	8260 ¹			Analyzed immediately
	C Isotope ratios	C CSIA ²	VOA	H ₂ SO ₄ , 4°C	n/a ³
	Cl Isotope ratios	Cl CSIA ²	VOA	H ₂ SO ₄ , 4°C	n/a ³
	H Isotope ratios	Cl CSIA ²	VOA	H ₂ SO ₄ , 4°C	n/a ³

¹ Modified analytical protocol described in Section 5.6

² In-house analytical CSIA protocols described in Section 5.6

³ Preserved (pH <2, 4°C) CE samples can be analyzed for their isotope ratios after as much as several months of storage.

The following paragraph is a GCMS method description for VOCs concentration determination, modified after the publication on the laboratory study of this project (Kuder et al., 2013). Analysis of CEs and ethene concentrations was performed by purge and trap (model 4660 by OI Analytical, College Station, US) combined with GC/MS (GC/MS model 7890/5975, Agilent, Santa Clara, USA). The purge and trap was fitted with a custom-order adsorbent trap (Supelco, Bellefonte, USA) with 8 cm bed of Carbopack B and 16 cm bed of Carbosieve S-III to permit satisfactory retention of ethene and VC. The GC column was PoraPLOT-Q (Agilent), 25 m x 0.32 mm. Control samples for concentration analysis were prepared immediately prior to analysis from concentrated aqueous stock solutions and analyzed at least daily (see the following section for description of the standards). Analytical uncertainty for each of the analytes was determined from a 4-point calibration line (0.3-40 µg/l). The low end of the calibration range was met by using a custom cryofocusing interface between the purge and trap and the GC/MS, which permitted splitless transfer of the sample in the detector. Samples where the concentrations were above the calibration limit were reanalyzed after dilution. The chlorinated hydrocarbons concentration measurements were associated with uncertainty of $\pm 7\%$. For ethene, the error was $\pm 15\%$.

The CSIA laboratory methods do not require additional sample pretreatment except extraction of VOCs by purge and trap (PT). Similar to the standard USEPA SW846 methods, VOCs recovered by PT are separated by gas chromatography (GC). C and H isotope analyses involve post-separation thermal conversion of individual compounds to CO₂ or H₂, respectively, occurring without losing chromatographic separation between individual compound peaks. The conversion is followed by analysis by IRMS. The CI CSIA method utilizes conventional GC/MS equipment and the analytical protocol has been adopted and Sakaguchi-Soder et al. (2007). In the CI method, the MS is operated in single ion mode, scanning for the molecular ions characteristic of the target analyte with and without ³⁷Cl, respectively.

The following paragraphs give a CSIA description, modified after the publication on the laboratory study of this project (Kuder et al., 2013). CSIA was performed using a combination of a purge and trap (OI Analytical 4660) with a GC and a detector appropriate for given element isotope ratio. An isotope-ratio mass spectrometer was used for C and H CSIA (Agilent 6890 GC with a Thermo-Finnigan MAT 252 for C CSIA or a Thermo-Finnigan Delta XL for C and H CSIA; Thermo-Finnigan, Bremen, Germany). CI CSIA was performed on the GC/MS instrument described above. The analytical protocol for C CSIA of TCE and cDCE was similar to that described in the past (Kuder et al., 2009). For VC and ethene, the method used the Carbosieve S-III trap and the Q-Plot GC column, similar as in the concentration analysis. The GCMS-based CI CSIA method is described in more detail by McHugh et al. (McHugh et al., 2011). H CSIA was performed using a custom chromium metal reactor for conversion of the CEs and/or ethene to H₂ (Kuder and Philp, 2013). The purge and trap peripherals and the GC were identical to those in C CSIA

For all CSIA methods, the performance of the instruments was validated daily, by analysis of the target analytes of known isotope composition (lab control samples; see the following section for the description of the CSIA standards used), following identical procedures as those applied to the microcosm samples. Raw output of H CSIA required an accuracy correction (Kuder and Philp, 2013). No $\delta^2\text{H}$ standard was available for VC; consequently, the correction for raw VC

was based on the average of corrections cDCE and TCE. Based on the performance of the daily standards, the analytical uncertainty of C CSIA was $\pm 0.5\%$. For Cl CSIA of TCE and VC, the uncertainty was $\pm 0.8\%$, whereas for cDCE it was $\pm 1.0\%$ or better. The uncertainty of H CSIA was $\pm 15\%$.

CSIA and GC/MS reference standards. For the analyte concentration analysis, a commercial chlorinated VOCs mixture (QTM Volatile Halocarbons Mix) was obtained from Sigma-Aldrich (St. Louis, MO, USA) and diluted in water to 2500 $\mu\text{g/l}$. A tank of compressed ethene (UHP grade) was obtained from Airgas, Inc (Tulsa, OK, USA). Ethene was injected into a headspace-free serum bottle filled with water to obtain a concentration of 700 $\mu\text{g/l}$. The aqueous stock solutions were used to prepare daily standards for purge and trap-GC/MS analysis.

For C CSIA, ethene (the same as above), VC (1000 ppmv in nitrogen, a commercial standard from Scott Specialty Gases, Plumsteadville, PA, USA), cDCE and TCE (ACS grade, Sigma-Aldrich) were used. The values of the $\delta^{13}\text{C}$ of ethene, cDCE, and TCE were obtained by off-line conversion to CO_2 and analysis by dual-inlet IRMS. The value of $\delta^{13}\text{C}$ of VC was obtained by direct injection of the 1000 ppmv standard into the GC-IRMS. While no independent VC standard was available to verify that the obtained VPDB values were accurate, the same GC-IRMS instrument produced accurate $\delta^{13}\text{C}$ results for direct injection of methane, ethane, ethene, cDCE and TCE. For Cl CSIA, the standards were calibrated to SMOC by analysis of pure cDCE and TCE (Sigma-Aldrich) and pure VC (Specialty Gases of America, Toledo, OH, USA) by the offline MeCl method, by the laboratory of Dr. N. Sturchio at the University of Chicago.

The standards for H CSIA were calibrated to the VSMOW scale by analysis of cDCE ($\delta^2\text{H} = +729\%$) and TCE ($\delta^2\text{H} = +506\%$) by offline combustion of the CE to water followed by reduction of water to H_2 and dual inlet-IRMS, by Dr. A. Schimmelmann at the Indiana University. The ethene standard was calibrated by analysis of pure phase ethene at Indiana University ($\delta^2\text{H} = -73\%$).

CSIA Quality Assurance

Quality Assurance/Quality Control (QA/QC) for CSIA has been described in more detail in Section 3 of the User's Guide for this project (ESTCP ER-201029). QAQC samples are required to control the analytical precision and accuracy of isotope ratio determination. The main QAQC evidence is obtained by analysis of Laboratory Control Samples (LCS), prepared in identical matrix to that of the field samples (e.g, water) and analyzed under identical conditions as the field samples. The LCS is prepared using target compounds of known isotope composition (if available).

5.7 SAMPLING RESULTS

In this section, Table 5.3 provides a summary of the sampling program. Figure 5.2 shows a map of the sampling locations. Figure 5.3 shows the analytical data (CEs concentrations and C isotope ratios) plotted using a topographic cross-section format.

Table 5.3 Project sampling program, analytes and analyses

Component	Matrix	Number of Samples	Analytes	Analyses	Location
Microcosm Study	Microcosm water medium	Time series samples from microcosms	PCE, TCE, cDCE, tDCE, VC, ethylene	Concentration by GC CSIA by Isotope Ratio GCMS	Laboratory experiment
Field Program (2011)	Groundwater	83 Locations	PCE, TCE, cDCE, tDCE, VC, ethylene	Concentration by GC; CSIA by Isotope Ratio GCMS	See Fig. 5.2 (map of the well locations); Table D1 identifies all sampling points.
	Groundwater	83 Locations	Field Parameters	Temperature pH, groundwater elevation, DO, conductivity, turbidity	See Fig. 5.2 (map of the well locations); Table D1 identifies all sampling points.
Field Program (2014)	Groundwater	22 Locations	PCE, TCE, cDCE, tDCE	Concentration by GC; CSIA by Isotope Ratio GCMS	See Fig. 5.2 (map of the well locations); Table D2 identifies all sampling points.

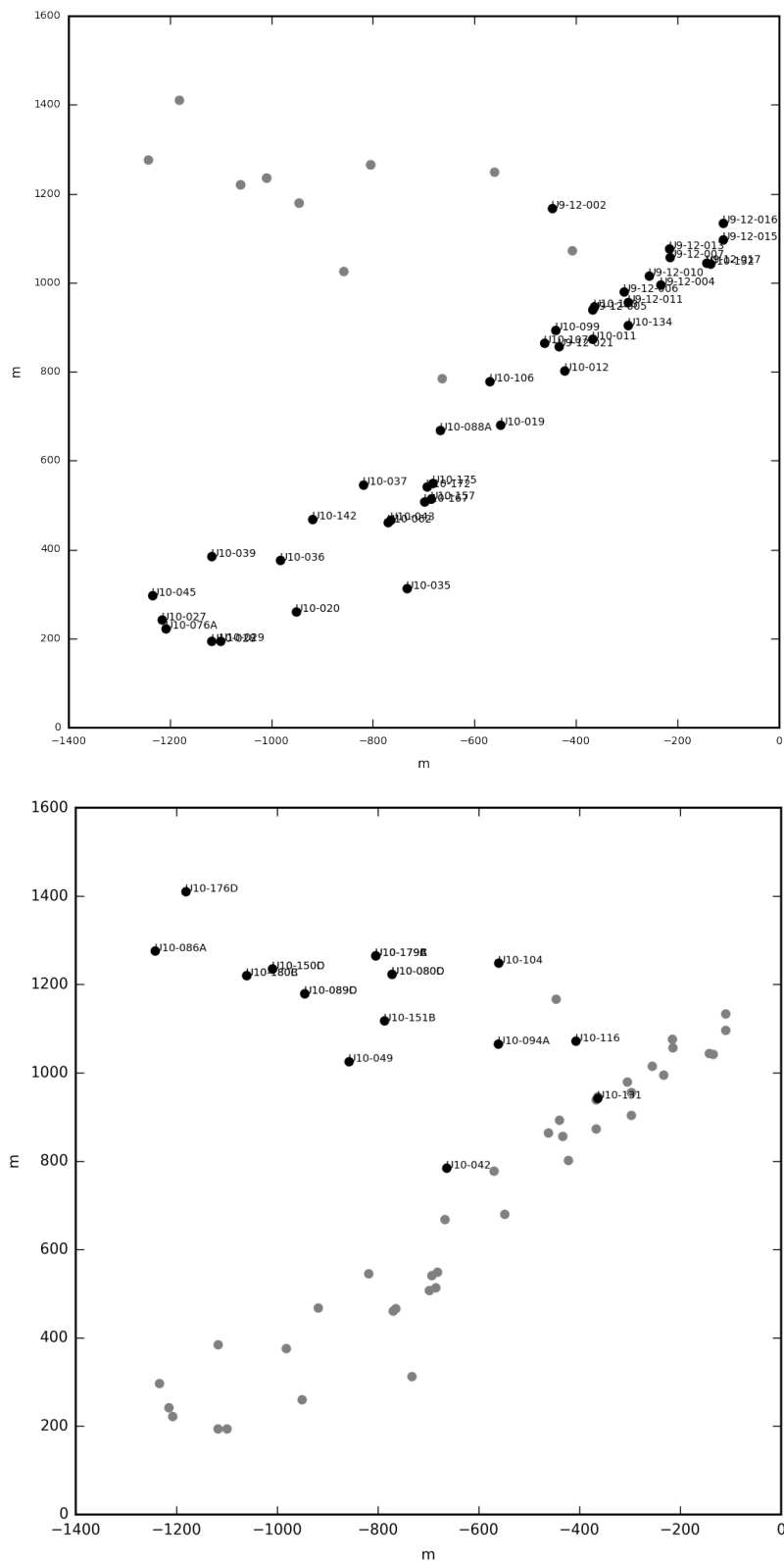


Figure 5.2. Locations of wells sampled for CSIA. Top: Shallow Plume; Bottom: Deep Plume. See Table D1 for well screen depth information.

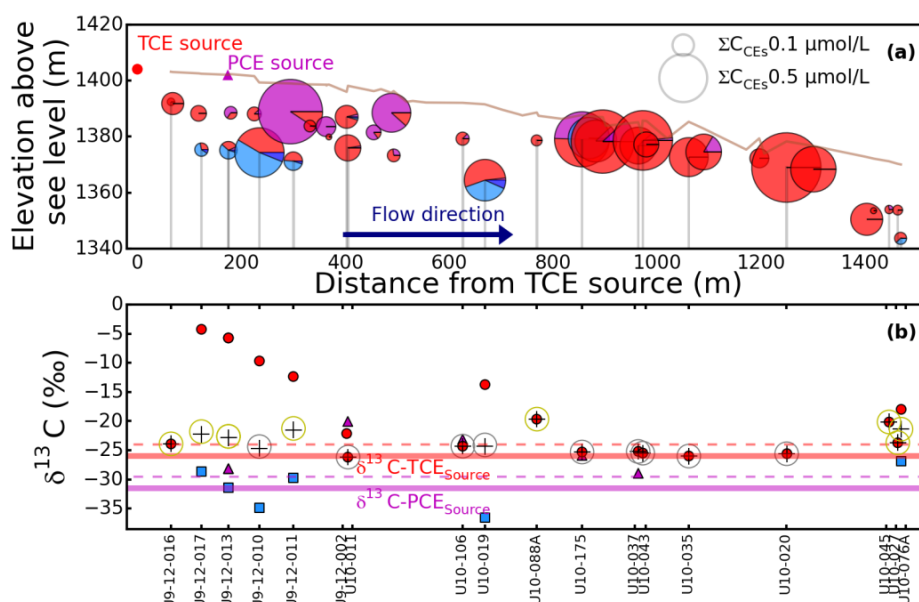


Figure 5.3A. CEs concentration and C isotope ratios, cross-section view, Shallow Plume, 2011 sample set. Red = TCE; Purple = PCE; Light blue = cis-DCE; Dark blue = trans-DCE; + = C-IMB values. The solid line corresponds to the TCE and PCE source signatures, the dashed lines show the 2 ‰ minimum $\delta^{13}C$ threshold indicative of degradation.

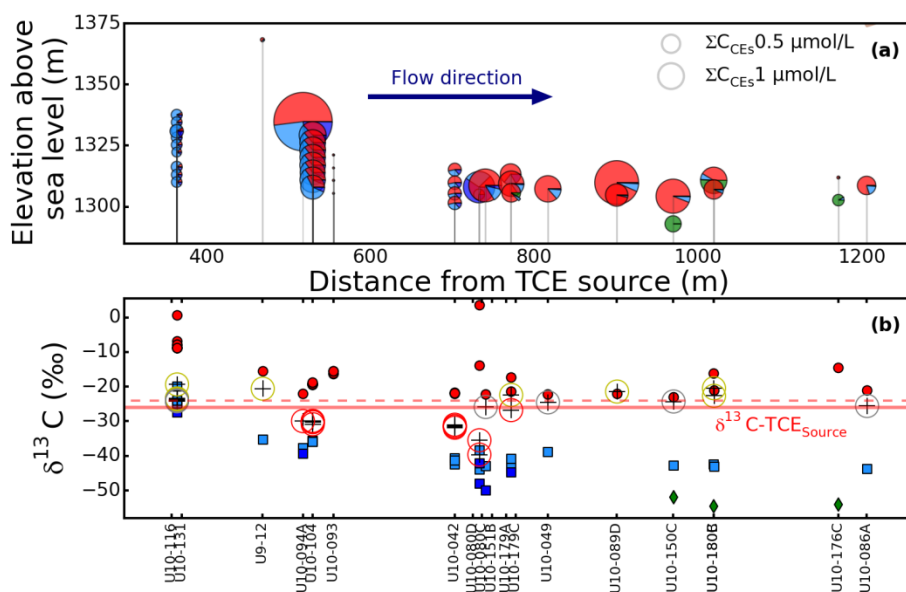


Figure 5.3B. CEs concentration and C isotope ratios, cross-section view, Deep Plume, 2011 sample set. See Fig. 5.3A for an explanation of the symbols.

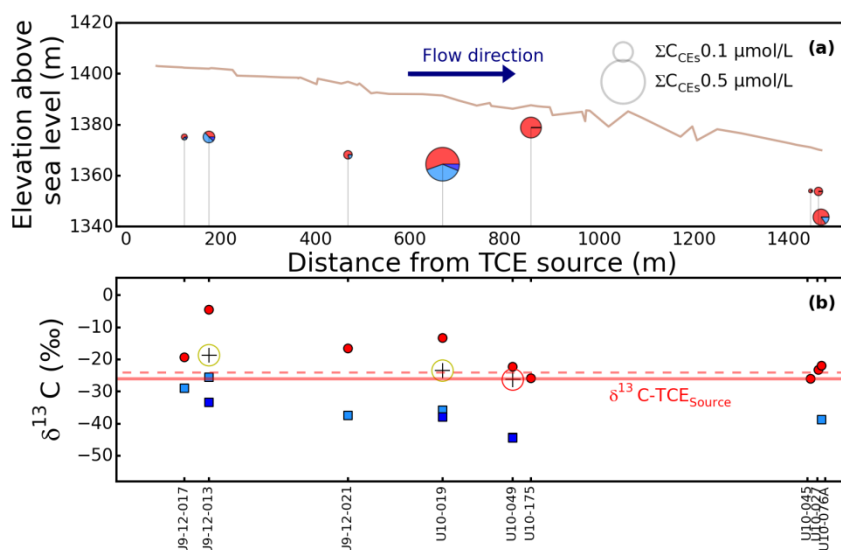


Figure 5.3C. CEs concentration and C isotope ratios, cross-section view, Shallow Plume, 2014 sample set. See Fig. 5.3A for an explanation of the symbols.

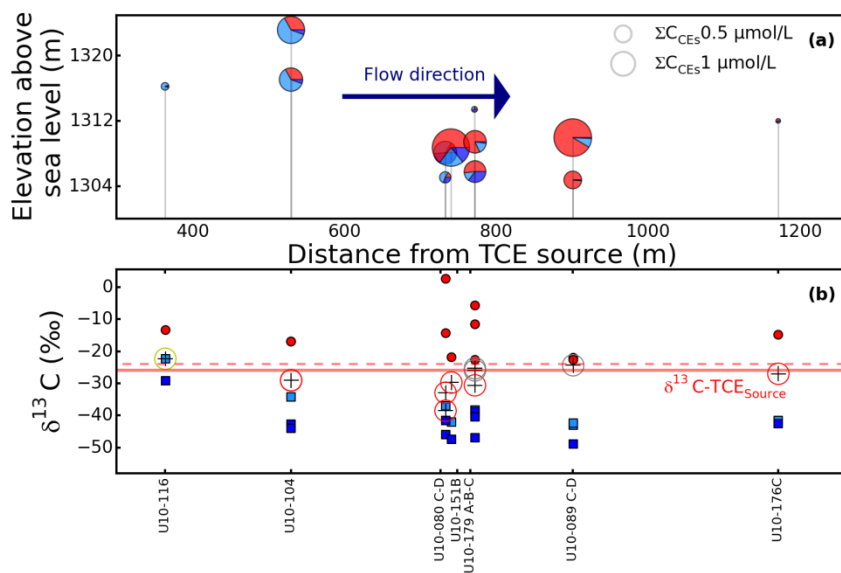


Figure 5.3D. CEs concentration and C isotope ratios, cross-section view, Deep Plume, 2014 sample set. See Fig. 5.3A for an explanation of the symbols.

6.0 PERFORMANCE ASSESSMENT

6.1 PERFORMANCE OBJECTIVE 1: OPTIMIZE CSIA METHOD FOR C, H, CL

The main novel element of the analytical methodology developed in the early performance stage of this project was the H CSIA method for analysis of chlorinated compounds. The detailed description of the method development and performance has been published by the *Environmental Science and Technology* journal (Kuder and Philp, 2013). The performance of C, Cl and H method was adequate. The data are reported in Appendix C, in Tables C5 and C6.

6.2 PERFORMANCE OBJECTIVE 2: ADAPT 0/1-D PHREEQC MODEL FOR H ISOTOPE ENRICHMENT

The H fractionation model was developed using mechanistic information from the lab study summarized in Section 5.3. A full description of the lab study was published by the *Environmental Science and Technology* journal (Kuder et al., 2013).

Simulation of Hydrogen Isotope Fractionation

Figure 6.1 illustrates that H isotope fractionation during sequential RD lacks primary KIEs and only involves secondary KIEs and the effects of inserting new H atoms into the RD products ($\epsilon_{H_{\text{protonation}}}$). The model only considered the averages of the applicable hydrogen KIEs of each reaction step to limit model complexity. As the H atoms transferred from the parent to the daughter products experience little isotope fractionation, the bulk $\delta^2\text{H}$ of a daughter product is mostly affected by the $\delta^2\text{H}$ of the H atom replacing the Cl atom during dechlorination/protonation (Kuder et al. 2013).

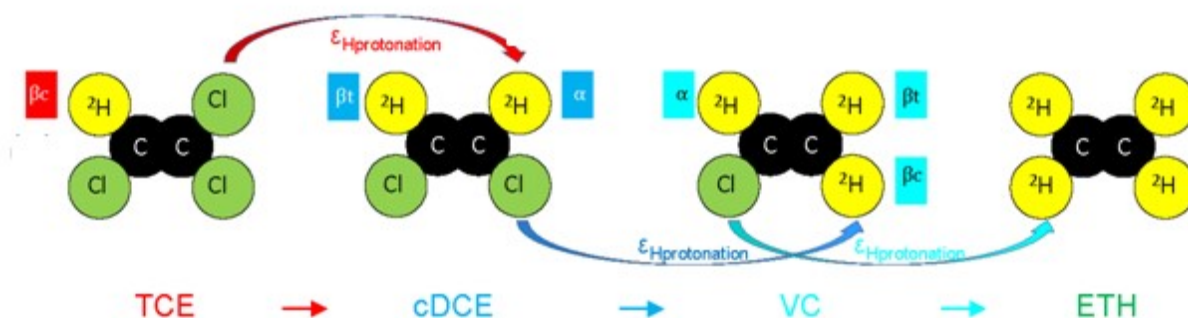


Figure 6.1. A conceptual model of H isotope fractionation in RD of TCE to ethene. The scheme combines secondary KIEs (in TCE transformation, type β_c) and the effects of inserting H atoms by protonation, $\epsilon_{H_{\text{protonation}}}$. For simplicity, the reactions involving tDCE are omitted.

Hydrogen isotope ratios were simulated with an extended “bulk isotope” method (van Breukelen et al., 2005). To simulate $\delta^2\text{H}$ of a daughter product, the model considered (i) isotope fractionation of the H atoms transferred from the parent to daughter product (ϵ_{bulk}) consisting of solely secondary KIEs); and (ii) the rates of the light, $\text{Rate}_{1\text{H}}$, and the heavy, $\text{Rate}_{2\text{H}}$, H isotopes

replacing the Cl atom of the parent compound, *i.e.*, through protonation, at each dechlorination step calculated as the total rate multiplied with the hydrogen isotopic abundance (Equations 5A and 5B):

$$Rate_{1H} = -Rate_m \cdot \left[1 + (\delta^2H_{water} + \epsilon_{H\text{protonation}} + 1) \cdot VSMOW \right]^{-1} \quad \text{Eq. 5A}$$

$$Rate_{2H} = -Rate_m \cdot \left(1 - \left[1 + (\delta^2H_{water} + \epsilon_{H\text{protonation}} + 1) \cdot VSMOW \right]^{-1} \right) \quad \text{Eq. 5B}$$

$Rate_m$ is the degradation rate of the corresponding parent compound, $\epsilon_{H\text{protonation}}$ is the overall H isotopic enrichment factor expressed with respect to δ^2H of groundwater and associated with this reaction step, and VSMOW is the international standard for the isotopic composition of water. The rates of H addition through protonation and of H transfer from the parent compound were weighted to account for the different numbers of H atoms involved. For example, in case of VC having three H atoms, two H atoms are transferred from DCE, whereas one H atom is added via protonation. Consequently, the H transfer flux is multiplied by $\frac{2}{3}$ and the protonation flux by $\frac{1}{3}$.

Model Calibration

For the sake of continuity, calibration of the H fractionation model is discussed in Section 6.3, as part of the “complete” C, Cl, H PHREEQC model calibration.

6.3 PERFORMANCE OBJECTIVE 3: CALIBRATE 0/1-D GEOCHEMICAL MODEL FOR C, CL AND H ENRICHMENT

After completing the H CSIA model development described above in Section 6.2, the complete three-element isotope fractionation 0/1-D PHREEQC model was calibrated using the lab study data. While examples of less comprehensive models (only C or Cl isotope fractionation) were described previously, only the C isotope fractionation model was validated previously using experimental data.

Model Calibration

Model developed for this project was validated based on a laboratory study data (a microcosm experiment). Details of the laboratory study have been published elsewhere (Kuder et al., 2013). The laboratory study is also summarized in Section 5.3. Figure 6.2 shows the results for the model calibrated with the experimental observations. The template models discussed in Section 6.5 below are based on this model. Further details of the model calibration will be published by van Breukelen et al. (2016, manuscript submitted).

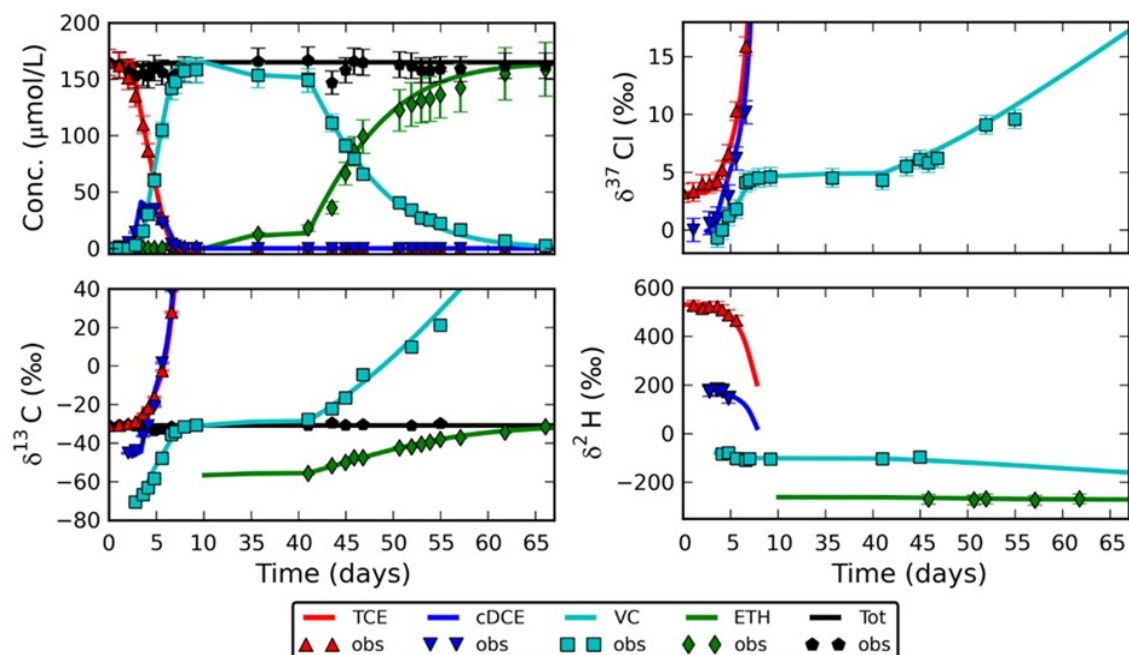


Figure 6.2. Calibration results for the C, Cl and H isotope fractionation model. The model accurately simulates concentrations, and C, Cl, and H isotope ratios of CEs and ethene over the course of sequential dechlorination.

6.4 PERFORMANCE OBJECTIVE 4: ADAPT MODEL TO 2/3-D IN PHAST AND PHT3D

This performance objective has been addressed as Case 3 in the User's Guide prepared for this project (cf. section 4.2.3 in the User's Guide). Case 3 is a simulation of a 2-D cross-section of a TCE plume degrading through reductive dechlorination in the anoxic plume core and through oxidative transformation at the plume fringes where the pollution plume mixes with clean aerobic water. Identical simulations were made using PHAST and PHT3D. The model input files needed to run the models are explained in section 7.3 of the ER-201029 User's Guide.

The goal of the simulations was to illustrate that the developed models are able to simulate complex situations (core and fringe degradation) in 2-D and should, therefore, be applicable as PHT3D in actual complex groundwater solute transport models setup with the widely used MODFLOW-MT3DMS codes. The model input files needed to run the model are explained in detail in Section 7.3 of the User's Guide. The developed model can simulate complete dechlorination of PCE to ethene together with oxidative transformation of DCE and VC under aerobic conditions. However, because the number of solutes which can be simultaneously simulated with the PHT3D graphical user interface (GUI) PMWIN was limited to 60, the PCE to TCE RD step and DCE oxidation step were discarded. The complete model worked without problems in PHAST (results not shown). Figure 6.3 illustrates the hydrogeological model setup and Table 6.1 shows the input parameters selected for the degradation and isotope fractionation processes. For each compound, the input parameters include k_{RD} (per year), the degradation rate per year for the RD pathway only, k_{OX} (per year), the degradation rate per year for the OX pathway, ϵ_C (‰) the isotope enrichment factor for C for each transformation reaction, and ϵ_{Cl}

ESTCP Final Report:

Integrated Stable Isotope –
Reactive Transport Model Approach
for Assessment of Chlorinated
Solvent Degradation

(‰) the isotope enrichment factor for Cl for each transformation reaction. Secondary Cl KIEs were omitted from that model.

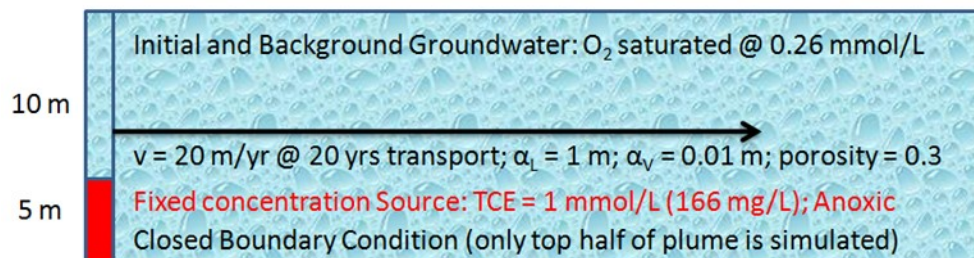


Figure 6.3. Case 3 (ESTCP ER-201029, User's Guide). Model setup for reductive dechlorination of TCE to ethene under anoxic conditions in the core of the plume together with oxidative transformation of VC at the fringe of the plume under aerobic conditions.

Table 6.1. Parameter values selected for Case 3

	TCE	DCE	VC
k_{RD} (per year)	1	0.5	0.25
ϵ_C (‰)	-12	-20	-25
ϵ_{Cl} (‰)	-3	-2	-2
k_{OX} (per year)	-	-	2
ϵ_C (‰)	-	-	-7.2
ϵ_{Cl} (‰)	-	-	-0.3

k_{RD} (per year) = degradation rate per year for RD pathway; k_{OX} (per year) = degradation rate per year for oxidative transformation pathway; ϵ_C (‰) – isotope enrichment factor for C; ϵ_{Cl} (‰) – isotope enrichment factor for Cl. The values of ϵ represent typical values reported in the literature for degradation of these compounds (see ER-201029 User's Guide Appendix B)

Figures 6.4 and 6.5 show output from the PHAST and PHT3D models, respectively, applied in cross-sectional 2-D mode. The model output shows the following: (i) concentration peaks increasingly downgradient in the order from TCE to ETH; (ii) relatively high levels of TCE and DCE in the top fringe area where reductive dechlorination is impeded by elevated oxygen concentrations; (iii) correspondingly, the C isotope ratios of TCE and DCE increase downgradient but decrease upwards due to increasing inhibition of RD by oxygen; and (iv) isotope enrichment of VC is noticeable in the diluted top parts of the fringe where its oxidative transformation is promoted by higher oxygen levels.

The spatial and temporal resolution was equal for both the PHAST and PHT3D model: 0.1 m and 2.0 m spatial resolution (node spacing) in vertical and horizontal direction, respectively, and a time step of 0.1 year. PHT3D has a better solver (TVD) than PHAST to simulate transverse dispersion accurately. Indeed, numerical dispersion seems a bit larger in the PHAST model as the fringe in the PHT3D model seems slightly sharper. However, these small differences are probably not relevant in practical applications.

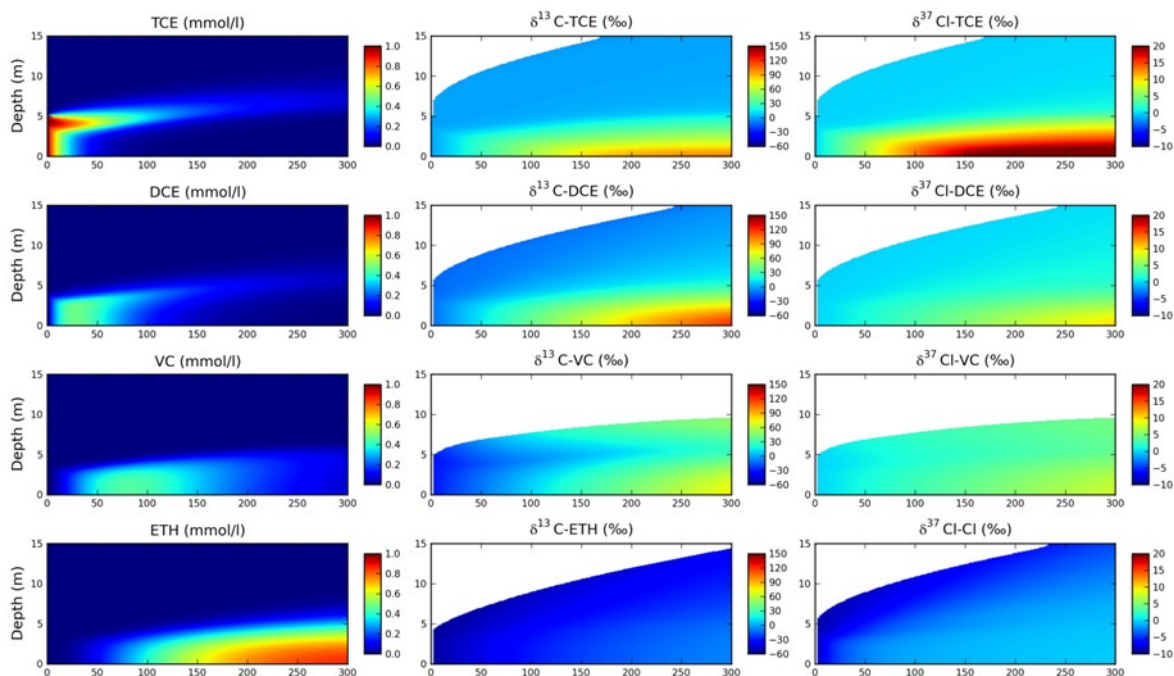


Figure 6.4. Results of 2-D PHAST simulation of reductive dechlorination (TCE to ethene) in the core of the plume and oxidation of VC at the fringe (Case 3, cf. Figure 6.3).

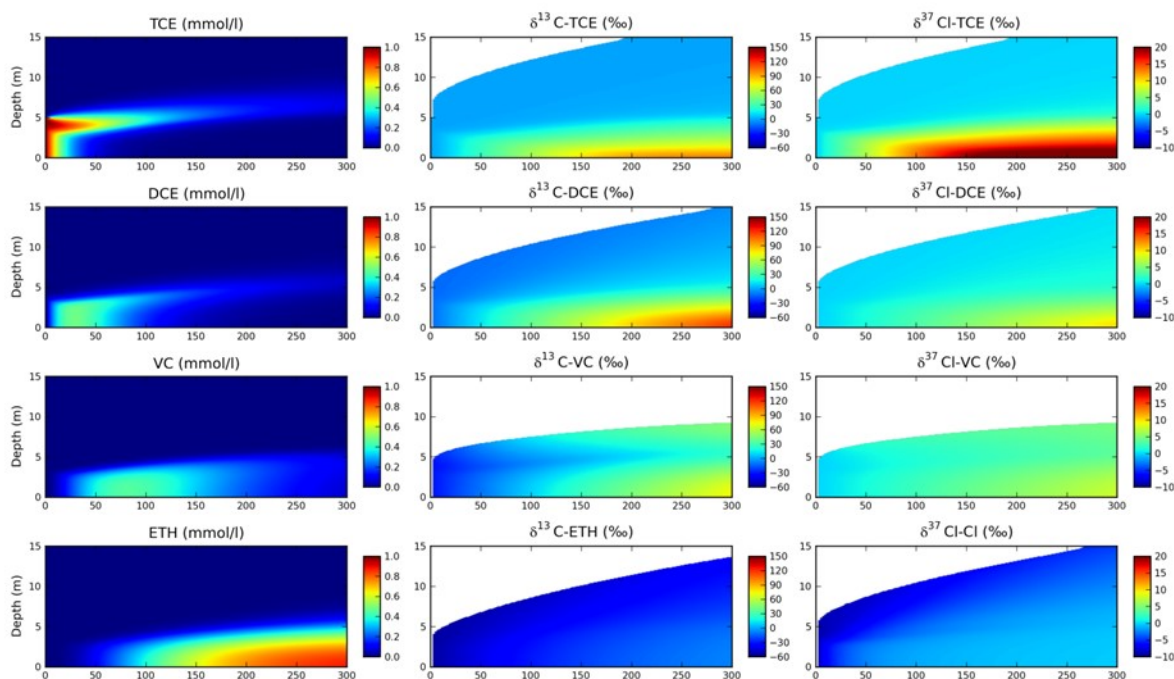


Figure 6.5. Results of 2-D PHT3D simulation of reductive dechlorination (TCE to ethene) in the core of the plume and oxidation of VC at the fringe (Case 3, cf. Figure 6.3).

6.5 PERFORMANCE OBJECTIVE 5: CALIBRATE 2/3-D MODEL WITH SITE-SPECIFIC DATA (REVISED: CALIBRATE 0-D MODEL WITH SITE-SPECIFIC DATA)

In this section, we discuss the application of the model to help in interpretation of the CSIA data from the Shallow and Deep TCE Plumes. The summary of “classic” interpretation of the CSIA data from Demonstration Site, which was the prerequisite to the modeling, is also given in Appendix A of the User’s Guide published previously (ESTCP ER-201029, User’s Guide).

This discussion centers on TCE plumes and on carbon and chlorine isotopes. Due to limited number of wells with PCE detections and even fewer wells with evidence of PCE degradation, modeling of PCE plume was not conducted. The present discussion of the model application is restricted to the lines of evidence that were informative in field site data evaluation. In this section, we do not discuss the model simulating chlorine isotope composition of cDCE, since that model’s output was not providing added benefit to the field site evaluation in the present case. Similarly, hydrogen data are not discussed in this section. The anticipated target for H isotope ratio modeling (a line of evidence for detection of TCE produced by reductive dechlorination of PCE) turned out to be not applicable at the Demonstration Site.

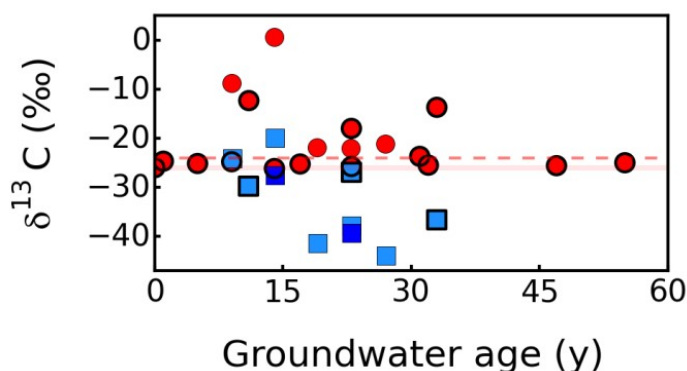


Figure 6.6. Carbon isotope ratios for TCE (red circles), cDCE (light blue squares) and tDCE (dark blue squares), versus the groundwater age. Shallow wells are identified by the black outline. The red line corresponds to the TCE source signature, the dashed line shows the 2 ‰ $\delta^{13}\text{C}$ threshold indicative of degradation (US EPA, 2008).

6.5.1 The rationale for the revision of the spatial dimensionality of the model to 0-D

Visualization of the CSIA field data showed irregular patterns of isotope ratios of TCE versus distance (Figures 5.3A-D) and vs. flow velocities (tritium-helium data, Figure 6.6), not matching the assumed homogeneous first-order TCE degradation rate constant postulated by the site’s conceptual model. CE degradation appeared to be limited to several disconnected zones in the Shallow Plume, while occurring predominantly in the source area of the Deep Plume (and with significant element of diffusion and back diffusion, see discussion below). A solution could be to simulate multiple flow paths covering multiple areas in the aquifer. However, we could not find areas like shallow/middle/deep parts of the aquifer where downgradient wells were hydraulically connected and the CSIA enrichment showed a steady pattern. Therefore, we applied the most basic and simple 0-D batch setup where a plume was considered a reaction vessel where

ESTCP Final Report:

Integrated Stable Isotope –

Reactive Transport Model Approach

for Assessment of Chlorinated

Solvent Degradation

concentrations and isotope ratios change in a logical fashion but where spatial locations of the individual samples do not need specific consideration. Such an approach was applied before by van Breukelen et al. (2005) to simulate CSIA data from a hydrogeologically complex site. Such a model approach is still highly valuable as it allows to model all site data with a single model (optionally with variations in model parameter values to capture the site's variation in rate constants for example) and should provide field isotope enrichment factors and prove/disprove various degradation pathways (Section 6.6). The enrichment factors obtained can subsequently be used in a Rayleigh equation (Eq. 3) to calculate the extent of transformation (Section 6.7).

6.5.2 Model approach

The existing CSM for OU 10 described complex attenuation mechanisms (CH2MHill, 2009). According to the CSM, TCE in the Shallow Plume was degraded via aerobic cometabolism. In addition to aerobic cometabolism, reductive dechlorination evidence was reported from the toe of the plume, where TCE enters the Lower Lithologic Unit. The CSM of the Deep Plume proposed that the contaminants reside in mobile (sand) and immobile (clay and silt) porosities. Geochemical conditions likely range from highly anaerobic and strongly reducing in the immobile porosity, conducive to reductive dechlorination, to aerobic in the mobile porosity, conducive to aerobic cometabolism and contaminant oxidation. The primary mechanism for degradation of TCE within the immobile porosity is reductive dechlorination and the degraded TCE and the degradation products may then diffuse into the mobile porosity. On the other hand, reductive dechlorination degradation rates may be relatively slow in the mobile porosity of the Deep Plume. However, degradation of TCE and the daughter products of reductive dechlorination present within the mobile porosity may also occur through cometabolic oxidation. The complex pattern of degradation processes is also apparent from the CSIA data discussed in Appendix A of the User's Guide (ESTCP ER-201029, User's Guide). Therefore, the plume-wide data cannot be easily explained by any single process alone.

- **The conclusion is that contaminant attenuation at OU 10 likely involves multiple degradation pathways, potentially both reductive dechlorination and aerobic cometabolic biodegradation.**

Tentative attenuation scenarios were proposed (Table 6.2), combining reductive dechlorination of TCE with other degradation pathways. The scenarios were then tested using the 0-D PHREEQC model. Model inputs (isotope enrichment factors, source isotope ratios and rates of individual reactions) are summarized in Tables 6.3 and 6.4. Historically, VC was detected only in a few wells at the site and at low concentrations. Therefore, VC disappearance was modeled through fast oxidation, which is a reasonable assumption since VC oxidation rates are generally relatively high (Alvarez-Cohen and Speitel, 2001).

Given the limitations of the 0-D approach, only the wells with evidence of degradation qualified for evaluation. This was because the model addresses the contaminant concentration through calculation of the molar fraction of individual contaminants. If no degradation products are present and the isotope ratio of the contaminant is identical to the source value, the data point cannot be interpreted beyond stating the lack of evidence of degradation.

Table 6.2. List of the modeled attenuation scenarios

#	Simulation	Variables	Figure
1	Scenario 1. Reductive dechlorination only, end product cis-DCE		6.9
2	Scenario 2. Simultaneous (TCE,DCE) RD and (DCE, VC) OX.	Variations in relative DCE degradation rate constant	6.10
3	Scenario 3. Sequential (TCE, DCE) RD and (TCE, DCE, VC) OX.	Rate constants, $\epsilon_{\text{C-TCE}}$ (oxidation) enrichment factor	6.11
4	Scenario 4. Simultaneous RD and OX.	Rate constants, $\epsilon_{\text{C-TCE}}$ (oxidation) enrichment factor	6.12
5	Similar to Scenario 1. Reductive dechlorination only, end product cis-DCE – alternative $\epsilon_{\text{C-TCE}}$ value	No variations	6.13

Selection of the isotope effects used in the model

This is a summary of the isotope effects used as inputs for the model variants discussed in this report (Table 6.4). See the User's Guide (ER-201029) for additional information, including details and input parameters for additional variants of the model.

$\epsilon_{\text{C TCE} \rightarrow \text{cDCE}}$. The default value of this parameter was defined as a difference between $\delta^{13}\text{C-TCE}$ and $\delta^{13}\text{C-DCE}$ at the initial stage of transformation (Hunkeler et al., 1999). We considered a DCE molar yield of less than 20 % as the maximum threshold for the reaction being in initial stage. The resulting $\epsilon_{\text{C TCE} \rightarrow \text{cDCE}}$ was approximately -20 ‰ (Table 6.3). That value is similar to the maximum isotope effect reported from various studies of reductive dechlorination of TCE (see Table B-1 in the ER-201029 User's Guide).

$\epsilon_{\text{C TCE} \rightarrow \text{tDCE}}$. The isotope effect in reductive dechlorination of TCE to trans-DCE, $\epsilon_{\text{C TCE} \rightarrow \text{tDCE}}$ was most likely larger than in the dechlorination to cis-DCE as suggested by the $\delta^{13}\text{C}$ of trans-DCEs values that were depleted by 1.4 ‰ to 7.5 ‰ vs. cis-DCE (Fig. 5.3). Therefore, $\epsilon_{\text{C TCE} \rightarrow \text{tDCE}}$ would likely be more negative in order to explain the ^{13}C depletion observed for trans-DCE. A value of -25 ‰ gave acceptable results in model fitting in Scenario 1; however, reductive dechlorination of TCE in trans-DCE did not improve the overall fit of the data in comparison of a model that omitted the $\text{TCE} \rightarrow \text{tDCE}$ transformation.

$\epsilon_{\text{C}}/\epsilon_{\text{Cl}}$. The $\epsilon_{\text{C}}/\epsilon_{\text{Cl}}$ slope of RD of TCE should be obtained using the samples that were unlikely to be affected by oxidation. For those samples, the field values of the isotope ratios matched the simulation of the Scenario 1 (Table 6.2) model with $\epsilon_{\text{C TCE} \rightarrow \text{cDCE}} = -20.2\text{ ‰}$. Most of those samples were collected from the Shallow Plume. The calculated $\epsilon_{\text{Cl}}/\epsilon_{\text{C}}$ is 0.19, which is similar to the literature range for RD (between 0.21 and 0.37, see Fig. 6.7).

ESTCP Final Report:

Integrated Stable Isotope –

Reactive Transport Model Approach

for Assessment of Chlorinated

Solvent Degradation

$\epsilon_{Cl\text{ bulk}}$. The Cl bulk enrichment factor for TCE reductive dechlorination was calculated using the ϵ_C/ϵ_{Cl} slope of TCE and $\epsilon_{C\text{ TCE} \rightarrow cDCE}$ value, following the method employed by Wiegert et al. (Wiegert et al., 2012). The subsequent $\epsilon_{Cl\text{ bulk}}$ is -3.8 ‰ . The values of $\epsilon_{Cl\text{ bulk}}$ in transformation of cis-DCE are taken from the literature (Abe et al., 2009; Kuder et al., 2013).

Table 6.3. Relative first-order degradation rate constants
Model/scenario numbers are identical as in Table 6.2

Scenario #	TCE \rightarrow cis-DCE	cis-DCE \rightarrow VC	TCE \rightarrow CO ₂	cis-DCE \rightarrow CO ₂	VC \rightarrow CO ₂	End reductive dechlorination/Start oxidation (fraction of TCE degraded through RD)
Model 1						
1.1	1	-	-	-	-	-
Model 2						
2.1	1	-	-	0.2	-	-
2.2	1	-	-	1	-	-
2.3	1	0.2	-	-	15	-
2.4	1	1	-	-	15	-
Model 3						
3.1*	1	-	1	0.45	-	8 %
3.2	1	1	-	0.8	200	52 %
3.3	1	1	0.8	0.8	200	40 %
3.4	1	1	2	0.8	200	22 %
3.5	1	0.4	-	-	200	46 %
Model 4						
4.1	1	-	-	-	-	-
4.2*	1	-	0.5	0.5	-	-
4.3	1	-	0.5	0.5	-	-
4.4	1	-	2	2	-	-
4.5	1	-	2	0.2	-	-
Model 5						
5.1**	1	-	-	-	-	-

* $\epsilon_{C\text{-TCE}}$ for TCE oxidation = -4 ‰ (See table 6.4)

** $\epsilon_{C\text{-TCE}}$ for TCE reductive dechlorination = -10 ‰ (see Table 6.4)

Table 6.4A. Carbon isotope fractionation factors used in the models

Scenario #	TCE → cis-DCE	cis-DCE → VC	TCE → CO ₂	cis-DCE → CO ₂	VC → CO ₂
1.1,1.2,1.3	-20.2 ‰	-	-	-	-
2.1, 2.2, 2.3, 2.4	-20.2 ‰	-26.8 ‰	-	-8.5 ‰	-
3.2, 3.3., 3.4, 3.5	-20 ‰	-26.8 ‰	-15 ‰	-8.5 ‰	-
3.1	-20 ‰	-	-4 ‰	-8.5 ‰	-
4.1, 4.3, 4.4, 4.5	-20 ‰	-	-15 ‰	-8.5 ‰	-
4.2	-20 ‰	-	-4 ‰	-8.5 ‰	-
5.1	-10 ‰	-	-	-	-

Table 6.4B. Bulk chlorine isotope fractionation factors used in the models

Scenario #	TCE → cis-DCE	cis-DCE → VC	TCE → CO ₂	cis-DCE → CO ₂	VC → CO ₂
1.1,1.2,1.3	-3.8 ‰	-	-	-	-
2.1, 2.2, 2.3, 2.4	-3.8 ‰	-1.7 ‰	-	-0.3 ‰	-
3.2, 3.3., 3.4, 3.5	-8 ‰	-1.7 ‰	0 ‰	-0.3 ‰	-
3.1	-8 ‰	-	0 ‰	-0.3 ‰	-
4.1, 4.3, 4.4, 4.5	-8 ‰	-	0 ‰	-0.3 ‰	-
4.2	-8 ‰	-	0 ‰	-0.3 ‰	-
5.1	-	-	-	-	-

6.5.3 Modeling results: Shallow Plume

Based on the “classic” approach to CSIA evaluation of site data (Case Study, Appendix A of the User’s Guide, ESTCP ER-201029, User’s Guide), TCE reductive dechlorination was likely in 11 out of 38 wells at the Shallow Plume, as evidenced by detections of DCE isomers and/or the presence of isotope enrichment of TCE (Figures 5.3A and 5.3C). The dual-element C+Cl CSIA of TCE of the Shallow Plume showed a strong bimodal separation of the wells (Figure 6.7). One group of samples followed a trend consistent with reductive dechlorination (that trend included all samples where RD products were detected plus additional samples, where only TCE was present). Remaining wells followed a trend consistent with TCE attenuation by diffusion out of the mobile porosity of the dissolved plume. One possible outlier was well U9-12-021. In that sample, cis-DCE was detected and TCE showed significant ¹³C enrichment (+10 ‰ enrichment vs. the source TCE), but there was no fractionation of Cl isotopes (the δ³⁷Cl signature was identical to the source, within the analytical uncertainty margin). Finally, the samples within the RD-like group (as well as U9-12-021) displayed enriched values of C-IMB (Fig. 5.3A and 5.3C) (for definition of C-IMB, see the User’s Guide, Section 3.3.5), suggesting that additional degradation process, not simply TCE to DCE transformation, was involved.

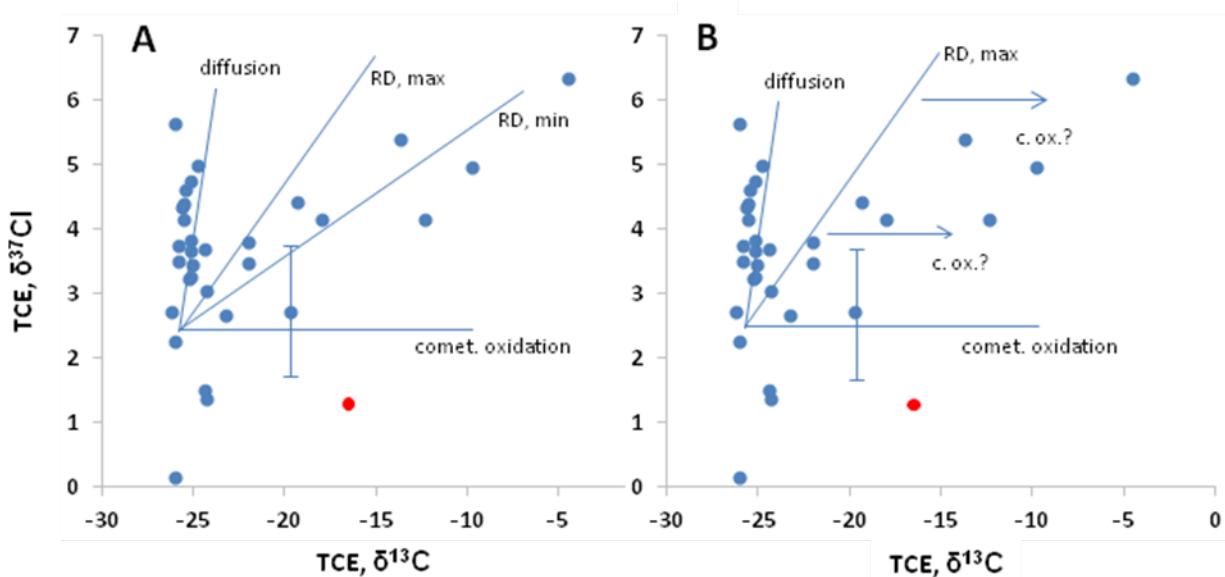


Figure 6.7. Dual-element CSIA plots, TCE in the Shallow Plume. A) Data rationalization by RD and diffusion accounting for isotope fractionation. B) Data rationalization by TCE oxidation following RD. The red marker indicates one outlier well, U9-12-021 (see text for explanations). The dual-CSIA reference trends are shown for RD (minimum and maximum range) and diffusion based on published experimental data (see the summary of isotope effect in TCE biodegradation, Appendix B of the User's Guide, ER-201029; see Wanner and Hunkeler, 2015 for the isotope effects in TCE diffusion). The reference line for cometabolic oxidation is theoretical (the absence of Cl fractionation accounting for the known reaction mechanism with formation of an epoxide intermediate).

Questions remaining after “Classic CSIA”

While the evidence for RD occurring in certain Shallow Plume wells was strong, uncertainties remained: (i) the role of oxidation of TCE (compare cases A and B in Figure 6.7); and (ii) can the enriched C-IMB values (Figure 5.3A and 5.3C) be also explained by differences in sorption or diffusion/back-diffusion of DCE vs. TCE, which separates the depleted daughter products from the enriched parent compound, rather than by degradation proceeding beyond DCE?

Scenario test results

TCE reductive dechlorination was confirmed as a significant degradation process. All scenarios without TCE oxidation yielded good fit of the simulated TCE isotope ratios and concentrations to the field data (Figures 6.9 and 6.10). As already suggested in the preceding section, sample U9-12-021 was an exception in that a better fit was obtained for the scenarios involving TCE oxidation (Figure 6.11 and 6.12).

The RD-only model (Scenario 1, Figure 6.9A-D) showed a poor fit to the field data, in particular, the C isotope ratios of DCE (Fig. 6.9B) and the C-IMBs (Fig. 6.9C). Scenario 1 overpredicted the production of cDCE and/or underpredicted the isotope ratios of cDCE. That result was not

ESTCP Final Report:

*Integrated Stable Isotope –
Reactive Transport Model Approach
for Assessment of Chlorinated
Solvent Degradation*

unexpected, since C-IMB data evaluation has already suggested the possibility of CEs mineralization proceeding past cDCE. Model Scenario 2 (Figure 6.10A-C) confirmed that hypothesis. Introduction of a sink for cDCE (either through direct oxidation or through production of VC which is subsequently oxidized) produced a much better data fit for cDCE, without significant worsening of the fit for TCE. In that model, there was a clear effect of the relative rates of cDCE production and degradation. The model required that the rate of cDCE degradation was low in comparison to the rate of TCE degradation through reductive dechlorination. Clear identification of the sink for cDCE was not possible, but based on existing site data (relatively high content of DO and the presence of aerobic bacteria capable of CEs degradation, combined with virtual absence of VC), oxidation of the reductive dechlorination products appears a likely option. Finally, Figures 6.11 (TCE reduction followed by TCE and DCE oxidation) and 6.12 (simultaneous reduction and oxidation of TCE and DCE) illustrate the potential of TCE oxidation. In Figure 6.11, reductive and oxidative processes were simulated by applying a lag time for oxidation and an end time for reductive dechlorination. This illustrates the transition from reductive to oxic conditions. Both scenarios can be forced (by adjusting model inputs) to match the dual-element field data for the RD and oxidation of TCE (following the scheme shown in Figure 6.7B), however, such an outcome is not very realistic. While obtaining a reasonable fit of the model with TCE oxidation to the dual-element CSIA distribution of field data is possible (Figures 6.11D and 6.12D), it would require hand-picked input parameters for each well to maintain the appearance of a dual-element trend for a group of wells. Moreover, the models with TCE oxidation overpredict the C isotope ratios of TCE in relation to its molar ratio (Figures 6.11A and 6.12A).

In regards to the potential effects of diffusion/back-diffusion on the C-IMB results, the present results do not indicate such influence. Specifically, the ^{13}C -enriched C-IMB observed in the field data would have to be rationalized by the following: (i) the depleted RD products being selectively removed (e.g., cis-DCE migrating preferentially in the mobile porosity; or (ii) the ^{13}C -enriched degraded TCE being preferentially released by back-diffusion into the mobile porosity. Both effects are unlikely, since the modeling confirms the relative distribution of TCE and cis-DCE in the samples can be explained well by degradation processes alone, consistently for the whole Shallow Plume data set.

Conclusions

- *Model results confirm that cis-DCE has been degrading (most likely, by cometabolic oxidation). cis-DCE degradation is necessary in the model to fit the field cis-DCE results.*
- *The model combining reductive dechlorination of TCE and relatively slower degradation of the RD products yields a very good fit to the field TCE and reasonable fit to the DCE data.*
- *Introduction of TCE oxidation into the model helps to explain the CSIA results for U9-12-021. That sample's isotope ratios and the observed concentrations appear to be consistent with the effects of combined reductive dechlorination of TCE and aerobic degradation of both TCE and DCE.*
- *For most wells, there is no clear evidence of TCE oxidation.*
- *Oxidation of TCE cannot be excluded, but the present results imply that (i) the degradation process would have to be associated with minimal isotope fractionation*

ESTCP Final Report:

Integrated Stable Isotope –

Reactive Transport Model Approach

for Assessment of Chlorinated

Solvent Degradation

(such as reported for cometabolic sMMO organisms, but not the organisms utilizing toluene oxygenases); and (ii) at least for the wells that were discussed in the preceding section, the rates of TCE and cis-DCE oxidation would have to be closely balanced to maintain the observed RD-like data pattern (such balance is unlikely to be consistent for several discrete monitoring points situated in different sections of the plume).

- Note that the present discussion does not concern the Shallow Plume wells that were not exhibiting C isotope fractionation. TCE in those wells was not affected by RD. If TCE oxidation occurred, it must have been limited or the degradation pathway did not involve isotope fractionation (the enrichment factor of the aerobic degradation would be near zero).
- In addition to TCE degradation, the Shallow Plume shows isotope signature of significant TCE mass attenuation by diffusion out of the mobile porosity (Fig. 6.7).

6.5.4 Modeling results: Deep Plume

Based on the “classic” approach to CSIA evaluation of site data (Case Study, Appendix A, User’s Guide for this project), evidence of at least some TCE reductive dechlorination was apparent in nearly all sampling points at the Deep Plume. The dual-element CSIA of TCE from the site showed a trend that was generally consistent with the range of values reported from reductive dechlorination (Figure 6.8). However, the apparent slope of the trend was poorly defined and the observed dual-element CSIA slope could be rationalized by at least three different degradation/attenuation scenarios, always involving RD, but with possible contributions of isotope fractionation caused by TCE diffusion or TCE undergoing aerobic degradation.

The samples in the eastern/northeastern section of the plume showed largest net values of both C and Cl enrichment. Surprisingly, the values of C-IMB in several samples (also in the eastern/northeastern section of the plume) were depleted relatively to the primary source signature of TCE.

Questions remaining after “Classic CSIA”

While the evidence for RD occurring in the Deep Plume was strong, uncertainties remained: (i) the role of other mechanisms affecting the slope of the dual-element CSIA trend of TCE (compare cases A, B and C in Figure 6.7); (ii) can the enriched C-IMB values be also explained by differences in sorption or diffusion/back-diffusion of DCE vs. TCE rather than by degradation proceeding past DCE; and (iii) how to explain the depleted C-IMB values?

Scenario test results

Figs. 6.9A and 6.10A showed that the wells in the western section of the Deep Plume (green symbols) are consistent with the RD model that also successfully simulated the data from the Shallow Plume. On the other hand, the model showed significant fit deviations vs. the majority of samples from the eastern/northeastern area the plume. The model (all scenarios tested) significantly overpredicted the molar fractions of TCE and/or the isotope ratios of TCE if the applied enrichment factor was -20 ‰ (the value used in the Shallow Plume modeling). While the

applied TCE isotope enrichment factor seems too large compared to the observations, the model using a smaller enrichment factor to fit $\delta^{13}\text{C}$ of TCE (for example -10 ‰ shown in Figure 6.13A) does not reproduce the depleted $\delta^{13}\text{C}$ of cis-DCE in the same samples (Figure 6.13B).

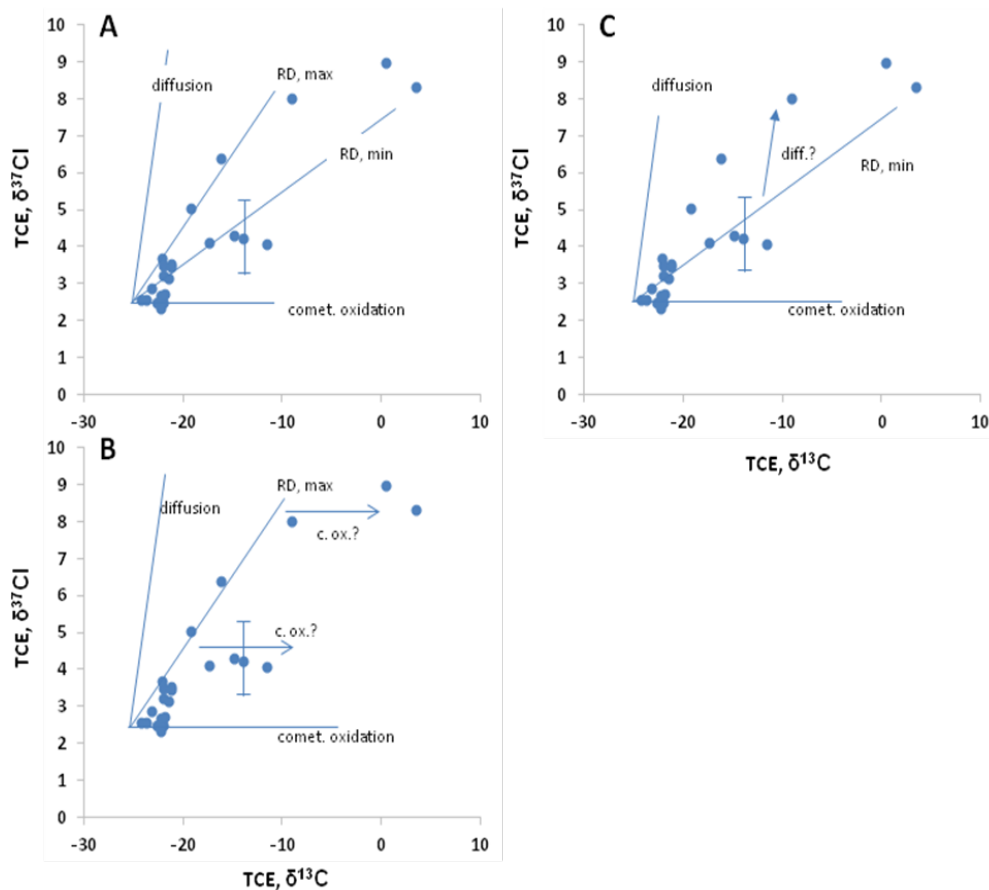


Figure 6.8. Dual-element CSIA plots, TCE in the Deep Plume. The dual-CSIA reference trends are shown for RD (minimum and maximum range) and diffusion based on published experimental data (see the summary of isotope effect in TCE biodegradation, Appendix B of the User's Guide, ER-201029; see Wanner and Hunkeler, 2015 for the isotope effects in TCE diffusion). The reference line for cometabolic oxidation is theoretical (the absence of Cl fractionation accounting for the known reaction mechanism with formation of an epoxide intermediate). A) Data rationalization by RD only; B) Data rationalization by TCE oxidation following RD; C) Data rationalization RD, with additional Cl fractionation resulting from TCE diffusion.

It appears that the present model approach does not address the attenuation mechanisms in the Deep Plume. The present model accounts for chemical reactions, but not for contaminant transport. Note that the Deep Plume is situated in heterogeneous lithology, with a significant

element of fine-grained sediment. While conventional knowledge is that transport phenomena do not significantly affect isotope ratios (USEPA, 2008), more recent work (e.g. Wanner and Hunkeler, 2015) shows that in certain hydrogeological context, physical processes may exert significant controls over isotope composition of groundwater contaminants. Diffusion and back-diffusion of contaminants is significant at the Deep Zone, in particular in the E/NE area. For example, if TCE degradation occurs in the clay layer only, the transfer of DCEs from the clay layer to the aquifer due to concentration gradients will differ from TCE transport, and potentially lead to the observed anomalies of TCE molar fractions and isotope ratios. Preferential back-diffusion of DCEs might enhance C-IMB depletion, since daughter compounds (DCEs) are depleted with respect to the parent compound (TCE) (Figure 2.1). Preferential migration of depleted DCE into the mobile porosity would have the effect observed in the data set, of producing the C-IMB values that are depleted vs. the source value of the parent compound. While no other satisfying explanation could be suggested, we expect transport processes to considerably influence the molar ratios and the distribution of the pollutants at this site.

Conclusions

- *Model results are consistent with a major role of RD of TCE.*
- *The model results concerning the fate of degradation products and potential oxidation of TCE are inconclusive.*
- *Significant problems with fitting the simulation results to the field data suggest that the concentrations and isotope ratios of the contaminants in the mobile porosity are largely controlled by back-diffusion from clay layers.*

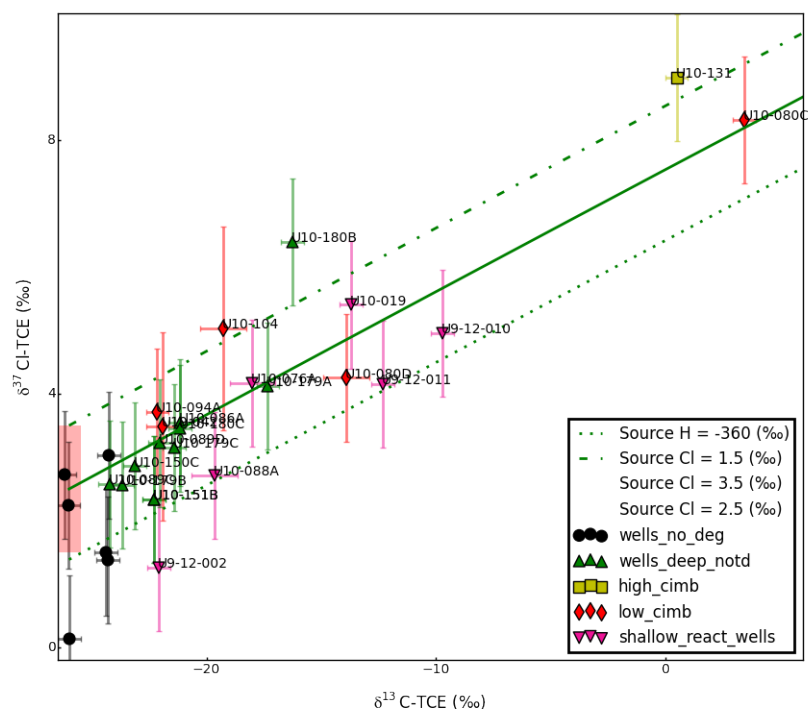
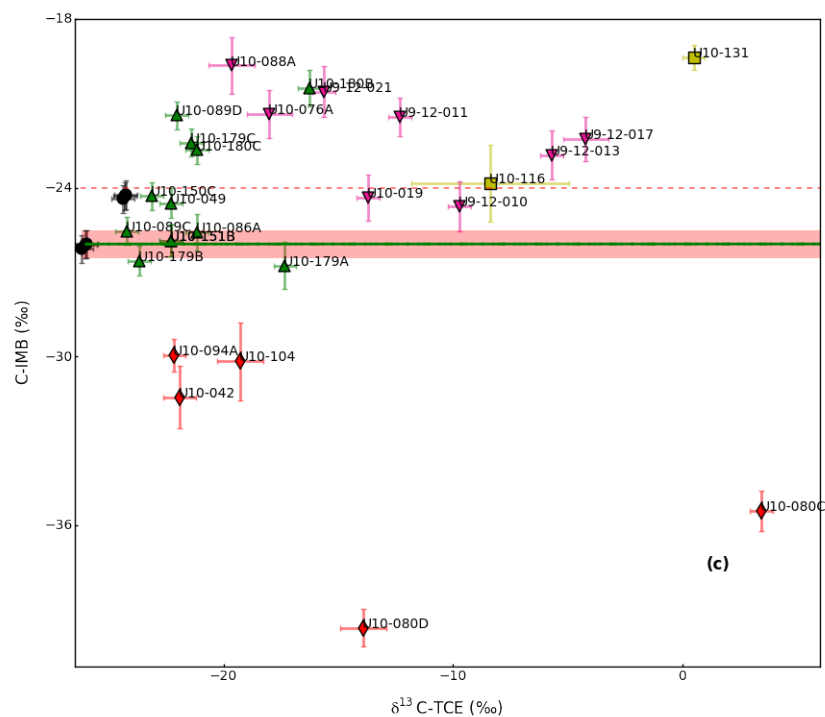


Fig. 6.9CD. Scenario 1 (Table 6.2): Model for TCE reductive dechlorination only, cis-DCE stall. C) C-IMB vs. C isotope ratios of TCE; D) Dual-element, C/Cl plot. The shaded rectangle represents the carbon and/or chlorine TCE source signature's uncertainty range. Symbols depict individual monitoring wells: Shallow Plume (pink); western part of the Deep Plume (green); wells with depleted C-IMB, E/NE area of the Deep Plume (red); wells with enriched C-IMB, E/NE area of the Deep Plume (yellow).

ESTCP Final Report:

Integrated Stable Isotope –
Reactive Transport Model Approach
for Assessment of Chlorinated
Solvent Degradation

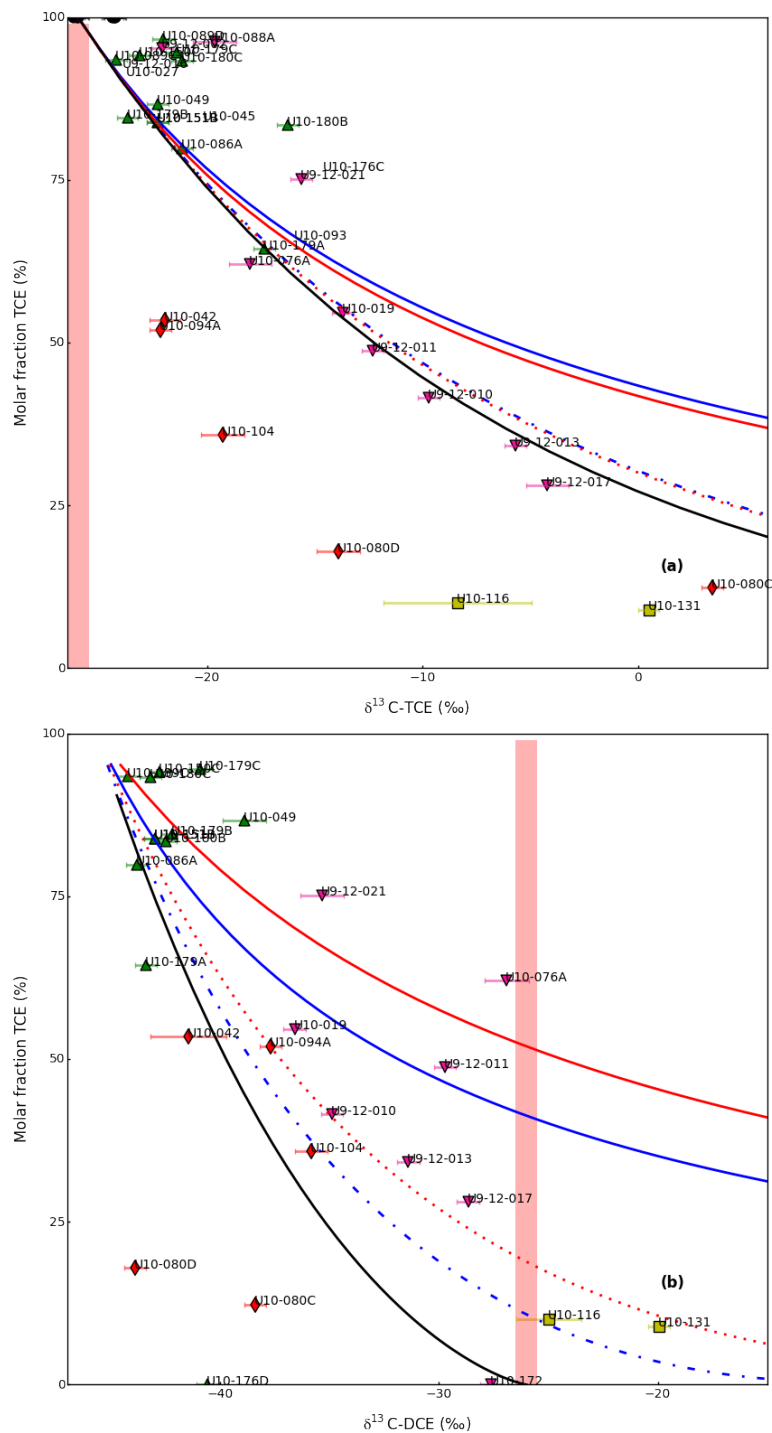


Fig. 6.10AB. Scenario 2 (Table 6.2): RD of TCE with DCE oxidation model (blue dashed, $k_{DCE} = 0.2 \times k_{TCE}$; blue solid, $k_{DCE} = 1 \times k_{TCE}$) versus TCE, DCE reductive dechlorination followed by quick VC oxidation model (red dashed, $k_{DCE} = 0.2 \times k_{TCE}$; red solid, $k_{DCE} = 1 \times k_{TCE}$). A) C isotope ratios of TCE vs. molar fraction of TCE; B) C isotope ratios of cis-DCE vs. molar fraction of TCE. Black line represents the model with TCE reductive dechlorination only (Scenario 1). Symbols: identical as in Fig. 6.9.

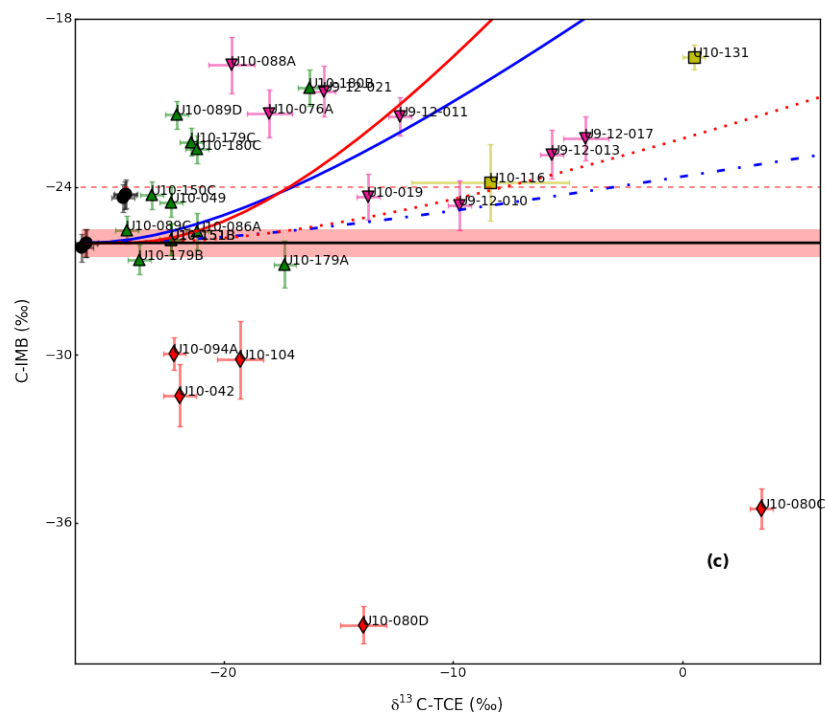


Fig. 6.10C. Scenario 2 (Table 6.2): RD of TCE with DCE oxidation model (blue dashed, $k_{DCE} = 0.2 \times k_{TCE}$; blue solid, $k_{DCE} = 1 \times k_{TCE}$) versus TCE, DCE reductive dechlorination followed by quick VC oxidation model (red dashed, $k_{DCE} = 0.2 \times k_{TCE}$; red solid, $k_{DCE} = 1 \times k_{TCE}$). C) C-IMB vs. C isotope ratios of TCE. Black line represents the model with TCE reductive dechlorination only (Scenario 1). Symbols: identical as in Fig. 6.9.

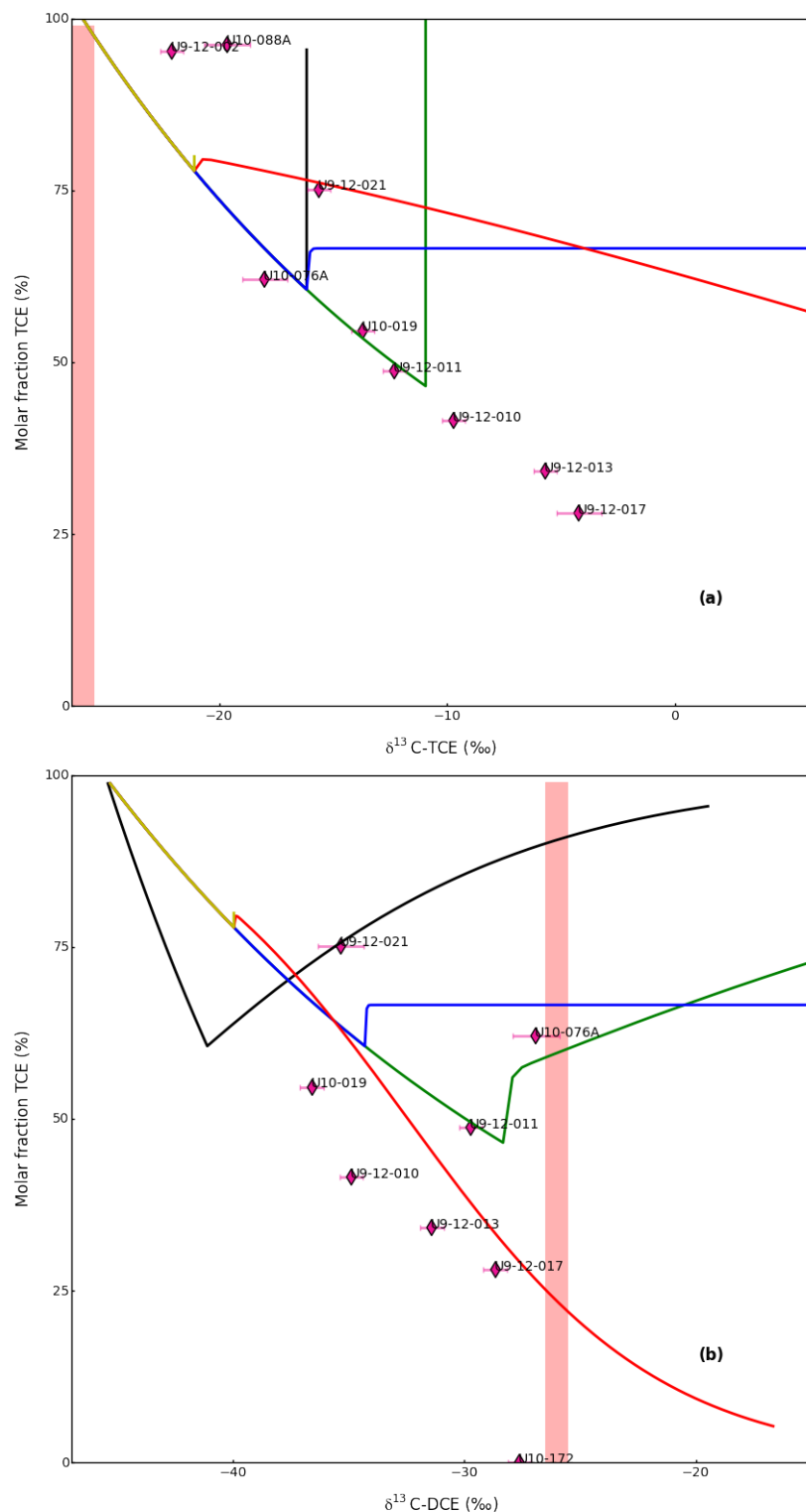


Fig. 6.11AB. Scenario 3 (Table 6.2): Sequential RD/oxidation model. Shallow Plume data only. A) C isotope ratios of TCE vs. molar fraction of TCE; B) C isotope ratios of cis-DCE vs. molar fraction of TCE. Symbols: identical as in Fig. 6.9.

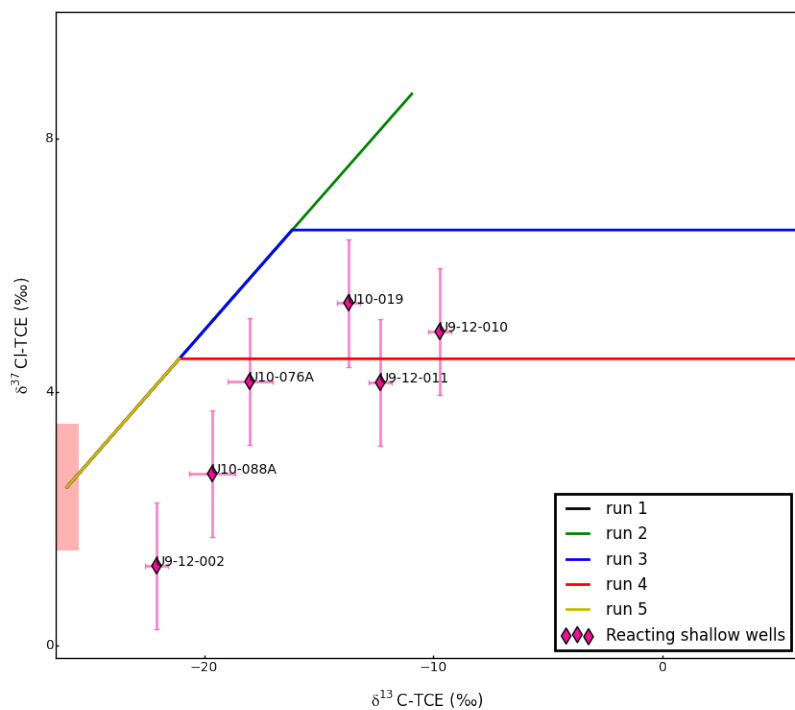
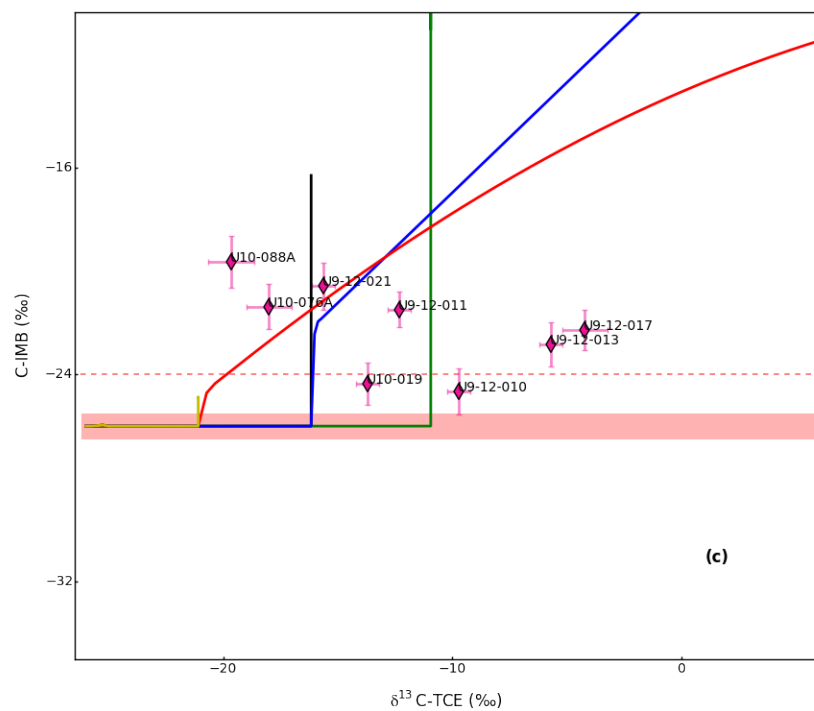


Fig. 6.11CD. Scenario 3 (Table 6.2): Sequential RD/TCE oxidation model. Shallow Plume data only.
C) C-IMB vs. C isotope ratios of TCE; D) Dual-element, C/Cl plot. Symbols: identical as in Fig. 6.9.

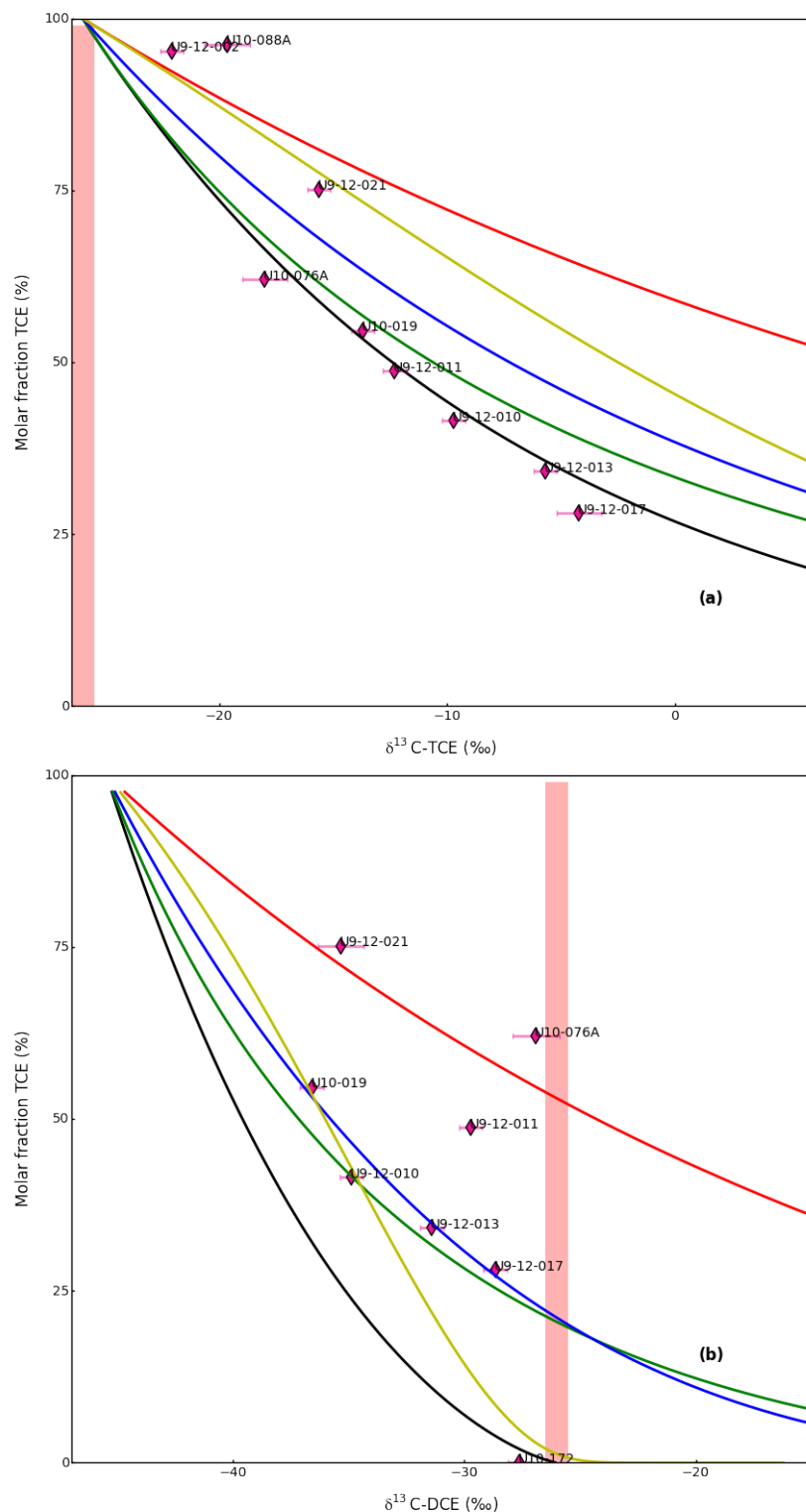


Fig. 6.12AB. Scenario 4 (Table 6.2): Simultaneous RD/TCE oxidation model. Shallow Plume data only. A) C isotope ratios of TCE vs. molar fraction of TCE; B) C isotope ratios of cis-DCE vs. molar fraction of TCE. Symbols: identical as in Fig. 6.9. Black line: RD of TCE only (Scenario 1) shown for reference.

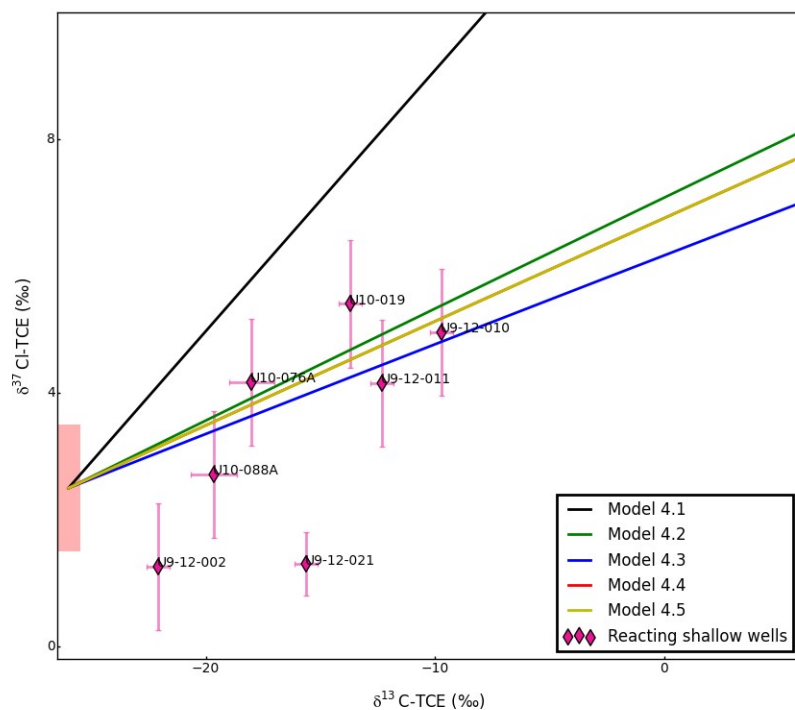
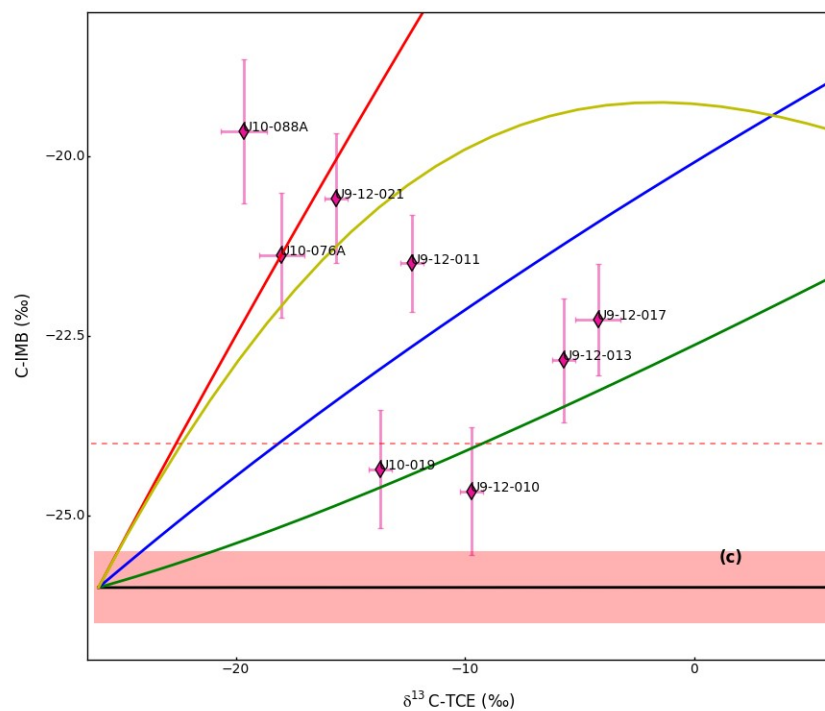


Fig. 6.12CD. Scenario 4 (Table 6.2): Simultaneous RD/TCE oxidation model. Shallow Plume data only. C) C-IMB vs. C isotope ratios of TCE; D) Dual-element, C/Cl plot. Symbols: identical as in Fig. 6.9. Black line: RD of TCE only (Scenario 1) shown for reference.

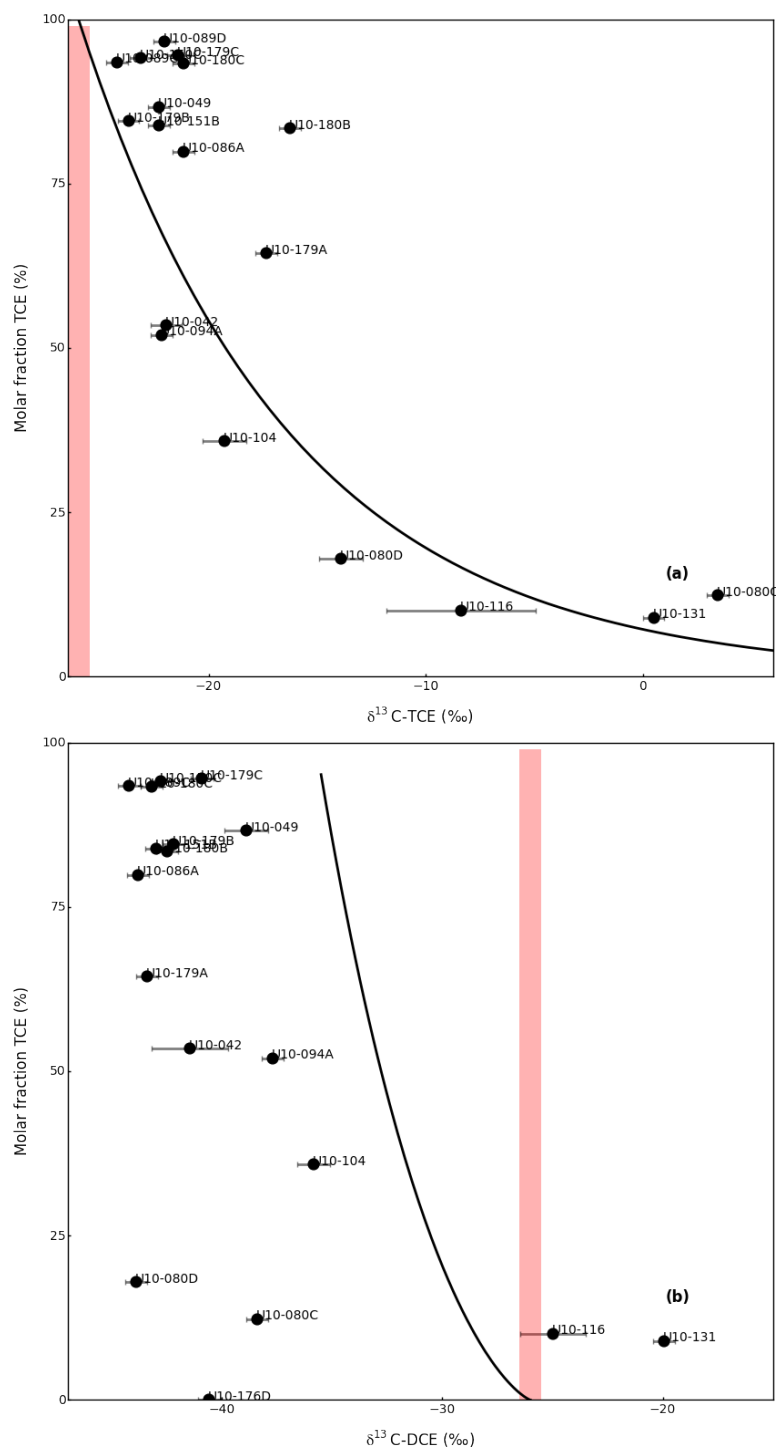


Fig. 6.13AB. Scenario 5 (Table 6.2): Model for TCE reductive dechlorination only, using a lower value of carbon isotope effect (epsilon = -10 ‰). Deep Plume only. A) C isotope ratios of TCE vs. molar fraction of TCE; B) C isotope ratios of cis-DCE vs. molar fraction of TCE. The shaded rectangle represents the carbon TCE source signature's uncertainty range. Symbols depict individual monitoring wells in the Deep Plume.

6.6 PERFORMANCE OBJECTIVE 6: USE CSIA/MODEL TECHNOLOGY TO DEMONSTRATE THE PRESENCE OF MULTIPLE DEGRADATION PATHWAYS

As discussed in Section 6.5, in the process of “classic” evaluation of concentration and CSIA data, followed by the scenario modeling, we obtained evidence of several biodegradation mechanisms and physical processes contributing to contaminant attenuation at the site.

The initial lines of evidence were: (i) the dual-isotope CSIA (cf. Figures 6.7 and 6.8), used to identify the patterns of two-element (C, Cl) isotope fractionation consistent with known degradation/attenuation mechanisms, and (ii) calculation of C-IMB for the sum of CEs, individually for each sample, to identify oxidation of the RD dechlorination products. The next level of mechanism identification was the scenario modeling, performed to resolve ambiguities in the initial evidence. The results are summarized below:

1. **Reductive dechlorination of TCE in Shallow and Deep Plumes.** Dual-isotope CSIA provided strong evidence of RD occurring in both plumes. Direct validation of that interpretation by the model was not necessary, but model scenarios combining RD with oxidation of RD products and/or TCE permitted to assess the relative significance of RD in the overall degradation budget.
2. **Degradation of cis-DCE in Shallow and Deep Plumes.** In the Shallow plume, the evidence from the enriched C-IMBs was consistent with model results. Together, the “classic” CSIA and the model permitted a robust confirmation of cis-DCE degradation. In the Deep Plume, the evidence was more ambiguous. Due to significant element of diffusion/back-diffusion, C-IMB data varied significantly, in particular in the E/NE section of the plume where several depleted readings of C-IMB were obtained. Scenario simulations involving DCE degradation appear to fit only certain individual wells, but the overall fit to the data set is poor.
3. **Oxidation of TCE in Shallow Plume.** Only one well (U9-12-021) produced isotope signatures consistent with significant contribution of TCE oxidation. The evidence from dual-element CSIA was confirmed by the model results. Scenario modeling excludes significant overall contribution from oxidation mechanisms that are known to produce relatively strong isotope fractionation (e.g., cometabolic degradation by toluene oxygenase organisms). However, as discussed in the previous section, we cannot exclude TCE oxidation is occurring if the associated isotope fractionation factor is minimal.
4. **TCE mass attenuation by diffusion out of the mobile porosity in Shallow Plume.** Strong evidence of TCE mass removal by diffusion is provided by dual-element CSIA (Figure 6.7). The 0-D model used in this study does not address that process.
5. **Diffusion/back-diffusion of CEs in Deep Plume.** Anomalous C-IMB values recorded for several wells in the Deep Plume and problems with fitting the simulations suggest that the isotope ratios and concentrations of TCE and DCEs are affected by non-degradative processes that are not included in the model. In the Deep Plume the difficulties are likely caused by diffusion/back-diffusion.

Conclusions

- Consistent conclusion from “classic” CSIA and the modeling provide the most robust mechanism identification.
- Degradation and non-degradative pathways can be identified.
- Existing model is not adequate for accurate simulation of certain data sets. In the Deep Plume, the role of diffusion/back-diffusion appears to be too significant to accurately apply the 0-D modeling approach.

6.7 PERFORMANCE OBJECTIVE 7: ESTIMATE DEGRADATION CONSTANTS FOR CONTAMINANTS OF CONCERN AT DEMONSTRATION SITE

In 0-D modeling, the field degradation rates are not obtained directly from the simulation but can be estimated indirectly, using the extent of overall CEs degradation and the time elapsed since the onset of degradation at given monitoring wells, using Eq. 6, where A is the groundwater age at the sampling location (years), and f_{CE} , the fraction of the remaining contaminant (TCE, DCE, or the total CEs). In principle, this is the approach of CSIA-based calculation of the rates of degradation that was already described by various authors, including in Sections 4.3 and 4.4 of the CSIA Guidance Document published by USEPA (USEPA, 2008).

$$k_{CE} = -\frac{\ln(f_{CE})}{A} \quad (\text{Eq. 6})$$

Using Eq. 6 is most straightforward for evaluation of the primary contaminant (TCE at this site), because f_{CE} is directly calculated by the Rayleigh equation (Eq. 3, Section 2.1.1). To calculate f_{DCE} (DCE degradation product), $\delta^{13}C_{DCE,0}$ must be obtained first, using Eq. 7 (Hunkeler et al., 2005).

$$\delta^{13}C_{DCE,0} = \delta^{13}C_{TCE,0} + \frac{\varepsilon_{TCE \rightarrow cDCE} \cdot f_{TCE} \cdot \ln(f_{TCE})}{1 - f_{TCE}} \quad (\text{Eq. 7})$$

The values of enrichment factors for Eq. 3 and Eq. 7 can be taken from the modeling, given that the model fitted the field data. If that is not possible, conservative values of enrichment factors should be taken from the literature, to avoid over prediction of the extent of degradation (USEPA, 2008).

Finally, cumulative mineralization of CEs (inclusive of the parent CE and the RD products) can be also obtained, using Eq. 8 (f_{CEs} is the cumulative fraction of all CEs remaining after degradation). For TCE and DCE, Eq. 8 is written as:

$$f_{CEs} = 1 - (1 - f_{TCE})(1 - f_{DCE}) \quad (\text{Eq. 8})$$

Figure 6.14 shows an example of model-assisted estimation of the fraction of mineralized (oxidized) CEs. The modeled reference lines are based on model Scenario 2 (RD of TCE combined with oxidation of RD products, see Tables 6.3 and 6.4 for model characteristics). It should be noted that Fig. 6.14 is not absolutely quantitative even if the reference model displayed good fit to the field data. Calculation of the remaining fraction of the contaminant (f in Eq. 3) is sensitive to the chosen value of the enrichment factor. In the present case, no analysis was performed on the goodness of model fit for a wider range of enrichment factors.

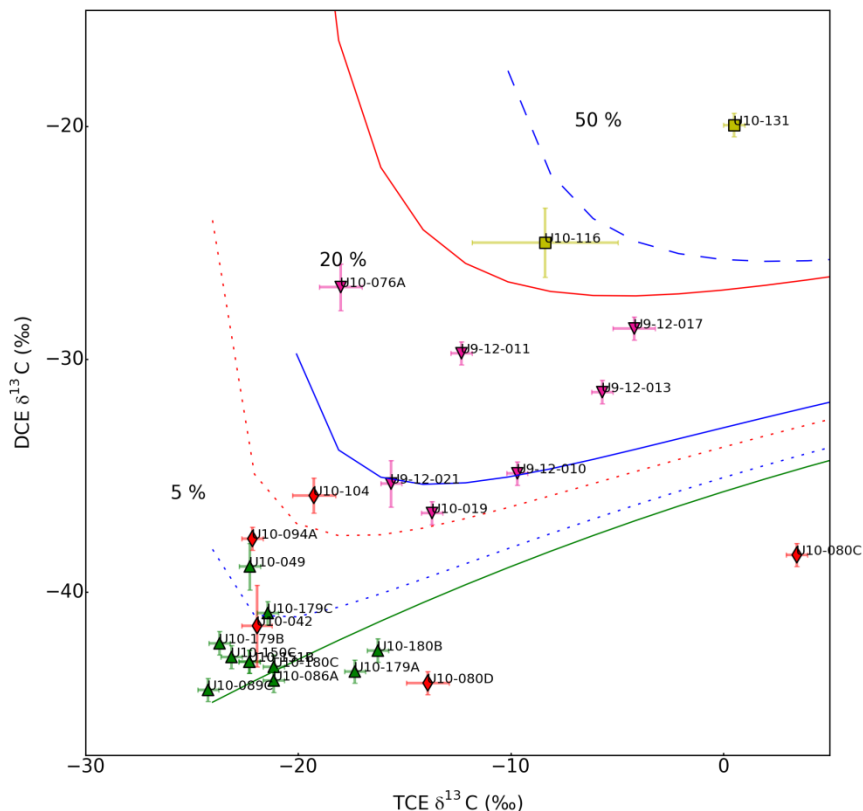


Figure 6.14. Estimation of cumulative CEs mineralization, comparing observed values (symbols) with the modeled contour lines of the percentage of total CEs mineralization. The modelled lines are based on model Scenario 2, where RD of TCE was followed by DCE reductive dechlorination followed by quick VC oxidation (red), or DCE reductive dechlorination was followed directly by DCE oxidation (blue). The percentage of mineralization: short dashes, 5 %; solid lines, 20 %; long dashes, 50 %. As a reference, a contour line of the model without further DCE transformation is shown in green (this model represents 0 % of mineralization). Symbols depict individual monitoring wells: Shallow Plume (pink); western part of the Deep Plume (green); wells with depleted C-IMB, E/NE area of the Deep Plume (red); wells with enriched C-IMB, E/NE area of the Deep Plume (yellow). Note that based on the model fit quality discussed in Section 6.5, the most reliable data are those from the Shallow Plume and the western part of the Deep Plume.

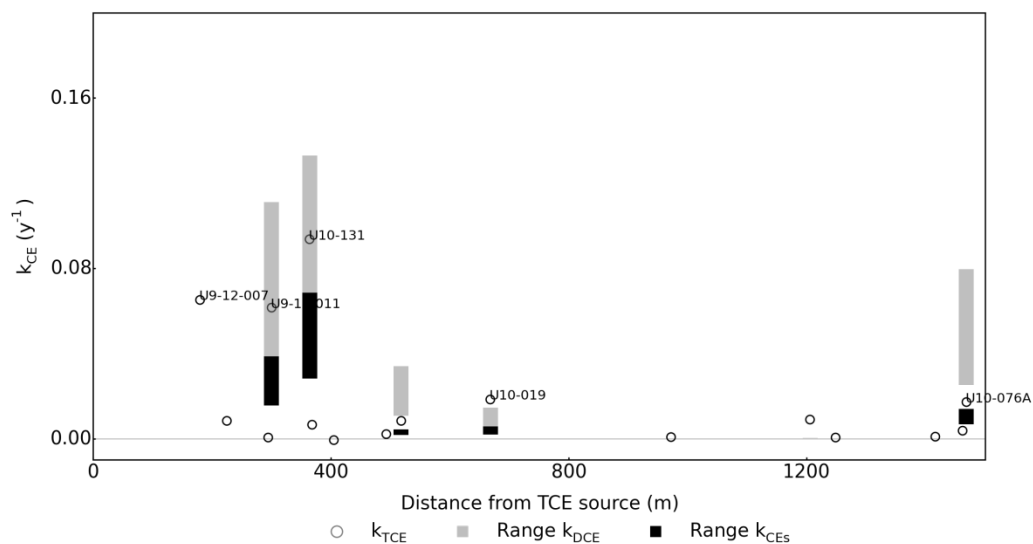


Figure 6.15. First-order integral degradation rate constants. TCE (circles), DCE (grey bars), and CEs mineralization (black bars). Bars indicate the range obtained with different model parameters for low-fractionating oxidative degradation of DCE (upper end) and for high-fractionating reductive degradation of DCE (lower end). Both shallow and deep wells are included. Age of groundwater was obtained by tritium-helium dating (cf. Figure 6.6 and Table C8) Note that the rate constants represent average values along the flow paths leading to the specific monitoring wells.

Figure 6.15 shows the results from applying Eq. 6 to calculate the first-order degradation rate constants using the Demonstration Site data. The calculated rate constants confirmed the presence of ‘hotspots’ of degradation, where TCE and DCEs degrade at relatively high rates, as opposed to the rest of the aquifer, where $\delta^{13}\text{C}$ enrichments are limited and the CEs degradation rate constants are generally low. Rate constants determined in this heterogeneous aquifer using groundwater ages might over- or underestimate the localized degradation rate constants. Large degradation rate constants close to the source, in the vicinity of the aquitard, are likely overestimated by back-diffusion of highly degraded and thus enriched TCE and DCE from clay into water with relatively recent age. However, generally it can be assumed that degradation occurs in local zones and thus the obtained integral rate constants underestimate the true rates at these local hotspots. A more conservative approach, similar to the standard CSIA data evaluation protocol, would be to use the age of the spill as the maximum age of the contaminant (see Sections 4.3 and 4.4 of the CSIA Guidance Document published by USEPA; USEPA, 2008).

Conclusions

- The main benefit of the 0-D model is a decrease of uncertainty of the applicable range of enrichment factors.
- The modeling permitted a quantitative assessment of the fate of the RD intermediates (cf. Figure 6.14). “Classic” CSIA-based assessment of the fate of the RD intermediates is qualitative.

- *The accuracy of the calculated rate constants improves for well-defined reaction mechanisms, with well-defined enrichment factors.*
- *The groundwater age is not directly representative of the time of degradation and introduces some uncertainty in the calculated degradation rate constants.*

6.8 PERFORMANCE OBJECTIVE 8: DEVELOP A NEW FRAMEWORK FOR INTERPRETING CSIA DATA

This element of performance was addressed by the User's Guide deliverable, published online in 2014. The Guide summarizes the "classic" CSIA data interpretation and then describes in detail the modeling methods for CSIA data interpretation. The Guide also includes a Case Study (Appendix A), discussing the interpretation of results from the Demonstration Site. The model templates (Cases 1-4, described in the User's Guide and available for download) can be tailored to the site specific conditions for future applications.

6.9 PERFORMANCE OBJECTIVE 9: REFINE CSM FOR DEMONSTRATION SITE

The conclusions from characterization of CEs attenuation in the Shallow and Deep Plumes are summarized here, following Sections 6.5, 6.6 and 6.7. That information contributes to the existing CSM of the Demonstration Site. The type of information obtained is relatively similar to that provided by the "classic" CSIA, with the most significant added benefit of more accurate quantitative conclusions regarding the degradation rates and the extent of contaminant mass attenuation.

Shallow Plume assessment

- *Model results confirm that cis-DCE is degrading (most likely, by cometabolic oxidation). The element of cis-DCE degradation is necessary in the model to fit the field cis-DCE results.*
- *The model combining reductive dechlorination of TCE and relatively slower degradation of the RD products yields a very good fit to the field TCE data and a reasonable fit to the DCE data.*
- *Introduction of TCE oxidation into the model helps to explain the CSIA results for well U9-12-021. That sample's isotope ratios and the observed concentrations appear to be consistent with the effects of combined reductive dechlorination of TCE and aerobic degradation of both TCE and DCE.*
- *For most wells, there is no clear evidence of TCE oxidation.*
- *Oxidation of TCE cannot be excluded, but the present results imply that (i) the degradation process would have to be associated with minimal isotope fractionation (such as reported for cometabolic sMMO organisms, but not the organisms utilizing toluene oxygenases); and (ii) at least for the wells that were discussed in the preceding section, the rates of TCE and cis-DCE oxidation would have to be closely balanced to maintain the observed RD-like data pattern (such balance is unlikely to be consistent for several discrete monitoring points situated in different sections of the plume).*
- *Note that the present discussion does not concern the Shallow Plume wells that were not exhibiting C isotope fractionation. TCE in those wells was not affected by RD. If TCE*

oxidation occurred, it must have been limited or the degradation pathway did not involve isotope fractionation (the enrichment factor of the aerobic degradation would be near zero).

- *In addition to TCE degradation, the Shallow Plume shows isotope signatures of significant TCE mass attenuation by diffusion out of the mobile porosity.*

Deep Plume assessment

- *Model results are consistent with a major role of RD of TCE.*
- *The model results concerning the fate of degradation products and potential oxidation of TCE are inconclusive.*
- *Significant problems with fitting the simulation results for various reaction chain scenarios to the field data suggest that the concentrations and isotope ratios of the contaminants in the mobile porosity are largely controlled by back-diffusion from clay layers.*

Reaction mechanism identification

- *Consistent conclusion from “classic” CSIA and the modeling provide the most robust mechanism identification.*
- *Degradation and non-degradative pathways can be identified.*
- *Existing model is not adequate for accurate simulation of certain data sets. In the Deep Plume, diffusion/back-diffusion appears to be too significant to apply the 0-D modeling approach.*

Estimates of degradation constants

- *The main benefit of the 0-D model is a decrease of uncertainty of the applicable range of enrichment factors.*
- *The modeling permitted a quantitative assessment of the fate of the RD intermediates (cf. Figure 6.14). “Classic” CSIA-based assessment of the fate of the RD intermediates is qualitative.*
- *The accuracy of the calculated rate constants improves for well-defined reaction mechanisms, with well-defined enrichment factors.*
- *The groundwater age is not directly representative of the time of degradation and introduces some uncertainty in the calculated degradation rate constants.*

The relative contribution of the modeling to reach those conclusions varied. On qualitative level, “classic” CSIA permitted relatively similar site data interpretation. The main benefits of the model were:

1. In the Shallow Plume, the 0-D model was a good approximation of the transformations of the contaminants of concern. For that data set, validation of the conclusions from the “classic” lines of CSIA evidence (e.g., mechanism identification using the dual-element CSIA plot) and then by validation of the proposed degradation scenarios by means of modeling was informative and strengthened the final conclusion.
2. Modeling (scenario testing) can be applied as a negative evidence (to confirm the absence or insignificance of given reaction mechanism or scenario). For example, the potential for

TCE oxidation (specifically, cometabolic oxidation by toluene oxygenase that is known to result with significant carbon isotope fractionation) appears to be small after scenario modeling (Section 6.5). This conclusion could not be reached using the “classic” approach (compare Figures 6.7A vs. 6.7B).

3. Possibly the most valuable contribution of the modeling is the improved precision of quantitative assessment of biodegradation, for the RD intermediates (cf. Figure 6.14), and for the parent CEs. Modeling helps to constrain the values of enrichment factors needed to calculate the extent of contaminant degradation (Equations 3 and 8). Typically, estimates of degradation rates obtained from CSIA are highly conservative. The chance of a major underestimate of degradation increases for the degradation pathways associated with a large variability of isotope effects among different degraders utilizing that pathway. For example, the reported range of enrichment factors in RD of TCE is very wide, varying from -2.5 to -19 ‰ (Appendix B, ESTCP ER-201029, User’s Guide). Modeling helped to restrict the \pm uncertainty of the field site-specific enrichment factors and to improve the precision of the calculated extent of biodegradation.

7.0 COST ASSESSMENT

7.1 COST MODEL

The cost analysis is based on actual costs of tasks completed for this project. The scale of the present demonstration was significantly larger than the anticipated scale of routine applications for support of MNA as a selected remedy. In routine application, fewer samples will be collected and analyzed and two-element or three-element CSIA data will be required only on a case-specific basis. Where possible, costs below are reported on a modular basis (e.g. per sample or per labor hour) to support cost estimates for CSIA projects.

The cost estimates are based on the following assumptions:

- The initial site characterization and conceptual site model (CSM) have been completed and the site is in the remedial investigation phase for selecting an MNA remedy;
- Groundwater samples are collected from existing wells or sampling locations. Cost estimate do not include installation of additional temporary or permanent monitoring locations.
- The cost estimates assume that the CSIA is performed by a commercial lab charging fixed price per sample (the cost of method development is not included).
- The cost estimates assume that data interpretation and modeling are performed by trained consultants and that the model will be implemented similarly to the present study, using the 0/1-D option.
- Cost of software training and additional software (e.g. GIS software, MODFLOW-based modeling software) is not included in the estimates.

Cost Elements: Project planning

Project planning should consider available site data and a comprehensive CSM to decide if CSIA and or CSIA/modeling are necessary. The decision to use CSIA to support remedial decision making should be based on uncertainties surrounding the rate of degradation of VOCs at various locations within the subsurface. Project planning should include articulation of clear sampling goals and data quality objectives (DQOs) for the CSIA program. Goals and objectives for a CSIA program targeted to supporting selection of an MNA remedy should include rationale for analytes and sampling locations including hydrogeologic intervals (e.g. saturated units, fine or coarse-grained sediments), as well as high and low concentration areas of the plume. Given the high cost CSIA, preliminary evaluation of the CSM and goals of the study by a trained consultant is recommended.

Cost Elements: Groundwater Sampling

Groundwater samples are typically collected from pre-existing monitoring wells. Costs associated with groundwater sampling include mobilization of the sampling crew to the site, supplies and equipment usage for sampling and shipping of samples to the laboratory for analysis. For the cost analysis, the sampling cost is expressed as \$/well. For CSIA work the cost of groundwater sampling can be lowered by collecting the CSIA samples during the routine site monitoring events. Work performed at the demonstration site included sampling by both permeable diffusion bags (PDBs) and low-flow techniques. Cost estimates for sampling are based on average costs incurred during the demonstration project.

Cost Elements: Laboratory Analyses

Laboratory analyses include: (i) concentration analysis by conventional methods (e.g., USEPA 8260); (ii) CSIA; and (iii) optionally, groundwater geochemistry parameters. Cost saving is possible if CSIA sampling is coordinated with routine site assessment sampling including contaminant concentration and geochemistry parameters analysis, to avoid duplication of those analyses. Typically, the analyses will be provided by a commercial laboratory (or laboratories, if separate facilities are used for CSIA and for the routine analyses) on price per sample basis. Price per sample depends on the scope of analysis (the list of target analytes, the isotope ratios requested, and the type of sample matrix). No additional cost for method development should be included for routine projects.

Cost Elements: Data Interpretation

CSIA data have to be interpreted and reported to the end user, typically, within the context of the protocols laid out by the EPA (USEPA, 1998; USEPA, 2008). CSIA will likely be chosen as a tool when results of data collected as per the EPA *Technical Protocol for Evaluating Natural Attenuation of Chlorinated Solvents in Groundwater* (USEPA, 1998) are inconclusive or do not provide sufficient detail to identify rates of decay. The results from that first-stage CSIA interpretation would serve to justify (or not) proceeding with the modeling. The modeling effort for routine application includes adaptation of the existing model to site-specific parameters, scenario testing and data interpretation. CSIA interpretation and modeling costs can be estimated using the number of hours spent and the average consultant costs.

Table 7.1. Cost model for a CSIA/model application

Cost Element	Data Tracked
Project Planning	Unit Cost: \$ per labor hour <ul style="list-style-type: none"> • Labor hours for CSM review and sampling objectives • Labor hours for developing Sampling and Analysis Plan (SAP)
Groundwater Sampling	Unit Cost: \$ per monitoring well <ul style="list-style-type: none"> • Mobilization and sampling, including personnel labor, sampling supplies and shipping of the samples to the laboratory
Laboratory Analysis	Unit Cost: \$ per analysis <ul style="list-style-type: none"> • Number of routine concentration analyses • Number of CSIA analyses • Number of groundwater geochemistry parameter analyses
Data Interpretation	Unit Cost: \$ per labor hour <ul style="list-style-type: none"> • Labor hours for preliminary (‘classic’) CSIA interpretation (consultant) • Labor hours for modeling CSIA data (consultant) • Labor hours for reporting CSIA results (consultant)

7.2 COST DRIVERS

The main cost drivers are: (i) the total cost of CSIA per sample, which depends on the isotope ratios determined and on the analytical techniques involved; (ii) the size and complexity of the study site, defining the number of samples to be collected and analyzed. The cost of data interpretation and reporting will be relatively low in comparison with the total cost of sample collection and laboratory analysis.

Cost of CSIA per sample

Unlike conventional VOCs concentration analysis, the CSIA cost per sample varies significantly, depending on the number of target analytes and on the isotope ratios to be determined. The costs in Table 7.2 are based on the current commercial service prices at the OU laboratory.

Number of samples collected

The USEPA guide for CSIA (USEPA, 2008) recommends collecting 12-20 samples from separate monitoring wells for “classic” CSIA projects. If CSIA data modeling is potentially to be used, the number of samples should probably fall close the maximum of the recommended range. Model fitting works best is the simulation is matched vs. a group of field data, to identify common mechanisms affecting the target contaminants. Results from modeling of smaller data sets may be also useful, if the tested scenarios are relatively simple and the hydrogeology conditions suggest low heterogeneity.

Table 7.2. CSIA, cost per sample (based on current costs at the OU laboratory)

	C CSIA	Cl CSIA	H CSIA	Total for three-element CSIA
Standard methodology, single target compound (e.g., only TCE)	\$400	\$400	\$400	\$1200
Standard methodology, two target compounds (e.g., TCE + cis-DCE)	\$450	\$450	\$450	\$1350
Standard methodology, three target compounds (e.g., TCE+cis-DCE+vinyl chloride)	\$500	\$500	\$500	\$1500
2D-GC methodology, single target compound (e.g., only TCE)*	\$400	- **	\$400	\$800**
* 2D-GC cost applies at per compound basis. 2D-GC may be required if a high-priority sample contains significant load of non-target VOCs, e.g., for commingled plumes of CEs and gasoline; **2D-GC is usually not required for Cl CSIA, due to different isotope ratio detection approach.				

7.3 COST ANALYSIS

Cost analysis is shown for three hypothetical Case Studies utilizing methodology similar to that applied at the Demonstration Site (C, or C+Cl CSIA, 0-D modeling). The cost is compared to the cost of conventional MNA sampling and analysis and to the cost of bench top-scale biodegradation testing (microcosms). The rationale of the comparison with MNA is to illustrate the added cost of the CSIA/modeling in the overall site assessment expenditures. CSIA provides evidence supporting MNA, but it does not replace the need for conventional MNA monitoring. The rationale of cost comparison between CSIA and a microcosm test is that both provide evidence of biodegradation in support of MNA. However, the choice between the two approaches should not be based exclusively on the cost, since the potential information gained from the two approaches is not fully equivalent.

Case 1: Evaluation of a simple data set to detect evidence of TCE RD. 10 samples are collected. C CSIA is conducted for TCE and for cis-DCE (Table 7.3).

Case 2: Evaluation of a simple data set to answer whether RD stalls at cis-DCE or whether cis-DCE is also mineralized. 10 samples are collected. C and Cl CSIA are conducted for TCE and for cis-DCE (Table 7.4).

Case 3: Evaluation of a large data set, for evidence of competing degradation mechanisms. The site scenario is somewhat similar to the Shallow Plume at Hill AFB, OU10 discussed in this report. 20 samples are collected. C and Cl CSIA are conducted for TCE, cis-DCE and VC. C CSIA is also conducted for ethene (Table 7.5).

The cost analysis demonstrates that CSIA and CSIA/modeling (totals include sample collection, analysis and interpretation) compare favorably with standard MNA sampling (cost of 3 year, semiannual sampling and lab analyses) and significant cost saving is possible if sample collection and routine analytical work is integrated into scheduled site monitoring activities. The added cost of modeling conducted by a consultant who is already set for this type of work is relatively minor in comparison of the total cost of implementation.

The cost of CSIA/modeling at relatively simple sites (Cases 1 and 2, Tables 7.3 and 7.4) is lower or similar to the cost of a simple bench-scale microcosm test of biodegradation. The cost of a CSIA study of a large site (Case 3, Table 7.5) is significantly higher than that of a small-scale microcosm study. However, CSIA/modeling provides much more information than simple verification of the biodegradation potential. Also, note that the main cost driver in microcosm work is the number of experimental variables to be tested and the number of samples collected and analyzed over the period of microcosms incubation. The monitoring cost for a long-term microcosm study, or a study involving setting up experiments with multiple sediment samples, would easily exceed the estimate for CSIA/modeling.

Table 7.3. Cost analysis: Case 1. CSIA and microcosms: single event; MNA: 3 years

Cost element	Cost Unit (CSIA, MNA)	No. units	Subtotal Classic CSIA	Subtotal CSIA+ model	Subtotal MNA (3 yrs, semiannual)	Subtotal Microcosm Study
Project Planning	\$150/hour	4	\$600	\$600	\$ 600	\$ 600
Samples Collection	\$100/well (MNA)	10	-	-	\$ 6,000	\$6,000*
	\$125/well (CSIA)	10	\$1,250	\$1,350	-	
Laboratory Analysis	\$100/sample; VOCs (8260) and geochemistry.	10	\$1,000	\$1,000	\$6,000	\$1,500***
	\$450/sample; CSIA	10	\$4,500	\$4,500	-	-
Data Interpretation	\$150/hour ("classic" CSIA)	15	\$2,250	\$2,250	\$6,000**	\$3,000
	\$180/hour (modeling)	15	-	\$2,700		
TOTAL			\$9,600	\$12,400	\$18,600	\$11,100
TOTAL (sampling cost excluded) ****			\$7,600	\$10,050		

*Includes setup of Laboratory Microcosm; ** Data reporting tables and figures over 3 years; *** A minimum of 15 samples (3 trials with 5 samples each); ****Assumes the sample collection and VOCs data are shared with the routine site assessment. Monitoring well mobilization cost and standard VOCs and geochemistry analyses are removed from the total.

Table 7.4. Cost analysis: Case 2. CSIA and microcosms: single event; MNA: 3 years

Cost element	Cost Unit	No. units	Subtotal Classic CSIA	Subtotal CSIA+ model	Subtotal MNA (3 yrs, semiannual)	Subtotal Microcosm Study
Project Planning	\$150/hour	4	\$600	\$600	\$600	\$600
Samples Collection	\$100/well (MNA)	10	-	-	\$ 6,000	\$6,000*
	\$125/well (CSIA)	10	\$1,250	\$1,250	-	
Laboratory Analysis	\$100/sample; VOCs concentrations and geochemistry	10	\$1,000	\$1,000	\$6,000	\$1,500***
	\$900/sample; CSIA (see Table 7.2 for further cost details)	10	\$9,000	\$9,000	-	-
Data Interpretation	\$150/hour (“classic” CSIA)	15	\$2,250	\$2,250	\$6,000**	\$3,000
	\$180/hour (modeling)	15	-	\$2,700		
TOTAL			\$14,100	\$16,800	\$18,600	\$11,100
TOTAL (sampling cost excluded)****			\$12,100	\$14,800		

*Includes setup of Laboratory Microcosm; ** Data reporting tables and figures over 3 years; *** A minimum of 15 samples (3 trials with 5 samples each); ****Assumes the sample collection and VOCs data are shared with the routine site assessment. Monitoring well mobilization cost and standard VOCs and geochemistry analyses are removed from the total.

Table 7.5. Cost analysis: Case 3. CSIA and microcosms: single event; MNA: 3 years

Cost element	Cost Unit	No. units	Subtotal Classic CSIA	Subtotal CSIA+ model	Subtotal MNA (3 yrs, semiannual)	Subtotal Microcosm Study
Project Planning	\$150/hour	6	\$900	\$900	\$600	\$600
Samples Collection	\$100/well (MNA) \$125/well (CSIA)	20 20	- \$2,500	- \$2,500	\$12,000 -	\$6,000*
Laboratory Analysis	\$100/sample; VOCs concentrations and geochemistry	20	\$2,000	\$2,000	\$12,000	\$1,500***
	\$1050/sample; CSIA (see Table 7.2 for further cost details)	20	\$21,000	\$21,000	-	-
Data Interpretation	\$150/hour ("classic" CSIA)	30	\$4,500	\$4,500	\$6,000**	\$3,000
	\$180/hour (modeling)	30	-	\$5,400		
TOTAL			\$30,900	\$36,300	\$30,600	\$11,100
TOTAL (sampling cost excluded)****			\$26,900	\$32,300		
*Includes setup of Laboratory Microcosm; ** Data reporting tables and figures over 3 years; *** A minimum of 15 samples (3 trials with 5 samples each); ****Assumes the sample collection and VOCs data are shared with the routine site assessment. Monitoring well mobilization cost and standard VOCs and geochemistry analyses are removed from the total.						

Qualitative Cost Analysis

The main driver for the use of MNA is the relatively lower cost of that remedy in comparison with active remedies, such as pump and treat or permeable reactive barriers (PRB). CSIA data can provide strong evidence for selecting an MNA remedy, through a demonstration of degradation processes even in the absence of daughter products. Accelerated selection of MNA in lieu of active remedies could lower or eliminate the expenses of remedy installation and operating costs. CSIA can be also used alongside PBR or other in situ remedies, to document the efficacy of degradation processes. For example, CSIA data can provide support for assessing the performance of remedies that rely on stimulating reductive dechlorination.

The scale of potential savings can be illustrated by a comparison to the cost of two typical remedies: (i) groundwater extraction and treatment (pump and treat), and (ii) permeable reactive barriers (PRBs). Note that the cost versus performance estimates for groundwater remedies vary widely depending on specific technologies used, hydrogeologic conditions, location and length of operation, among other factors.

- Pump and treat remedies can cost in the range of \$200,000 for initial design and installation with long-term treatment costs varying widely depending on treatment technologies and disposal requirements (Khan et al. 2004). Operation and maintenance costs can be on the order of hundreds of thousands of dollars per year.
- Passive remedies such as permeable reaction barriers (PRBs) can cost between \$1 M and \$1.5 M for design and installation, depending on the size and fill material (NAVFAC, 2012), but have little long-term associated O&M costs. In situ treatments to reduce the oxidation reduction potential in aquifers can have similar costs, depending on the size of the area treated and the number of mobilizations required to attain complete contaminant degradation.

Costs associated with an MNA remedy include collection of data to support selection of the remedy and routine monitoring, data management and reporting. Estimates of the cost of long-term well sampling and analysis are in the range of \$500 per sample (ER-1601, Final Report). Depending on the number of monitoring wells and the monitoring frequency, MNA remedy costs are in the range of several thousand to tens of thousands dollars per year as opposed to several hundred thousand dollars per year for active remedies such as pump and treat. Other than installation of monitoring wells, no significant capital costs are involved in MNA (unlike in the case of PRBs).

8.0 IMPLEMENTATION ISSUES

The interaction with the Demonstration Site is limited to collection of field samples (groundwater), and identical implementation issues apply as for routine site monitoring work. Therefore, no implementation issues are expected in regards of field sample collection. Also, from the point of view of the end user, no equipment or software procurement is involved.

Two potential implementation issues are: (i) availability of consultants with appropriate CSIA and modeling training; and (ii) availability of CSIA laboratory facilities. Currently, few consultants in the US specialize in CSIA data and probably no consultants specialize in isotope effect modeling. Self-training material provided in the in the User's Guide is intended to be the reference for consultants with general modeling background. Currently, few laboratories in the North America offer CSIA on commercial basis. Moreover, sample processing capability for certain types of CSIA samples is even more restricted. Therefore, the processing of CSIA samples is usually less timely than in the case of standard groundwater analytical data.

It is also possible that the implementation results may be inconclusive or the modeling may bring no additional benefit vs. "classic" CSIA. The preliminary stage of a routine application should be an assessment of available site data, to first decide that CSIA should be pursued. The cost

increment added by the modeling is relatively small in comparison with the cost of sample collection and CSIA. Moreover, once the CSIA data are available, the modeling of the data is not time-sensitive. The decision to pursue the modeling should be made based on the results from the “standard” CSIA data (are there uncertainties remaining that can be potentially resolved by scenario modeling?). Finally, the confidence of data interpretation, both in “classic” CSIA and in CSIA/modeling, require good understanding of isotope effects associated with degradation pathways to be investigated. Currently, relatively few publications are available on isotope effects of Cl and even more so, on isotope effects of H, in key degradation pathways relevant to CEs studies. Preliminary assessment of the site should consider what can be achieved, based on up-to date status of the subject literature.

9.0 REFERENCES

- Abe, Y. and D. Hunkeler (2006) Does the Rayleigh equation apply to evaluate field isotope data in contaminant hydrogeology? *Environ. Sci. Technol.* 40: 1588-1596.
- Abe, Y., R. Aravena, J. Zopfi, O. Shouakar-Stash, E. Cox, J. D. Roberts and D. Hunkeler (2009) Carbon and chlorine isotope fractionation during aerobic oxidation and reductive dechlorination of vinyl chloride and cis-1,2-dichloroethene. *Environ. Sci. Technol.* 43: 101-107.
- CH2MHILL (2009) Operable Unit 10 Remedial Investigation Report. Salt Lake City, UT, CH2M Hill for Air Force Center for Engineering and the Environment and Hill Air Force Base, Utah.
- CH2MHILL (2011) Hill AFB OU10 ERPIMS Database.
- D'Affonseca, F. M., H. Prommer, M. Finkel, P. Blum and P. Grathwohl (2011) Modeling the long-term and transient evolution of biogeochemical and isotopic signatures in coal tar-contaminated aquifers. *Water Resources Research* 47: W05518.
- Eckert, D., S. Qiu, M. Elsner and O. A. Cirpka (2013) Model complexity needed for quantitative analysis of high resolution isotope and concentration data from a toluene-pulse experiment. *environ. Sci. Technol.* 47: 6900-6907.
- ER-1601 (2013) New cost-effective method for long-term groundwater monitoring programs. Final Report. Available online at <https://www.serdp-estcp.org/Program-Areas/Environmental-Restoration/Contaminated-Groundwater/Monitoring/ER-1601>
- ER-201025 (2012) Use of compound specific stable isotope analysis to distinguish between vapor intrusion and indoor sources of VOCs. Laboratory Validation Report. Available online at <https://www.serdp-estcp.org/Program-Areas/Environmental-Restoration/Contaminated-Groundwater/Emerging-Issues/ER-201025/ER-201025>
- ER-201029 (2014) Integrated Stable Isotope – Reactive Transport Model Approach for Assessment of Chlorinated Solvent Degradation. User's Guide. Available online at <https://serdp-estcp.org/Program-Areas/Environmental-Restoration/Contaminated-Groundwater/ER-201029>
- Hunkeler, D., B. M., van Breukelen and M. Elsner (2009) Modeling chlorine isotope trends during sequential transformation of chlorinated ethenes. *Environ. Sci. Technol.* 43: 6750-6756.

- Hunkeler, D., R., Aravena and B. J. Butler (1999) Monitoring microbial dechlorination of tetrachlorethene (PCE) in groundwater using compound-specific stable carbon isotope ratios: microcosm and field studies. *Environ. Sci. Technol.* 33: 2733-2738.
- Jin, B., M. Rolle, T. Li and S. B. Haderlein (2014) Diffusive fractionation of BTEX and chlorinated ethenes in aqueous solution: Quantification of spatial isotope gradients. *Environ. Sci. Technol.* 48: 6141-6150.
- Karlsen, R. H., F. J. C. Smits, P. J. Stuyfzand, T. N. Olsthoorn and B. M. van Breukelen (2012) A post audit and inverse modeling in reactive transport: 50 years of artificial recharge in the Amsterdam Water Supply Dunes. *J. Hydrology* 454: 7-25.
- Khan, F. I., et al. (2004) An overview and analysis of site remediation technologies. *Journal of Environmental Management* 71: 95-122.
- Kuder, T. and P. Philp (2013) Demonstration of compound-specific isotope analysis of hydrogen isotope ratios in chlorinated ethenes. *Environ. Sci. Technol.* 47: 1461-1467.
- Kuder, T., B. M. van Breukelen, M. Vanderford and P. Philp (2013) 3D-CSIA: Carbon, chlorine, and hydrogen isotope fractionation in transformation of TCE to ethene by a *Dehalococcoides* culture. *Environ. Sci. Technol.* 47: 9668-9677.
- Lesser, L. E.; Johnson, P. C.; Aravena, R.; Spinnler, G. E.; Bruce, C. L.; Salanitro, J. P., An evaluation of compound-specific isotope analyses for assessing the biodegradation of MTBE at Port Hueneme, CA. *Environ. Sci. Technol.* 2008, 42: 6637-6643.
- Liang, X., Y. Dong, T. Kuder, L. R. Krumholz, R. P. Philp and E. C. Butler (2007) Distinguishing abiotic and biotic transformation of tetrachloroethylene and trichloroethylene by stable carbon isotope fractionation. *Environ. Sci. Technol.* 41: 7094-7100.
- Mak, K. S., Griebler, C., Meckenstock, R.U., Liedl R. and Peter A. (2006) Combined application of conservative transport modelling and compound-specific carbon isotope analyses to assess in situ attenuation of benzene, toluene, and o-xylene. *J. Contaminant Hydrology* 88: 306–320.
- NAVFAC (2012). Permeable reactive barrier cost and performance report. Naval Facilities Engineering Command. Available online at http://www.navfac.navy.mil/content/dam/navfac/Specialty%20Centers/Engineering%20and%20Expeditionary%20Warfare%20Center/Environmental/Restoration/er_pdfs/c/navfacesc-ev-tr-1207-cp-prb-201203.pdf.
- Prommer, H., B. Anneser, M. Rolle, F. Einsiedl and C. Griebler (2009) Biogeochemical and isotopic gradients in a BTEX/PAH contaminant plume: Model-based interpretation of a high-resolution field data set. *Environ. Sci. Technol.* 43: 8206-8212.
- Sakaguchi-Soder, K., J. Jager, H. Grund, F. Mattaus and C. Schuth (2007) Monitoring and evaluation of dechlorination processes using compound-specific chlorine isotope analysis. *Rapid Communications in Mass Spectrometry* 21: 3077-3084.
- Steeffel, C.I., Yabusaki, S.B. and U. Mayer (2015) Reactive transport benchmarks for subsurface environmental simulation. *Comput. Geosci.* 19: 439–443.
- USEPA (1998) Technical protocol for evaluating natural attenuation of chlorinated solvents in ground water. Washington DC, US Environmental Protection Agency.
- USEPA (2008) A Guide for assessing biodegradation and source identification of organic ground water contaminants using compound specific isotope analysis (CSIA) USEPA. Washington, DC, US Environmental Protection Agency Office of Research and Development National Risk Management Laboratory: 82.

- van Breukelen, B. M. and H. Prommer (2008) Beyond the Rayleigh equation: Reactive transport modeling of isotope fractionation effects to improve quantification of biodegradation. *Environ. Sci. Technol.* 42: 2457-2463.
- van Breukelen, B. M. and M. Rolle (2012) Transverse hydrodynamic dispersion effects on isotope signals in groundwater chlorinated solvents' plumes. *Environ. Sci. Technol.* 46: 7700-7708.
- van Breukelen, B. M., D. Hunkeler and F. Volkerling (2005) Quantification of sequential chlorinated ethene degradation by use of a reactive transport model incorporating isotope fractionation. *Environ. Sci. Technol.* 39: 4189 - 4197.
- van Breukelen, B. M., P.E. Stack, H. Thouement, M.Vanderford, P. Philp and T. Kuder (2016) Modeling 3D-CSIA data: Carbon, chlorine, and hydrogen isotope fractionation during reductive dechlorination of TCE to ethene. Submitted to *Environmental Science & Technology*.
- Wanner, P. and D. Hunkeler (2015) Carbon and chlorine isotopologue fractionation of chlorinated hydrocarbons during diffusion in water and low permeability sediments. *Geochimica et Cosmochimica Acta*, 157: 198-212.
- Wiegert, C., C. Aeppli, T. Knowles, H. Holmstrand, R. Evershed, R. D. Pancost, J. Macháčkova and Ö. Gustafsson (2012) Dual carbon–chlorine stable isotope investigation of sources and fate of chlorinated ethenes in contaminated groundwater. *Environ. Sci. Technol.* 46: 10918-10925.

APPENDICES

Appendix A: Points of Contact

POINT OF CONTACT Name	ORGANIZATION Name Address	Phone Fax E-mail	Role in Project
Paul Philp	Univ. of Oklahoma, 100 E. Boyd St., Norman Oklahoma 73019	405-325-4469 (phone) 405-325-3140 (fax) pphilp@ou.edu	PI Supervising the project
Tomasz Kuder	Univ. of Oklahoma, 100 E. Boyd St., Norman Oklahoma 73019	405-325-3253 (phone) 405-325-3140 (fax) tkuder@ou.edu	Co-PI Supervising the Analytical Lab
Boris van Breukelen	Delft University of Technology, Stevinweg 1, 2628 CN Delft, The Netherlands	+31-15-278-5227 (phone) b.m.vanbreukelen@tudelft.nl	Performer Developing the Models
Héloïse Thouement	VU University Amsterdam, De Boelelaan 1085, 1081 HV Amsterdam, The Netherlands	+31-20-5983851 (phone) h.a.a.thouement@vu.nl	Performer Developing the model, conducting data modeling
Mindy Vanderford	HydroGeoLogic, Inc., 4407 Jane St., Bellaire, Texas 77401	713-838-7778 (phone) mvanderford@hgl.com	Performer Supervising Field Program and Logistics

Appendix B: List of Software

This list summarizes the software used in the project. This list is a revised version of the information included in the User's Guide for this project.

PHREEQC – A one dimensional (1-D) geochemical transport model developed by the U.S. Geological Survey (USGS) that can also simulate irreversible kinetic reactions such as degradation of CEs. The software is free and can be downloaded from the following websites: http://wwwbrr.cr.usgs.gov/projects/GWC_coupled/PHREEQC/ (USGS web page; PHREEQC 3 version) or <http://pfw.antipodes.nl/download.html> (PHREEQC 2 for Windows version). All work for this project was done with the PHREEQC 2 but the models run as well with PHREEQC 3.

PHAST – 3-D groundwater flow and transport model capable of simulating the same set of reactions as PHREEQC. PHAST couples PHREEQC to the groundwater flow and solute transport model HST3D. PHAST is a practical platform to run 2-D simulations of plume cross-sections or even fully 3-D simulations. A freely available graphical user interface (GUI) is available. For simple conceptual models a GUI is however not needed. PHAST models are very simple to develop once the user understands the 1-D PHREEQC version of the model. PHAST can be downloaded at http://wwwbrr.cr.usgs.gov/projects/GWC_coupled/phast/

PHT3D – A three dimensional (3D) groundwater flow and transport model capable of simulating the same set of reactions as PHREEQC. PHT3D couples PHREEQC to the groundwater flow model MODFLOW and the solute transport model MT3DMS. PHT3D is mostly practical to run 2-D simulations of plume cross-sections or even fully 3-D simulations. The potential advantage of PHT3D with respect to PHAST is the option to simulate isotopologue diffusion which is not possible with PHAST. Diffusion-induced isotope fractionation might be relevant at the upper/lower fringes of pollution plumes. PHT3D can be downloaded at <http://www.pht3d.org>. However, to run PHT3D a commercial GUI is practically required which is a disadvantage compared to PHAST if the goal is to make a simple model. PHT3D takes more time to setup than PHAST. A large advantage of PHT3D is that the model is part of some commercially available GUIs like Visual Modflow or Processing Modflow (PMWIN; <http://www.simcore.com/>), which, in principle implies endless possibilities to simulate contaminant transport including isotope fractionation.

Python – A general purpose scripting language esigned to be highly readable and easy to use. For viewing model results of the template files, Python scripts have been developed for this project and are available for download from the project website (see below). Python is a free alternative for MATLAB and enables plotting of graphs and 2-D contour plots in a programming environment. Alternatively, plots can be made with PHREEQC for Windows or with Microsoft (MS) Excel. Python implementations can be downloaded for free as open-source softwares which run in a variety of Windows, Macintosh or Linux environments. Python can be downloaded at <http://python-xy.github.io/downloads.html>

Model template files: A ZIP file with templates, Cases 1-4, described in the User's Guide of this project.

ESTCP Final Report:

Integrated Stable Isotope –

Reactive Transport Model Approach

for Assessment of Chlorinated

Solvent Degradation

Appendix C: Tabulated Sampling Results

Table C1. Sampling Locations Hill OU10, the 2011 sample set.

Table C2. Sampling Locations Hill OU10, the 2014 sample set.

Table C3. Chlorinated ethenes concentrations, 2011 sample set.

Table C4. Chlorinated ethenes concentrations, 2014 sample set.

Table C5. CSIA data, 2011 sample set.

Table C6. CSIA data, 2014 sample set.

Table C7. Redox parameters, 2011 sample set.

Table C8. Miscellaneous: Toluene and benzene concentrations (historical), groundwater age (historical), screened depth.

Table C9. Redox and groundwater parameters statistics, 2011 sample set.

Table C1. Sampling Locations Hill OU10, the 2011 sample set

Location ID	Sample Interval	Depth Zone	Sampling Method	Sample Date	Sample Rationale
U10-011	71.5–73.5	Shallow A zone	LF	Aug/Sept. 2011	Lower shallow A zone TCE
U10-012	74–76	Shallow A zone	LF	Aug/Sept. 2011	Lower shallow A zone
U10-019	87.6–89.6	Shallow B zone	LF	Aug/Sept. 2011	South shallow plume, cDCE
U10-020	29.5–31.5	Shallow A zone	LF	Aug/Sept. 2011	Shallow plume upgradient, high TCE
U10-027	53–55	Shallow A zone	LF	Aug/Sept. 2011	South lobe shallow zone - low concentrations
U10-028	60–62	Shallow A zone	LF	Aug/Sept. 2011	South lobe shallow zone - low concentrations
U10-029	72–74	Deep C zone	LF	Aug/Sept. 2011	South lobe Shallow part of C zone
U10-035	40.35–42.35	Shallow A zone	LF	Aug/Sept. 2011	Lower A zone
U10-036	22.62–24.62	Shallow	LF	Aug/Sept. 2011	TCE only
U10-037	26.25–28	Shallow	LF	Aug/Sept. 2011	TCE only
U10-039	26.24–28.24	Shallow	LF	Aug/Sept. 2011	Center of shallow plume
U10-042	243–250	Deep C zone	PDB	Aug/Sept. 2011	Deep zone between main lobes of plume, TCE and cDCE detections
U10-042	260–270	Deep C zone	PDB	Aug/Sept. 2011	
U10-042	275–280	Deep C zone	PDB	Aug/Sept. 2011	
U10-042	280–290	Deep C zone	PDB	Aug/Sept. 2011	
U10-043	22–24	Shallow A zone	LF	Aug/Sept. 2011	High TCE concentrations
U10-045	16–18	Shallow A zone	LF	Nov/Dec. 2014	TCE and PCE
U10-049	258–260	Deep	LF	Dec. 2011	North lobe, history of VC
U10-062	26.75–28.75	Shallow A zone	LF	Dec. 2011	TCE concentrations lower than adjacent U10-043
U10-064	93.8–95.8	Deep C zone	LF	Aug/Sept. 2011	south lobe
U10-076A	85.4–87.4	Deep C zone	LF	Dec. 2011	TCE detections
U10-080C	260.5–263.5	Deep	BC	Dec. 2011	North lobe

ESTCP Final Report:

Integrated Stable Isotope –

Reactive Transport Model Approach

for Assessment of Chlorinated

Solvent Degradation

U10-080D	270.5–273.5	Deep	BC	Dec. 2011	North Lobe
U10-086A	213–215	Deep C zone	LF	Dec. 2011	North lobe downgradient
U10-088A	32–34	Shallow	LF	Dec. 2011	Very low conc. Of TCE
U10-089C	242–242.5	Deep C zone	BC	Dec. 2011	North lobe center
U10-089D	259–259.5	Deep C zone	BC	Dec. 2011	North lobe center
U10-093	232–234	Deep C zone	PDB	Dec. 2011	Upgradient of deep plume, delineates edge
U10-093	249–251	Deep C zone	PDB	Dec. 2011	
U10-093	266–268	Deep C zone	PDB	Dec. 2011	
U10-093	283–285	Deep C zone	PDB	Dec. 2011	
U10-094A	188–190	Deep C zone	LF	Dec. 2011	High concentrations, history of VC
U10-099	47.5–49.5	Shallow A zone	LF	Dec. 2011	Near groundwater elevation surface
U10-104	207–209	Deep C zone	PDB	Dec. 2011	Higher concentrations of TCE, cDCE and historical detections of VC at multiple depths
U10-104	217–219	Deep C zone	PDB	Dec. 2011	
U10-104	227–229	Deep C zone	PDB	Dec. 2011	
U10-104	237–239	Deep C zone	PDB	Dec. 2011	
U10-104	247–249	Deep C zone	PDB	Dec. 2011	
U10-104	257–259	Deep C zone	PDB	Dec. 2011	
U10-104	267–269	Deep C zone	PDB	Dec. 2011	
U10-104	277–279	Deep C zone	PDB	Dec. 2011	
U10-106	41–43	Shallow	LF	Dec. 2011	Low TCE concentrations
U10-107	22.5–24.7	Shallow	LF	Dec. 2011	High PCE concentrations
U10-116	198–200	Deep	PDB	Sept/Oct 2011	Edge of deep plume, cDCE concentrations higher than TCE
U10-116	208–210	Deep	PDB	Sept/Oct 2011	
U10-116	218–220	Deep	PDB	Sept/Oct 2011	
U10-116	228–230	Deep	PDB	Sept/Oct 2011	
U10-116	238–240	Deep	PDB	Sept/Oct 2011	
U10-116	248–250	Deep	PDB	Sept/Oct 2011	
U10-116	258–260	Deep	PDB	Sept/Oct 2011	
U10-116	268–270	Deep	PDB	Sept/Oct 2011	
U10-116	278–280	Deep	PDB	Sept/Oct 2011	
U10-116	288–290	Deep	PDB	Sept/Oct 2011	
U10-131	221–223	Deep C zone	LF	Dec. 2011	Near source
U10-132	46–48	Shallow	LF	Dec. 2011	TCE low concentrations
U10-133	48–50	Shallow A zone	LF	Dec. 2011	High PCE
U10-134	48–50	Shallow	LF	Dec. 2011	TCE low concentrations
U10-142	26–28	Shallow A zone	LF	Dec. 2011	PCE and TCE
U10-150C	252.5–253	Deep C zone	BC	Dec. 2011	Historical high TCE and cDCE
U10-150D	290–291	Deep C zone	BC	Dec. 2011	Recent TCE detections
U10-151B	258–259	Deep C zone	BC	Dec. 2011	Historic high TCE
U10-157	27–30	Shallow	LF	Dec. 2011	TCE concentrations relatively high
U10-167	27–30	Shallow	LF	Dec. 2011	Low concentration of TCE
U10-172	24–27	Shallow A zone	LF	Dec. 2011	TCE and cDCE and historical detections of VC

U10-175	27–30	Shallow	LF	Dec. 2011	TCE only
U10-176C	207.5–208	Deep	BC	Dec. 2011	cDCE only
U10-176D	238–238.5	Deep	BC	Dec. 2011	North lobe - low concentrations
U10-179A	242.5–243.0	Deep	BC	Dec. 2011	TCE, cDCE and tDCE
U10-179B	255.5–256	Deep	BC	Dec. 2011	TCE, cDCE and tDCE
U10-179C	267.5–268	Deep	BC	Dec. 2011	No data
U10-180B	224.5–225	Deep	BC	Dec. 2011	No data
U10-180C	237–237.5	Deep	BC	Dec. 2011	No data
U9-12-004	43–45	Shallow A zone	LF	Aug/Sept. 2011	TCE
U9-12-005	60–62	Shallow A zone	LF	Aug/Sept. 2011	Low concentration TCE
U9-12-006	32–34	Shallow A zone	LF	Aug/Sept. 2011	Low concentration TCE
U9-12-007	44–46	Shallow A zone	LF	Aug/Sept. 2011	TCE
U9-12-010	81–83	Shallow B zone	LF	Aug/Sept. 2011	TCE and cDCE
U9-12-011	90–92	Shallow B zone	LF	Aug/Sept. 2011	TCE and cDCE
U9-12-013	86–90	Shallow B zone	LF	Aug/Sept. 2011	B zone upgradient
U9-12-015	36–38	Shallow A zone	LF	Aug/Sept. 2011	shallow upgradient
U9-12-016	33–37	Shallow	LF	Aug/Sept. 2011	Low concentrations TCE
U9-12-017	87–91	Shallow B zone	LF	Aug/Sept. 2011	B zone upgradient - TCE and cDCE
U9-12-019	95–99	Shallow B zone	LF	Aug/Sept. 2011	South Lobe
U9-12-021	93–95	Deep	LF	Aug/Sept. 2011	TCE and cDCE

Notes:

1. Single well screens with multiple sample depths are shaded.
2. The sample interval is depth below ground surface.
3. LF = low flow, BC – BarCad, PDB = Permeable diffusion bags.

Table C2. Sampling Locations Hill OU10, the 2014 sample set

Location ID	Sample Interval	Depth Zone	Sampling Method	Sample Date	Sample Rationale
U10-019	87.6–89.6	Shallow B zone	LF	Apr. 2014	South shallow plume, cDCE
U10-027	53–55	Shallow A zone	LF	Apr. 2014	South lobe shallow zone - low concentrations
U10-045	16–18	Shallow A zone	LF	Apr. 2014	TCE and PCE
U10-049	258–260	Deep	LF	Apr. 2014	North lobe, history of VC
U10-076A	85.4–87.4	Deep C zone	LF	Apr. 2014	TCE detections
U10-080C	260.5–263.5	Deep	BC	Apr. 2014	North lobe
U10-080D	270.5–273.5	Deep	BC	Apr. 2014	North Lobe
U10-089C	242–242.5	Deep C zone	BC	Apr. 2014	North lobe center
U10-089D	259–259.5	Deep C zone	BC	Apr. 2014	North lobe center
U10-116	238–240	Deep	PDB	Apr. 2014	Edge of deep plume, cDCE concentrations higher than TCE
U10-116	268–270	Deep	PDB	Apr. 2014	
U10-151B	258–259	Deep C zone		Apr. 2014	Historic high TCE
U10-175	27–30	Shallow	LF	Apr. 2014	TCE only
U10-176C	207.5–208	Deep	BC	Apr. 2014	cDCE only
U10-179A	242.5–243.0	Deep	BC	Apr. 2014	TCE, cDCE and tDCE

ESTCP Final Report:

Integrated Stable Isotope –

Reactive Transport Model Approach

for Assessment of Chlorinated

Solvent Degradation

U10-179B	255.5-256	Deep	BC	Apr. 2014	TCE, cDCE and tDCE
U10-179C	267.5-268	Deep	BC	Apr. 2014	No data
U9-12-013	86–90	Shallow B zone	LF	Apr. 2014	B zone upgradient
U9-12-017	87–91	Shallow B zone	LF	Apr. 2014	B zone upgradient - TCE and cDCE
U9-12-021	93–95	Deep	LF	Apr. 2014	TCE and cDCE

Notes:

1. Single well screens with multiple sample depths are shaded.
2. The sample interval is depth below ground surface.
3. LF = low flow, BC – BarCad, PDB = Permeable diffusion bags.

Table C3. Chlorinated ethenes concentrations, 2011 sample set.

Chlorinated ethenes concentrations (µmol/L – Micromoles per Liter). Minimum analytical error ± 10 %						
Sample ID	PCE	TCE	Cis-DCE	Trans-DCE	1,1-DCE	VC
U10-011	3.5E-03 ⁽¹⁾	1.4E-01	0	0	0	0
U10-012	9.6E-03	2.6E-02	0	0	0	0
U10-019	6.4E-03 ⁽¹⁾	2.0E-01	1.4E-01	2.5E-02	0	0
U10-020	0	1.1E+00	0	0	0	0
U10-027	0	2.1E-02	0	0	0	0
U10-028	0	7.8E-03 ⁽¹⁾	0	0	0	0
U10-029	0	2.2E-01	0	0	0	0
U10-035	0	3.3E-01	0	0	0	0
U10-036	0	7.9E-02	0	0	0	0
U10-037	3.4E-02	2.6E-01	0	0	0	0
U10-039	0	4.5E-01	0	0	0	0
U10-042-243	0	1.4E-01	8.4E-02	3.3E-02	1.0E-03	0
U10-042-260	0	1.4E-01	9.1E-02	3.6E-02	1.0E-03	0
U10-042-275	0	1.4E-01	8.9E-02	3.4E-02	1.0E-03	0
U10-042-288	0	1.4E-01	8.9E-02	3.4E-02	1.0E-03	0
U10-043	1.1E-02 ⁽¹⁾	7.6E-01	0	0	0	0
U10-045	4.2E-03 ⁽¹⁾	1.1E-02 ⁽¹⁾	0	0	0	0
U10-049	0	9.1E-01	1.3E-01	1.4E-02	0	0
U10-062	0	1.4E-01	0	0	0	0
U10-076A	0	2.0E-02	1.2E-02 ⁽¹⁾	0	0	0
U10-080C	0	1.8E-01	4.2E-01	8.8E-01	1.0E-03	0
U10-080D	0	3.2E-02	9.7E-02	4.8E-02	0	0
U10-086A	0	4.1E-01	9.6E-02	4.1E-03	4.1E-03	0
U10-088A	0	2.6E-02	0	0	0	0
U10-089C	0	2.7E+00	1.7E-01	2.0E-02	5.3E-03	0
U10-089D	0	7.4E-01	2.0E-02	2.1E-03	4.1E-03	0
U10-093-232	0	5.6E-03 ⁽¹⁾	0	1.0E-03	0	0
U10-093-249	0	5.5E-03 ⁽¹⁾	0	0	0	0
U10-093-266	0	6.2E-03 ⁽¹⁾	0	1.0E-03	0	0
U10-093-283	0	4.6E-03 ⁽¹⁾	0	1.0E-03	0	0
U10-094A	0	2.7E+00	1.3E+00	1.1E+00	7.4E-03	0
U10-099	4.0E-02	7.1E-03 ⁽¹⁾	0	0	0	0
U10-104-207	0	4.1E-01	6.2E-01	7.1E-02	3.1E-03	0
U10-104-217	0	3.6E-01	5.7E-01	6.3E-02	3.1E-03	0
U10-104-227	0	3.7E-01	5.7E-01	6.4E-02	3.1E-03	0

ESTCP Final Report:

Integrated Stable Isotope –

Reactive Transport Model Approach

for Assessment of Chlorinated

Solvent Degradation

Chlorinated ethenes concentrations (µmol/L – Micromoles per Liter). Minimum analytical error ± 10 %

Sample ID	PCE	TCE	Cis-DCE	Trans-DCE	1,1-DCE	VC
U10-104-237	0	3.5E-01	5.6E-01	6.2E-02	3.1E-03	0
U10-104-247	0	3.6E-01	5.7E-01	6.2E-02	3.1E-03	0
U10-104-257	0	3.3E-01	5.5E-01	5.8E-02	3.1E-03	0
U10-104-267	0	3.4E-01	5.7E-01	6.0E-02	3.1E-03	0
U10-104-277	0	2.8E-01	5.3E-01	5.3E-02	3.1E-03	0
U10-106	4.8E-03 ⁽¹⁾	3.3E-02	0	0	0	0
U10-107	2.9E-01	3.8E-02	0	0	0	0
U10-116-198	0	1.3E-02	1.5E-01	1.7E-02	1.0E-03	0
U10-116-208	0	1.8E-02	1.4E-01	1.5E-02	0	0
U10-116-218	0	1.9E-02	1.4E-01	1.5E-02	0	0
U10-116-228	0	1.9E-02	1.4E-01	1.5E-02	0	0
U10-116-238	0	1.9E-02	1.4E-01	1.5E-02	0	0
U10-116-248	0	1.6E-02	1.2E-01	1.2E-02	0	0
U10-116-268	0	1.8E-02	1.5E-01	1.7E-02	4.1E-03	0
U10-116-278	0	1.7E-02	1.4E-01	1.7E-02	0	0
U10-116-288	0	1.7E-02	1.3E-01	1.7E-02	0	0
U10-131	0	2.4E-02	2.0E-01	4.6E-02	0	0
U10-132	0	5.4E-02	0	0	0	0
U10-133	8.5E-02	0	0	0	0	0
U10-134	0	3.0E-02	0	0	0	0
U10-142	4.6E-02	2.3E-01	0	0	0	0
U10-150C	0	1.7E+00	9.6E-02	6.3E-03	2.4E-03	0
U10-150D	0	0	0	0	0	4.0E-01
U10-151B	0	1.4E+00	2.0E-01	6.3E-02	2.1E-03	0
U10-157	4.6E-02	3.4E-01	0	0	0	0
U10-167	1.0E-01	7.7E-01	0	0	0	0
U10-172	0	0	3.6E-01	6.2E-03	0	0
U10-175	3.3E-01	3.3E-01	0	0	0	0
U10-176C	0	1.3E-02	0	0	0	0
U10-176D	0	0	1.6E-02	0	0	1.8E-01
U10-179A	0	4.2E-01	1.2E-01	1.1E-01	2.4E-03	0
U10-179B	0	8.2E-01	1.4E-01	1.2E-02	6.2E-04	0
U10-179C	0	4.6E-01	2.1E-02	3.1E-03	3.1E-03	4.1E-02 ⁽¹⁾
U10-180B	0	4.4E-01	7.9E-02	4.4E-03	4.1E-03	5.3E-01
U10-180C	0	5.3E-01	3.5E-02	3.1E-03	0	0
U9-12-002	4.3E-03 ⁽¹⁾	1.0E-01	3.1E-03	0	2.1E-03	0
U9-12-004	4.8E-03 ⁽¹⁾	3.7E-02	0	0	0	0
U9-12-005	0	7.2E-03 ⁽¹⁾	0	0	0	0
U9-12-006	8.2E-01	8.4E-02	0	0	0	0
U9-12-007	2.3E-02	1.2E-02	0	0	0	0
U9-12-010	0	2.2E-01	2.8E-01	3.1E-02	1.0E-03	0
U9-12-011	0	3.6E-02	3.4E-02	3.6E-03	0	0
U9-12-013	4.4E-03 ⁽¹⁾	2.1E-02	3.8E-02	2.9E-03	0	0
U9-12-015	0	1.1E-01	0	0	0	0
U9-12-016	0	1.2E-02	0	0	0	0
U9-12-017	0	1.1E-02	2.4E-02	3.5E-03	0	0
U9-12-021	0	1.9E-02	5.8E-03 ⁽¹⁾	3.9E-04	0	0

NOTES:

ESTCP Final Report:
Integrated Stable Isotope –
Reactive Transport Model Approach
for Assessment of Chlorinated
Solvent Degradation

Chlorinated ethenes concentrations (µmol/L – Micromoles per Liter). Minimum analytical error ± 10 %

Sample ID	PCE	TCE	Cis-DCE	Trans-DCE	1,1-DCE	VC
-----------	-----	-----	---------	-----------	---------	----

Sample ID is similar to the location identification at the Hill Site, except for wells sampling at different depth with PDBs for which the sampling depth (in feet) is added to the identification

(1)Analytical error of 20 % on concentrations

Table C4. Chlorinated ethenes concentrations, 2014 sample set

Chlorinated ethenes concentrations (µmol/L – Micromoles per Liter). Sampling campaign of 2014. VC, ethene, and 1,1-DCE were not detected.

Sample ID	PCE	TCE	Cis-DCE	Trans-DCE
U10-027		1.8E-03	1.8E-02	0
U10-045		0	4.1E-03	0
U10-049		0	5.8E-01	1.2E-01
U10-076A		0	5.7E-02	1.0E-02
U10-089C		0	2.3E+00	1.9E-01
U10-089D		0	5.4E-01	5.2E-03
U10-116-268		0	4.5E-03	9.2E-02
U10-151B		0	1.6E+00	5.2E-01
U10-175	3.4E-01	1.1E-01	0	0
U10-175-1	3.1E-01	1.5E-01	0	0
U10-176C	0	2.1E-02	4.1E-03	1.2E-02
U10-179C	0	4.3E-01	1.1E-01	2.9E-01
U9-12-017	0	6.1E-03	2.1E-03	1.0E-03
U9-12-021	0	1.5E-02	3.7E-03	0
U9-12-013	4.8E-03	1.3E-02	1.8E-02	4.1E-03
U10-019	1.8E-03	1.6E-01	1.1E-01	1.9E-02
U10-019-1	1.2E-03	1.5E-01	9.2E-02	1.8E-02
U10-080C	0	1.5E-01	3.2E-01	4.5E-01
U10-080C-1	0	1.4E-01	3.2E-01	4.3E-01
U10-080D	0	3.6E-02	1.2E-01	6.8E-02
U10-104-227	0	4.3E-01	8.0E-01	7.2E-02
U10-104-247	0	3.2E-01	5.9E-01	5.4E-02
U10-179A	0	1.4E-02	1.9E-02	2.6E-02
U10-179B	0	7.3E-01	1.4E-01	2.1E-02
U10-179B-1	0	7.0E-01	1.3E-01	1.9E-02
U10-151B-1	0	1.2E+00	4.1E-01	2.7E-01
U10-093-266	0	0	0	0

Table C5. CSIA data, 2011 sample set

Isotope ratios	$\delta^{13}\text{C}$ (‰)			$\delta^{37}\text{Cl}$ (‰)				$\delta^2\text{H}$ (‰)	
Chlorinated ethene	TCE	cis-DCE	trans-DCE	ETH	PCE	TCE	cis-DCE	TCE	cis-DCE
Minimum error	±0.5 ‰	±0.5 ‰	±0.5 ‰	±0.5 ‰	±1 ‰	±1 ‰	±1 ‰	±15 ‰	±15 ‰
Sample ID									
U10-011	-26.2					2.7		-251	
U10-012	-25.3								
U10-019	-13.7	-36.6				5.4	1.7		
U10-020	-25.6					4.4		-259	
U10-027	-23.7								
U10-028	-25.0								
U10-029	-25.0					3.5		-255	
U10-035	-26.0					0.1		-256	
U10-036	-24.3					3.0			
U10-037	-25.2				-0.2	3.2		-247	
U10-039	-24.4					3.7		-254	
U10-042-243	-22.0	-41.4				3.5	0.9		
U10-042-260	-22.2	-41.3				3.7	0.7		
U10-042-275	-21.9	-42.4				3.8	0.8		
U10-042-288	-21.8 ⁽¹⁾					3.0	1.0		
U10-043	-25.5					4.1		-260	
U10-045	-20.1 ⁽¹⁾								
U10-049	-22.3	-38.9					-0.1	-232	
U10-062	-25.4					4.6		-194	
U10-076A	-18.0 ⁽¹⁾	26.9 ⁽¹⁾				4.2			
U10-080C	3.5	-38.4	-42.2			8.3	1.3		-399
U10-080D	-13.9 ⁽¹⁾	-43.9	-48.0			4.3	0.4		
U10-086A	-21.2	-43.8				3.5	0.5	-247	-392 ⁽²⁾
U10-088A	-19.7 ⁽¹⁾					2.7			
U10-089C	-24.2	-44.2				2.6	-0.7	-266	
U10-089D	-22.1					3.2		-252	
U10-093-232	-15.5 ⁽³⁾								
U10-093-249	-15.5 ⁽³⁾								
U10-093-266	-16.3 ⁽³⁾								
U10-093-283	-16.4 ⁽³⁾								
U10-094A	-22.2	-37.7	-39.3			3.7	1.2	-288	-412
U10-099	-25.3 ⁽¹⁾				-1.3				
U10-104-207	-19.4	-35.8				4.8	0.4		
U10-104-	-19.5	-36.0				4.4	0.7		

Isotope ratios	$\delta^{13}\text{C}$ (‰)			$\delta^{37}\text{Cl}$ (‰)				$\delta^2\text{H}$ (‰)	
Chlorinated ethene	TCE	cis-DCE	trans-DCE	ETH	PCE	TCE	cis-DCE	TCE	cis-DCE
Minimum error	± 0.5 ‰	± 0.5 ‰	± 0.5 ‰	± 0.5 ‰	± 1 ‰	± 1 ‰	± 1 ‰	± 15 ‰	± 15 ‰
Sample ID									
217									
U10-104-227	-18.8	-36.0				5.2	1.2		
U10-104-237	-19.3	-36.0				5.2	0.8		
U10-104-247	-19.2	-35.6				5.3	0.3		
U10-104-257	-19.4	-35.7				4.7	0.3		
U10-104-267	-19.2	-35.7				5.6	0.8		
U10-104-277	-19.6	-36.0				5.1	0.1		
U10-106	-24.3					1.4			
U10-107	-25.2				-0.7	3.7			
U10-116-198	-8.9 ⁽⁴⁾	-24.0					2.1		-258
U10-116-208	-7.9 ⁽⁴⁾	-25.0					1.1		-253 ⁽²⁾
U10-116-218	-8.5 ⁽⁴⁾	-25.4					0.5		-265 ⁽²⁾
U10-116-228	-8.9 ⁽⁴⁾	-25.1					0.4		
U10-116-238	-8.9 ⁽⁴⁾	-24.9					0.6		-253
U10-116-248	-7.9 ⁽⁴⁾	-24.8					1.1		
U10-116-268	-8.9 ⁽⁴⁾	-25.3					0.6		
U10-116-278	-8.9 ⁽⁴⁾	-25.1					2.0		
U10-116-288	-7.0 ⁽⁴⁾	-25.3					0.1		-262 ⁽²⁾
U10-131	0.5	-19.9	-27.5			9.0	1.6		-293 ⁽²⁾
U10-132	-24.8					5.0			
U10-133					-0.5				
U10-134	-24.4					1.5			
U10-142	-25.2				0.2	3.8		-189	
U10-150C	-23.1	-42.8				2.9	-0.1	-256	
U10-150D			-52.0						
U10-151B	-22.3	-43.0	-50.0			2.3	-1.6	-245	-337 ⁽²⁾
U10-157	-25.5				-0.3	4.4		-188	
U10-167	-25.2				0.1	4.8		-192	
U10-172		-27.6					2.8		-258
U10-175	-25.3				-0.5			-198	
U10-176C	-14.6 ⁽¹⁾								

Isotope ratios	$\delta^{13}\text{C}$ (‰)			$\delta^{37}\text{Cl}$ (‰)				$\delta^2\text{H}$ (‰)	
Chlorinated ethene	TCE	cis-DCE	trans-DCE	ETH	PCE	TCE	cis-DCE	TCE	cis-DCE
Minimum error	± 0.5 ‰	± 0.5 ‰	± 0.5 ‰	± 0.5 ‰	± 1 ‰	± 1 ‰	± 1 ‰	± 15 ‰	± 15 ‰
Sample ID									
U10-176D	-40.6		-54.0						
U10-179A	-17.3	-43.4	-44.8			4.1	-1.8	-237	-359 ⁽²⁾
U10-179B	-23.7	-42.2				2.6	-0.6	-247	-320 ⁽²⁾
U10-179C	-21.4	-40.9				3.2		-251	
U10-180B	-16.3	-42.5		-54.5		6.4	-0.1	-178	
U10-180C	-21.2	-43.2				3.5	-0.6	-200	
U9-12-002	-22.1					1.3		-232	
U9-12-004	-25.2					3.3			
U9-12-005	-24.8 ⁽¹⁾								
U9-12-006	-25.8				-1.4	3.5			
U9-12-007	-24.7								
U9-12-010	-9.7	-34.9				5.0	0.3	-238	-459
U9-12-011	-12.3	-29.7				4.1	1.3		
U9-12-013	-5.7	-31.4					-0.5		
U9-12-015	-26.0					2.3		-256	
U9-12-016	-23.9 ⁽¹⁾								
U9-12-017	-4.2 ⁽¹⁾	-28.7							
U9-12-021	-15.6 ⁽¹⁾	-35.3							

NOTES:

Sample ID is similar to the location identification at the Hill Site, except for wells sampling at different depth with PDBs for which the upper boundary of the screen depth (in feet bgs) is added to the identification (see table miscellaneous)

‰ = permil

⁽¹⁾Error on $\delta^{13}\text{C}$ (‰) = 1 ‰

⁽²⁾Error on $\delta^2\text{H}$ (‰) = 30 ‰

⁽³⁾Error on $\delta^{13}\text{C}$ (‰) = 4 ‰

⁽⁴⁾Error on $\delta^{13}\text{C}$ (‰) = 2 ‰

Table C6. CSIA data, 2014 sample ses

Isotope ratios	$\delta^{13}\text{C}$ (‰)				$\delta^{37}\text{Cl}$ (‰)		$\delta^2\text{H}$ (‰)		
Chlorinated ethene	PCE	TCE	Cis-DCE	Trans-DCE	TCE	Cis-DCE	TCE	Cis-DCE	Trans-DCE
Minimum error	± 0.5 ‰	± 0.5 ‰	± 0.5 ‰	± 0.5 ‰	± 0.5 ‰	± 0.7 ‰	± 20 ‰	± 10 ‰	± 10 ‰
U10_027	-30.8	-23.2			2.7				
U10_045		-26.0			5.6				
U10_049		-22.3	-44.3	-44.4	2.7	0.1	-236	-387	
U10_049 ⁽¹⁾⁽²⁾⁽³⁾			-43.7	-46.2			-227	-380	
U10_076A ⁽²⁾		-22.0	-38.7		3.8	1.8			
U10_089C ⁽²⁾		-22.6	-42.4	-49.0	2.5		-241	-368	
U10_089D ⁽²⁾		-22.0	-43.0		2.5	-2.5			

ESTCP Final Report:

Integrated Stable Isotope –

Reactive Transport Model Approach

for Assessment of Chlorinated

Solvent Degradation

U10_116_268		-13.3	-22.4	-29.2	7.0	1.8			
U10_116_268 ⁽¹⁾		-6.2			8.7	1.3			
U10_151B ^{(2) (3)}		-21.9	-42.0	-47.4	2.7	0.2	-239	-382	-458
U10_175 ⁽²⁾	-29.1	-25.8			3.8				
U10_175 ^{(1) (2)}	-28.5	-25.2			3.4				
U10_175 ⁽¹⁾	-21.4	-25.4							
U10_175 ⁽¹⁾	-21.1	-25.7							
U10_176C		-14.8	-41.6	-42.5	4.3	0.2			
U10_179C ⁽²⁾		-11.6	-39.1	-40.4	4.1	1.6	-208	-418	-479
U10_179C ⁽¹⁾			-40.1	-39.9	4.3				
U10_179C ⁽¹⁾			-38.7	-40.1					
U9_12_017		-19.3	-28.9		4.4				
U9_12_021		-16.5	-37.5		1.3				
U9_12_013	-29.4	-4.5	-25.5	-33.3	6.3	-1.0			
U9_12_013 ⁽¹⁾	-28.1	-1.3	-25.1		6.6	0.3			
U9_12_013 ⁽¹⁾	-28.1	-2.3	-24.7			-0.5			
U10_019		-13.3	-35.8	-38.0		1.6			
U10_019 ^{(1) (3)}		-13.2	-35.2	-38.7		1.2			
U10_019 ⁽¹⁾			-35.7	-39.9		1.4			
U10_019 ⁽¹⁾			-35.6	-40.2					
U10_076A ⁽¹⁾		-22.4	-37.7						
U10_080C ⁽³⁾		2.6	-37.1	-41.6		0.2	-149	-396	-480
U10_080C ⁽¹⁾		2.3	-36.9	-41.6		1.3	-168	-398	-482
U10_080C ^{(1) (3)}		1.8	-37.3	-41.2		-0.3	-142	-392	-475
U10_080D ⁽³⁾		-14.3	-41.6	-46.0		-0.3			
U10_080D ⁽¹⁾		-12.7	-40.8	-45.6					
U10_104_227 ⁽³⁾		-17.0	-34.3	-42.8		0.9	-222	-309	-357
U10_104_247		-17.0	-34.2	-44.0		1.9	-241	-317	-341
U10_104_247 ⁽¹⁾							-229	-315	-337
U10_175 ⁽¹⁾	-21.4	-25.4							
U10_175 ⁽¹⁾	-21.1	-25.7							
U10_179A		-5.7	-38.4	-38.9		0.1			
U10_179B ⁽³⁾		-22.7	-39.8	-46.9		0.6	-240	-332	
U10_179B ⁽¹⁾						0.5	-241	-339	
U10_179C ⁽¹⁾			-38.7	-40.1					

NOTES:

⁽¹⁾Lab duplicate of the isotope data collected for this well

⁽²⁾TCE $\delta^{13}\text{C}$ and $\delta^{37}\text{Cl}$ data were measured in the same subsample

⁽³⁾Cis- DCE $\delta^{13}\text{C}$ and $\delta^{37}\text{Cl}$ data were measured in the same subsample

Sample ID is similar to the location identification at the Hill Site, except for wells sampling at different depth with PDBs for which the upper boundary of the screen depth (in feet bgs) is added to the identification (see table miscellaneous)

Table C7. Redox parameters, 2011 sample set

Sample ID	Total iron (mg/L)	Ferrous iron (mg/L)	Sulfide (mg/L)	Sulfate (mg/L)	Nitrate (mg/L)	Dissolved oxygen (mg/L)
U10-011	0.18	0	0.41	20	2.6	2.4
U10-012	0	0	0	80	25.3	1.7
U10-019	0.13	0.01	0	80	1.1	0.4
U10-020	0.13	0	0	0	0.4	0.2
U10-027	0.31	0	0	80	0.0	0.3
U10-028	0.23	0	0.03	52	0.8	0.2
U10-029	1.61	0.39	0	42	1.4	0.4
U10-035	0.27	0.07	0	80	1.1	0.1
U10-037	1.37	0.41	0	20	0.0	0.1
U10-039	1.52	0.31	0.04	80	0.0	0.1
U10-043	1.09	0.08	0.07	80	0.3	0.2
U10-045	0.07	0	0	80	0.1	0.2
U10-049	0.18	0.02	0	67	13.9	0.8
U10-062	0.08	0.05	0.22	80	80.2	0.4
U10-076A	0.12	0	0	80	1.0	2.4
U10-080C	2.29	1.14	0	4	28.3	4.8
U10-080D	1.9	1.17	0	2	28.9	4.4
U10-086A	2.88	0.98	0	14	1.4	4.4
U10-088A	0.08	0.03	0	39	0.0	4.8
U10-089C	0.36	0.17	0.12	20	1.8	4.3
U10-089D	0.07	0.02	0	4	2.1	4.5
U10-094A	1.3	0.16	0	33	0.8	0.9
U10-099	0.86	0	0	17	40.0	0.9
U10-106	0.18	0	0.08	80	29.5	2.1
U10-107	0.67	0.17	0.36	65	15.4	0.6
U10-131	1.58	0.07	0.8	0	2.0	1.8
U10-132	0.45	0.12	0.06	80	24.1	0.7
U10-133	0.07	0.04	0	14	3.7	2.2
U10-134	0.16	0.11	0.5	24	27.3	0.5
U10-142	0	0	0.2	80	30.4	0.7
U10-150C	0.63	0.33	0	15	122.9	4.3
U10-150D	1.29	0.88	0.49	80	600.2	4.5
U10-151B	0.2	0.18	0.03	20	130.5	4.6
U10-157	0.31	0.22	0.23	17	32.3	0.5
U10-167	0.79	0.32	0.05	80	21.9	1.9
U10-172	3.3	0.54	0.25	80	5.2	0.9
U10-175	0	0	0.06	54	27.4	1.7
U10-176C	1.84	0.67	0.06	0	6.5	2.4
U10-176D	2.38	0.37	0.1	80	1.3	3.7
U10-179A	0.44	0.13	0	4	2.2	4.0
U10-179B	2.98	1.23	0	4	42.9	4.7
U10-179C	1.69	0.63	0	44	91.0	4.9
U10-180B	1	0.09	0.11	80	1.6	3.2
U10-180C	0.67	0	0.07	80	7.2	3.8
U9-12-002	0.37	0.03	0.6	80	0.3	0.2

Sample ID	Total iron (mg/L)	Ferrous iron (mg/L)	Sulfide (mg/L)	Sulfate (mg/L)	Nitrate (mg/L)	Dissolved oxygen (mg/L)
U9-12-004	0	0	0.5	18	0.4	2.5
U9-12-005	0.4	0.03	0	80	0.7	1.7
U9-12-006	0.13	0	0.1	80	0.9	2.1
U9-12-007	0.21	0.13	0.15	44	1.4	2.4
U9-12-010	0.77	0.69	0	80	5.0	1.5
U9-12-011	0.41	0	0	80	0.0	0.5
U9-12-013	0.52	0.03	0.61	80	6.3	0.2
U9-12-015	0.71	0.22	0.1	28	0.9	2.0
U9-12-016	0.37	0.08	0.04	80	1.2	2.6
U9-12-017	0.03	0	0.04	80	3.3	1.2
U9-12-021	0.45	0.09	0.05	80	1.3	0.7

NOTES:

Results correspond to the sampling campaign of 2011

Sample ID is similar to the location identification at the Hill Site, except for wells sampling at different depth with PDBs for which the sampling depth (in feet) is added to the identification (see table miscellaneous)

mg/L = Milligrams per Liter

Sample ID is the identification of the well employed at the Hill Site

Table C8. Miscellaneous: Toluene and benzene concentrations (historical), groundwater age (historical), screened depth

Sample ID	Toluene ⁽¹⁾	Benzene ⁽¹⁾	Groundwater age (y) ⁽²⁾	Upper boundary well screen (feet bgs)	Lower boundary well screen (feet bgs)
	(µg/L)	(µg/L)			
U10-011	6.9E+00	7.2E+00	14	71.5	73.5
U10-012	0	0	17	74	76
U10-019	0	0	33	87.6	89.6
U10-020	0	0	47	29.5	31.5
U10-027	0	0	31	53	55
U10-028	0	0	55	60	62
U10-029	0	0		72	74
U10-035	0	0		40.35	42.35
U10-036	0	1.0E-01		22.62	24.62
U10-037	0	0		26.25	28
U10-039	9.7E+00	9.6E+00		26.24	28.24
U10-042-243	0	0	19	243	245
U10-042-260	0	0		260	262
U10-042-275	0	0		275	277
U10-042-288	0	0		288	290
U10-043	2.8E-01	0	32	22	24
U10-045	9.8E+00	9.6E+00		55.3	57.3

ESTCP Final Report:

Integrated Stable Isotope –

Reactive Transport Model Approach

for Assessment of Chlorinated

Solvent Degradation

U10-046	7.8E+00	7.2E+00	5	9.5	11.5
U10-049	0	0		258	260
U10-051	0	0	15	205	209
U10-060	0	0	27	34.8	36.8
U10-061	9.8E+00	9.7E+00	21	84.4	86.4
U10-062	2.9E+00	2.8E+00		26.75	28.75
U10-064	1.0E+01	1.0E+01	31	93.8	95.8
U10-065	0	0	31	95.25	97.25
U10-076A	4.0E+00	3.9E+00	23	85.4	87.4
U10-078A	0	0	44	97	99
U10-080C	0	0		260.5	263.5
U10-080D	8.0E+00	7.3E+00		270.5	273.5
U10-083B	0	0	21	265.5	268.5
U10-086A	0	0	27	213	215
U10-088A	7.6E+00	7.4E+00		32	34
U10-089C	0	0		242	242.5
U10-089D	0	0		259	259.5
U10-093-232	0	0		232	234
U10-093-249	0	0		249	251
U10-093-266	0	0		266	268
U10-093-283	0	0		283	285
U10-094A	0	0	23	188	190
U10-099	5.5E+00	5.1E+00		47.5	49.5
U10-104-207	0	0		207	209
U10-104-217	0	0		217	219
U10-104-227	0	0		227	229
U10-104-237	0	0		237	239
U10-104-247	0	0		247	249
U10-104-257	0	0		257	259
U10-104-267	0	0		267	269
U10-104-277	0	0		277	279
U10-106	0	0		41	43
U10-116-198	0	0	9	198	200
U10-116-208	0	0		208	210
U10-116-218	0	0		218	220
U10-116-228	0	0		228	230
U10-116-238	0	0		238	240
U10-116-248	0	0		248	250
U10-116-268	0	0		268	270
U10-116-278	0	0		278	280
U10-116-288	0	0		288	290
U10-124A	0	0	12	190	192
U10-124B	0	0	9	213	227
U10-130	0	0	16	286	288
U10-131	0	0	14	221	223
U10-132	0	0		46	48
U10-133	0	0		48	50
U10-134	0	0		48	50
U10-157	0	0		27	30

U10-167	8.6E+00	8.1E+00		27	30
U10-172	8.2E+00	8.1E+00		24	27
U10-175	0	0		27	30
U10-176C	0	0		207.5	208
U10-176D	4.3E+00	4.2E+00		238	238.5
U9-12-002	0	0		28	30
U9-12-004	9.4E+00	9.4E+00	5	43	45
U9-12-005	5.9E+00	5.9E+00	9	60	62
U9-12-006	0	0	23	32	34
U9-12-007	7.4E+00	7.2E+00	1	44	46
U9-12-010	0	0		81	83
U9-12-011	0	0	11	90	92
U9-12-013	0	0		86	90
U9-12-015	0	0	0	36	38
U9-12-016	0	0		33	37
U9-12-017	0	0		87	91
U9-12-021	9.6E+00	9.4E+00		93	95
U10-107				22.5	24.7
U10-142				30	28
U10-150C				252.5	253
U10-151B				258	259
U10-179A				242.5	243
U10-179B				255.5	256
U10-180B				224.5	225
U10-180C				237	237.5
U10-179C				267.5	268
U10-150D				290	291
U10-059			7	281	283
U10-074			36.5	170	172
U10-075A			37	220	222
U10-079			26	291	293
U10-083A			20	235	237
U10-087A			55	266	268
U10-122			0	76	78

NOTES:

⁽¹⁾Data from 2008 (CH2MHILL, 2011)

⁽²⁾Data from 2011 (CH2MHILL, 2011)

Table C9. Statistics on redox and groundwater quality parameters, 2011 sample set

Statistics	Total iron (mg/L)		Ferrous iron (mg/L)		Dissolved oxygen (mg/L)		Sulfate (mg/L)		Sulfide (mg/L)		Nitrate (mg/L)	
	Shallow	Deep	Shallow	Deep	Shallow	Deep	Shallow	Deep	Shallow	Deep	Shallow	Deep
Average value	0.5	1.3	0.1	0.6	1.2	3.7	60	31	0.1	0.1	11	60.3
Standard Deviation	0.6	0.9	0.2	0.4	1.0	1.3	27	31	0.2	0.2	17	137
Minimum Value	0	0.1	0	0	0.1	0.8	0.5	0.0	0.0	0.0	0.0	0.8
Maximum Value	3.3	3.0	0.7	1.2	4.8	4.9	80	80	1	1	80	600
Number of observations	38	18	38	18	38	18	38	18	38	18	38	18

NOTES:

mg/L = milligrams per Liter

Results correspond to the sampling campaign of 2011

Shallow corresponds to data collected in the Upper aquifer shallow plumes

Deep corresponds to the data collected in the Lower aquifer (within the deep plume)

Statistics	pH		Turbidity (NTU)		Specific conductance (mS/cm)		Oxidation reduction potential (mv)		Temperature (Celsius)	
	Shallow	Deep	Shallow	Deep	Shallow	Deep	Shallow	Deep	Shallow	Deep
Average value	7.0	7.5	6	26	1.2	0.9	177	131	14.8	16.7
Standard Deviation	0.3	0.5	19	71	0.3	0.5	46	48	2.2	1.5
3Minimum Value	6.4	6.7	1	0	0.7	0.6	102	58	11.3	15.0
Maximum Value	8.0	8.2	121	307	1.8	2.9	317	233	19.5	19.2
Number of observations	38	18	38	18	37	18	38	18	36	18

NOTES:

Results correspond to the sampling campaign of 2011

NTU = Number of Transfer Units

mS/cm = millisiemens per centimeter

mv = millivolt

Shallow corresponds to data collected in the Upper aquifer shallow plumes

Deep corresponds to the data collected in the Lower aquifer (within the deep plume)

Appendix D: Chains of Custody of the Field Samples

5301

*ESTCP Final Report:
Integrated Stable Isotope –
Reactive Transport Model Approach
for Assessment of Chlorinated
Solvent Degradation*

11/16 - 12/16

53012

*ESTCP Final Report:
Integrated Stable Isotope –
Reactive Transport Model Approach
for Assessment of Chlorinated
Solvent Degradation*

530/3

*ESTCP Final Report:
Integrated Stable Isotope –
Reactive Transport Model Approach
for Assessment of Chlorinated
Solvent Degradation*

530/4

530/4

530/5

*ESTCP Final Report:
Integrated Stable Isotope –
Reactive Transport Model Approach
for Assessment of Chlorinated
Solvent Degradation*

53016

*ESTCP Final Report:
Integrated Stable Isotope –
Reactive Transport Model Approach
for Assessment of Chlorinated
Solvent Degradation*

5/20/7

*ESTCP Final Report:
Integrated Stable Isotope –
Reactive Transport Model Approach
for Assessment of Chlorinated
Solvent Degradation*

Chain of Custody Record

530/8

Client Contact		Project Manager: Mandy Vanderford		Site Contact: Kalem Sessions		Date: 9-14-11		COC No: 261091407	
GSI Environmental Inc. 2211 Norfolk Suite 1000 Houston, Texas 77098 (713) 522-6300		Tel/Fax: (713) 522-6300		Lab Contact:		Carrier: FedEx		Job No. G-3493-103-MV	
Calendar (C) or Work Days (W)		Analysis Turnaround Time		TAT if different from Below STANDARD		SDG No.			
FAX		1 week		2 weeks					
Project Name: ESTCP Project ER-1029		1 day							
Site: Hill AFB OU 10									
P O # G-3493-103-MV									
Sample Identification		Sample Date	Sample Time	Sample Type	Sample Matrix	# of Cont.	Filtered Sample		
TB-14091101		9-14-11	0800	G	GA	1	GC-IRMS (C, CL, H isotope ratios)		
UID-0944		9-14-11	1238	LF	GA	12			
UID-116/118-200		9-15-11	1117	PDB	GA	12			
UID-116/263-310		9-15-11	1137	PDB	GA	12			
UID-116/218-220		9-15-11	1157	PDB	GA	12			
UID-116/228-230		9-15-11	1217	PDB	GA	12			
UID-116/238-240		9-15-11	1237	PDB	GA	12			
UID-116/248-250		9-15-11	1257	PDB	GA	12			
UID-116/253-260		9-15-11	1317	PDB	GA	12			
UID-116/263-270		9-15-11	1337	PDB	GA	12			
UID-116/273-280		9-15-11	1357	PDB	GA	12			
UID-116/288-290		9-15-11	1417	PDB	GA	12			
Preservation Used: 1=Ice, 2=HCl; 3=H2SO4; 4=HNO3; 5=NaOH; 6=Other									
Possible Hazard Identification									
<input type="checkbox"/> Non-Hazard		<input type="checkbox"/> Flammable		<input type="checkbox"/> Skin Irritant		<input type="checkbox"/> Poison B		<input type="checkbox"/> Unknown	
Special Instructions/QC Requirements & Comments: Dissolved Arsenic Samples need to be filtered by the laboratory.									
Sample Disposal (A fee may be assessed if samples are retained longer than 1 month)									
<input type="checkbox"/> Return To Client									
Disposal By Lab									
Archive For									
Months									
Retinquished by:		Company:		Date/Time:		Received by:		Company:	
Retinquished by: <i>Mandy Vest</i>		Company: <i>AEEC</i>		Date/Time: <i>9-15-11/1400</i>		Received by:		Company:	
Retinquished by:		Company:		Date/Time:		Received by:		Company:	
Retinquished by:		Company:		Date/Time:		Received by:		Company:	

6/02/9

*ESTCP Final Report:
Integrated Stable Isotope –
Reactive Transport Model Approach
for Assessment of Chlorinated
Solvent Degradation*

01/02/23

*ESTCP Final Report:
Integrated Stable Isotope –
Reactive Transport Model Approach
for Assessment of Chlorinated
Solvent Degradation*

11/08/23

*ESTCP Final Report:
Integrated Stable Isotope –
Reactive Transport Model Approach
for Assessment of Chlorinated
Solvent Degradation*

1/1/5

COC No:	261120761
_____ of _____	COCs
Job No.	G-3493-103-MW
SDG No.	

Attk
 1104

561/2

*ESTCP Final Report:
Integrated Stable Isotope –
Reactive Transport Model Approach
for Assessment of Chlorinated
Solvent Degradation*

5613

*ESTCP Final Report:
Integrated Stable Isotope –
Reactive Transport Model Approach
for Assessment of Chlorinated
Solvent Degradation*

Chain of Custody Record

561-4

Client Contact		Project Manager: Mindy Vanderford		Site Contact: Karen Sessions		Date: 12-19-11		COC No. 2011121901	
GSI Environmental Inc.		Tel/Fax: (713) 522-6300		Lab Contact:		Carrier: FedEx A		Job No. G-3483-103-MV	
2211 Norfolk Suite 1000		Analysis Turnaround Time						SDG No. 1104	
Houston, Texas 77098		Calendar (C) or Work Days (W)							
(713) 522-6300		TAT if different from Below STANDARD							
FAX		2 weeks							
Project Name: ESTCP Project ER-1029		1 week							
Site: Hill AFB OU 10		2 days							
P O # G-3483-103-MV		1 day							
Sample Identification		Sample Date	Sample Time	Sample Type	Sample Matrix	# of Cont.	Filtered Sample		Sample Specific Notes:
TB-19121161		12-19-11	0800	G	AA	2	GC-IRMS (C, CL, H isotope ratios)		
U9-12-010		12-19-11	1041	LF	GU	12			
U9-12-021		12-19-11	1134	LF	GU	12			
U10-011		12-19-11	1215	2F	GU	12			
U9-12-017		12-19-11	1256	LF	GU	12			
Preservation Used: 1=Ice, 2=HCl, 3=H2SO4, 4=HNO3, 5=NaOH, 6=Other									
Possible Hazard Identification									
<input type="checkbox"/> Non-Hazard		<input type="checkbox"/> Flammable		<input type="checkbox"/> Skin Irritant		<input type="checkbox"/> Poison B		<input type="checkbox"/> Unknown	
Special Instructions/QC Requirements & Comments: Dissolved Arsenic Samples need to be filtered by the laboratory.									
Sample Disposal (A fee may be assessed if samples are retained longer than 1 month)									
<input type="checkbox"/> Return To Client									
<input type="checkbox"/> Disposal By Lab									
<input type="checkbox"/> Archive For _____ Months									
Relinquished by:		Company:		Date/Time:		Received by:		Company:	
Relinquished by: <i>Debra Vard</i>		Company: <i>AEC</i>		Date/Time: <i>12/19/11 1800</i>		Received by: <i>hmk</i>		Company: <i>eu</i>	
Relinquished by:		Company:		Date/Time:		Received by:		Company:	
Relinquished by:		Company:		Date/Time:		Received by:		Company:	

26 Sample

822

[illegible]

*ESTCP Final Report:
Integrated Stable Isotope –
Reactive Transport Model Approach
for Assessment of Chlorinated
Solvent Degradation*

822

*ESTCP Final Report:
Integrated Stable Isotope –
Reactive Transport Model Approach
for Assessment of Chlorinated
Solvent Degradation*

Chain of Custody Record

[illegible]

Chain of Custody Record

[illegible]

822

*ESTCP Final Report:
Integrated Stable Isotope –
Reactive Transport Model Approach
for Assessment of Chlorinated
Solvent Degradation*